The Holographic Electron Star

Author:
YORAN TOURNOIS

Supervisors:
PROF. DR. IR. H. T. C. STOOF
V. P. J. JACOBS, MSC

June 30, 2015

Abstract

In this thesis, we study the application of the holographic duality to condensed-matter physics. Utilizing this duality, we consider the electron star as a holographic model for strongly correlated electrons at a non-zero charge density, in $3 + 1$ dimensions. The electron-star model consists of charged fermions, treated in a fluid limit, which backreact onto a $(4 + 1)$-dimensional Anti-deSitter spacetime. After solving the equations of motion in this model numerically, additional probe-fermions are added by constructing a Dirac action in the curved electron star spacetime. By solving the Dirac equation, the retarded Green's function and the spectral function for a chiral fermion are computed. Ultimately, the goal is to obtain a dual description of cold atomic gases in the unitarity limit.

Contents

Conventions

Throughout this thesis, natural units $c = \hbar = k_B = 1$ are always assumed. The dimensionality of the bulk spacetime is of the form $d + 1$, with d the number of spatial dimensions. Spacetime vectors are denoted by ordinary letters, while the spatial vectors are denoted with boldface symbols. The signature of the metric is mostly plus, i.e. $(-, +, \ldots, +)$.

A table of frequently used symbols and their meaning is shown below. Note that the inverse radial coordinate u is often denoted by z or r in the literature.

ℓ	AdS radius
κ	Gravitational coupling, $\kappa^2 = 8\pi G$
e	Fermion charge
r	Radial coordinate for (asymptotically) AdS: $r = 0$ is the interior, $r = \infty$ is the boundary
u	Inverse radial coordinate for (asymptotically) AdS: $u = 0$ is the boundary, $u = \infty$ is the interior
$\underline{a}$	Locally flat index (denoted by underline)
z	Dynamical critical exponent
Γ	Bulk gamma matrix
γ	Boundary gamma matrix

Chapter 1

Introduction

A challenge facing contemporary condensed-matter physics is providing a general description of systems that are strongly coupled, in which the comprising degrees of freedom have interaction energies which are not low compared to their kinetic energies. Although approaches to calculating some of the observables of these systems exist, a general method is lacking. This is in contrast to weakly coupled systems, which are characterized by weakly interacting degrees of freedom to which perturbative methods can be applied ubiquitously. Generally, pictures based on perturbative techniques fail in the strongly coupled regime, prompting condensed-matter physicists to seek new angles of attack.

A surprising approach to this problem comes from string theory, in the form of the holographic duality. This duality can be used to understand strongly coupled quantum field theories by mapping them onto a higher-dimensional theory of classical gravity, which is generally more tractable. The holographic duality earns its name in relation to holograms, which depict a lower dimensional representation of a higher dimensional object, but is also referred to as the gauge/gravity duality.

Typically, the classical gravity theory is defined on an Anti-deSitter (AdS) spacetime and is dual to a strongly coupled quantum field theory (QFT) defined on the lower dimensional boundary of this spacetime. Pictorially,

$$\text{Classical gravity in AdS}_{d+1} \quad \longleftrightarrow \quad \text{Strongly coupled QFT in } \partial\text{AdS}_{d+1}.$$

The most prominent example of the holographic duality is the well-known AdS/CFT correspondence relating an AdS_5 geometry to a four-dimensional conformal field theory (CFT), which is[1] a scale-invariant quantum field theory. Currently, the correspondence has been extended in numerous directions and has found numerous applications in other areas of physics. Most notably, the holographic duality is applied to condensed-matter physics, under the banner "AdS/CMT" (Anti-deSitter/Condensed Matter Theory). This application is motivated by the observation that a system undergoing a quantum phase transition - a phase transition at zero temperature - becomes *scale invariant* at the quantum critical point (QCP), see Figure 1.1, and is hence governed by a conformal field theory. By attempting a dual description in terms of classical gravity, the aim of AdS/CMT is to describe the universal behavior near quantum critical points.

Away from the QCP, there is a region in the phase diagram where the quantum fluctuations are relevant compared to the thermal fluctuations present at non-zero temperature. Referred to as the quantum critical region (QCR), it is the region where the physics of the QCP is probed at a non-zero temperature. This explains how such critical points can be found in experiments, which cannot be performed at absolute zero.

---

[1] Every CFT is a scale-invariant QFT, but the reverse statement need not hold. There are a few exotic examples of quantum field theories invariant under scaling symmetry which are not invariant under the full conformal group. In this thesis, we will take scale invariance and conformal invariance to be the same.
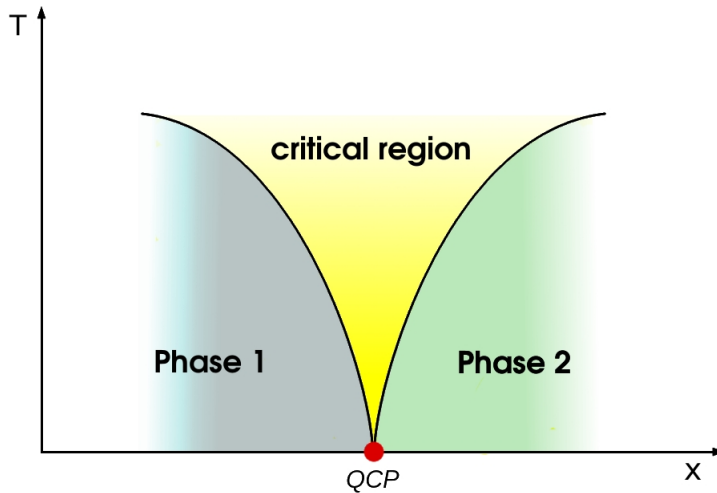
Figure 1.1: A sketch of a phase diagram showing a quantum phase transition with an associated quantum critical point (QCP) at zero temperature. At non-zero temperature, a (quantum) critical region extends over the quantum critical point. This figure is taken from ref. [1].

In this thesis we will study a specific gravitational model, the *electron star*, in the context of AdS/CMT. It is an Einstein-Maxwell-Dirac theory, which consists of charged fermions coupled to gravity, where the fermions are treated in a fluid limit. This model is aimed at providing a dual description of the quantum critical dynamics of fermionic systems at a non-zero charge density. A crucial aspect of the electron star is that, unlike many other models within AdS/CMT, the *backreaction* of the matter fields onto the metric is taken into account. That is, the matter fields explicitly appear in Einstein's equation and therefore affect the metric. Additional fermions are later added to the model, with the goal of calculating the *spectral function*. It is defined as

$$\rho\left(\omega, \mathbf{k}\right) = -\frac{1}{2\pi} \text{Im} \left[\text{Tr} \left[G_R\left(\omega, \mathbf{k}\right)\right]\right]$$

in terms of the retarded Green's function $G_R\left(\omega, \mathbf{k}\right)$, which we find by solving the fermion equations of motion in the electron-star background. Our approach here will be semi-holographic, which means we will add a term to the action *by hand*, yielding the free part of the Green's function which is not there in an ordinary holographic approach. The Green's function obtained this way can then be interpreted as a single-particle propagator.

The setup of the thesis is as follows. In Chapter 2, we will provide a brief introduction to the holographic duality and introduce a model, the Lifshitz black brane, as a warm-up exercise. Next, we will introduce the central model of this thesis, the electron star, and subsequently solve the model, in Chapter 3. In Chapter 4, we introduce additional fermions to the electron-star model and calculate the spectral function by solving the Dirac equation numerically. Finally, in Chapter 5, we turn to a conclusion and an outlook.

Chapter 2

Holography

In this chapter we provide an introduction to the holographic duality. We begin by introducing some key concepts, after which we discuss the AdS/CFT correspondence and its application to condensed-matter physics. This will lead us to consider the generalization of the holographic duality to anisotropic scale invariance, by means of the Lifshitz spacetime. There, we will consider an important model of a black hole in Lifshitz spacetime, referred to as the Lifshitz black brane, which is closely related to the electron-star model we will study in the next chapter.

2.1 The AdS/CFT correspondence

We provide a brief introduction to the AdS/CFT correspondence. First, we will thoroughly study the Anti-deSitter spacetime, after which we will introduce the AdS/CFT correspondence, discussing its essential structure. For more detailed introductions, we refer the reader to refs. [2],[3], and [4].

2.1.1 AdS spacetime

The central spacetime in the AdS/CFT correspondence is the Anti-deSitter (AdS) spacetime. Together with its cousin, the deSitter (dS) spacetime, it plays an important role in general relativity; these spaces are the vacuum solutions to Einstein's equations having constant positive (dS) or negative (AdS) curvature. One can think of them as the Lorentzian analogs of the sphere and the hyperboloid, respectively.

The deSitter spaces are maximally symmetric spaces, characterized by a Riemann tensor of the form

$$R_{\rho\sigma\mu\nu} = \alpha \left(g_{\rho\mu} g_{\sigma\nu} - g_{\rho\nu} g_{\sigma\mu} \right); \quad \alpha = \frac{R}{d \left(d+1 \right)},$$

see ref. [5], in $d+1$ dimensions. In particular, the Ricci tensor is proportional to the metric of the spacetime

$$R_{\mu\nu} = d\alpha g_{\mu\nu}$$

and hence, from Einstein's equation, the energy-momentum tensor

$$T_{\mu\nu} \equiv \frac{-2}{\sqrt{-g}} \frac{\delta S}{\delta g^{\mu\nu}}$$

is proportional to the metric as well

$$T_{\mu\nu} = -\frac{1}{2} d \left(d-1 \right) \alpha g_{\mu\nu}.$$

Such an energy-momentum tensor corresponds to a cosmological constant Λ, which is negative (positive) for $\alpha < 0$ ($\alpha > 0$), i.e. for negative (positive) curvature. The action for these spacetimes takes the form

$$S = \int d^{d+1}x \sqrt{-g}\,[R - 2\Lambda]\,.$$

Let us describe the Anti-deSitter spacetime, characterized by a negative Λ, more carefully as an embedding of a hyperboloid, allowing us to define coordinate frames. Consider the flat $(d+2)$-dimensional space described by the metric

$$ds^2 = -dX_0^2 - dX_{d+1}^2 + \sum_{i=1}^{d} dX_i^2$$

that embeds a hyperboloid given by the equation

$$-X_0^2 - X_{d+1}^2 + \sum_{i=1}^{d} X_i^2 = -\ell^2. \tag{2.1}$$

The constant ℓ, having the dimension of length, is called the AdS-radius (it is the radius of curvature). The set of coordinates

$$\begin{aligned}
X_0 &= \ell \cosh(\rho) \sin(t) \\
X_{d+1} &= \ell \cosh(\rho) \cos(t) \\
X_1 &= \ell \sinh(\rho) \cos\theta_1 \\
X_2 &= \ell \sinh(\rho) \sin\theta_1 \cos\theta_2 \\
&\vdots \quad \vdots \quad \vdots \\
X_d &= \ell \sinh(\rho) \sin\theta_1 ... \sin\theta_{d-1}
\end{aligned}$$

with $\rho \geq 0$ solves this constraint equation and induces a metric on the hyper-surface given by

$$ds^2 = \ell^2 \left(-\cosh^2(\rho)\,dt^2 + d\rho^2 + \sinh^2(\rho)\,d\Omega_{d-1}^2\right)$$

where $d\Omega_{d-1}^2$ is the metric on S^{d-1}. These coordinates[1] are global coordinates, i.e. they cover the entire spacetime.

An incredibly important property of the Anti-deSitter spacetime is that it admits a notion of a **boundary**, in the sense that spatial infinity is in causal contact with the interior of the spacetime. In particular, light rays can reach the boundary in finite time. The boundary is identified by conformal compactification, see ref. [5]. For this, one defines a new coordinate $\chi \in [0, \pi/2[$ related to ρ by

$$\cos\rho = \frac{1}{\cos\chi}.$$

Note that unlike ρ, the coordinate χ takes values in a finite (open) interval. The AdS metric in terms of χ takes the form

$$ds^2 = \frac{\ell^2}{\cos^2\chi}\left(-dt^2 + d\chi^2 + \sin^2\chi\, d\Omega_{d-1}^2\right). \tag{2.2}$$

In these coordinates, we can concretely identify the boundary of AdS spacetime as $\chi = \frac{\pi}{2}$ by compactification.

---

[1]Note that the time coordinate t is periodic, which allows for closed time-like curves [5]. The actual definition of AdS space is the covering space, which has the same metric but with t ranging from $-\infty$ to ∞.

Coordinate frames

We turn to two sets of coordinates parametrizing Anti-deSitter space which we will be important to us. For more details, we refer to ref. [6].

Begin by defining a new set of variables

$$
\begin{aligned}
a &= \frac{X_0 - X_d}{\ell^2} \\
b &= \frac{X_0 + X_d}{\ell^2} \\
x_i &= \frac{X_i}{\ell a} \\
t &= \frac{X_{d+1}}{\ell a}.
\end{aligned}
$$

In terms of these, equation (2.1) becomes

$$
\ell^2 = \ell^4 ab + \ell^2 a^2 \left(t^2 - x_i^2 \right)
$$

where $x_i^2 = \sum_i x_i^2$. This yields an equation for the coordinate b, which is reinserted in the equation for u and x_{d-1}. Transforming $a = \frac{1}{u}$ yields

$$
\begin{aligned}
X_0 &= \frac{1}{2u} \left(u^2 + x_i^2 + \ell^2 - t^2 \right) \\
X_{d+1} &= \frac{1}{2u} \left(u^2 + x_i^2 - \ell^2 - t^2 \right) \\
X_i &= \frac{\ell x_i}{u} \\
X_d &= \frac{\ell t}{u}.
\end{aligned}
$$

Then the metric takes the form

$$
ds^2 = \frac{\ell^2}{u^2} \left(-dt^2 + du^2 + dx_i^2 \right) \tag{2.3}
$$

where $u \in [0, \infty]$, which is referred to as the Poincaré form of the metric for the Anti-deSitter spacetime. We will refer to this system of coordinates simply as "u coordinates". The boundary of the spacetime is located at $u = 0$, and the interior is at $u = \infty$. Note that the boundary of the spacetime has a metric isomorphic to the Minkowski metric. It is the notion of a boundary which looks like Minkowski space that will play a crucial role in the AdS/CFT correspondence.

Another important coordinate system is obtained from the Poincaré metric simply by transforming

$$
u^2 = \frac{\ell^4}{r^2} \tag{2.4}
$$

and has the metric

$$
ds^2 = -\frac{r^2}{\ell^2} dt^2 + \frac{\ell^2}{r^2} dr^2 + \frac{r^2}{\ell^2} dx_i^2. \tag{2.5}
$$

We refer to this system of coordinates as "r coordinates". The radial coordinate r also ranges between 0 and infinity, but the boundary is at $r = \infty$ while the interior of the spacetime is at $r = 0$.

Transformations between coordinates

As will be explained in the next section, we will be concerned with *asymptotically* AdS spaces, which asymptote the pure AdS metric in the form (2.3) or (2.5) far away from the origin. In particular, we will consider a metric of the form

$$
ds^2 = -\tilde{f}(r) \frac{r^2}{\ell^2} dt^2 + \tilde{g}(r) \frac{\ell^2}{r^2} dr^2 + \frac{r^2}{\ell^2} dx_i^2 \tag{2.6}
$$

in r coordinates, with $\tilde{f}(r), \tilde{g}(r) \to 1$ as $r \to \infty$. We will also consider an asymptotically AdS metric in u coordinates, which we write down as

$$ds^2 = -\ell^2 f(u) \, dt^2 + \ell^2 g(u) \, du^2 + \frac{\ell^2}{u^2} dx_i^2, \tag{2.7}$$

i.e. the functions $f(u)$ and $g(u)$ do not asymptote 1 but rather u^{-2}. By transforming from the u to the r coordinate frame, using equation (2.4), one easily verifies that these functions are related by

$$
\begin{aligned}
f(u(r)) &= \frac{r^2}{\ell^4} \tilde{f}(r) \\
g(u(r)) &= \frac{r^2}{\ell^4} \tilde{g}(r)
\end{aligned}
\tag{2.8}
$$

This will be crucial later: this coordinate transformation is employed between Chapter 3 and Chapter 4, where we change from a metric of the form (2.7) to one of the form (2.6) .

2.1.2   The holographic duality

Roughly put, the holographic duality is an equivalence between non-gravitational quantum field theories and higher-dimensional gravity. In particular limits, the quantum field theory becomes strongly coupled while the dual gravity theory becomes classical. This is incredibly useful, as the conventional perturbative methods fail in the strongly coupled regime of QFTs, making them hard to describe. We will briefly cover the essential structure of this correspondence, skipping the string theoretical considerations. For a more thorough introduction, we refer the reader to refs. [2, 4].

The AdS/CFT correspondence embodies a realization of two fundamental concepts in theoretical physics. The first of these is the 't Hooft limit of quantum field theories. In order to illustrate this concept, consider the $SU(N)$ Yang-Mills theory described by the Lagrangian

$$\mathcal{L} = -\frac{1}{g^2} \text{Tr} \left[F^2 \right]$$

with the non-abelian field strength tensor $F_{\mu\nu} = \partial_\mu A_\nu - \partial_\nu A_\mu + [A_\mu, A_\nu]$. One can rewrite this as

$$\mathcal{L} = -\frac{N}{\lambda} \text{Tr} \left[F^2 \right]$$

by defining the 't Hooft coupling $\lambda = g^2 N$. The 't Hooft limit now consists of taking a large number of "colors" $N \to \infty$, the large N limit, and a small coupling $g \to 0$ while keeping λ fixed. The parameter N then organizes the amplitudes by topology; a diagram with E propagators, V vertices and F loops has a contribution

$$N^\chi \lambda^{E-V}$$

where $\chi = F - E + V$ is the Euler characteristic of the simplest surface triangulated by the diagram - see ref. [4]. In this limit, only the "planar" diagrams having $\chi = 2$ remain. Further, the full partition function becomes a sum over topologies, precisely as in the perturbative expansion of string theory. The forms of the partition functions are the same and the connection is made more explicit by identifying

$$g_s = N^{-1},$$

where g_s is the string coupling constant.

The second concept is the holographic principle in quantum gravity, which states that a given region of space can be described by a theory living on the boundary of that space. In black hole thermodynamics, for example, the entropy of a black hole is proportional to the area of the black hole,

rather than the volume. This concept is realized in the AdS/CFT correspondence, which is why it is also referred to as a holographic duality.

The original formulation, ref. [7], of the AdS/CFT correspondence involved type IIB string theory on $AdS_5 \times S^5$ and $\mathcal{N} = 4$ supersymmetric Yang-Mills theory, which is a conformal field theory. In the large N limit, g becomes small at a fixed 't Hooft coupling and the CFT becomes strongly coupled, while the string theory with $g_s = N^{-1}$ becomes classical gravity. This is an example of a holographic - or gauge/gravity - duality with a very high degree of symmetry. More examples have been found, and it is believed that the duality holds more generally, also for field theories without supersymmetry. The general duality, which we refer to as "the" holographic duality, relates classical gravity in $d + 1$ dimensional spacetime to a strongly coupled quantum field theory living in d dimensional spacetime. Typically, the gravity theory is on some $d + 1$ dimensional Anti-deSitter space, and the quantum field theory is said to live on the boundary (see section 2.1.1) of this spacetime.

The extra spatial dimension of the gravitational theory corresponds to the energy scale of the quantum field theory, i.e. the energy scale is placed on an equal footing with the other spatial dimensions of the field theory, see for instance ref. [2]. Invoking wisdom from the theory of the renormalization group (RG), we learn that the coupling constants g of the field theory depend on the energy scale r, evolving according to the RG flow equation

$$r \frac{\partial g}{\partial r} = \beta\left(g\right).$$

At the **critical point**, the field theory is scale invariant, which implies $\beta = 0$. Thus, the scale transformation

$$x^\mu \to \lambda x^\mu$$

is a symmetry. Insisting on the interpretation of r as an energy scale, we find it should transform as

$$r \to \frac{r}{\lambda}$$

under the scaling transformation. Thus, the complete set of coordinates, including r, can be combined into a $(d + 1)$-dimensional spacetime with the metric

$$ds^2 = \left(\frac{r}{\ell}\right)^2 \eta_{\mu\nu} dx^\mu dx^\nu + \frac{\ell^2}{r^2} dr^2.$$

This describes an AdS_{d+1} spacetime; it is precisely the metric in the form (2.5). The above considerations can be compressed into the saying "The AdS/CFT correspondence geometrizes the energy scale", and also in the "geek joke" $[G, R] = 0$, see ref. [8]. The different energy scales of the system foliate the higher-dimensional spacetime. The high-energy physics is encoded at the boundary of the space-time at $r = \infty$, while the low-energy physics is encoded in the interior of the spacetime at $r = 0$. These regimes are referred to as the ultra-violet (UV) and the infrared (IR) of the spacetime. See Figure 2.1.

Although the critical point provides a natural place to begin with the identification of a gravitational dual, deformations away from criticality are possible. This can be done, for instance, by considering ensembles such as a non-zero temperature or chemical potential, or by deforming the theory by relevant operators, ref. [3]. These effects break the scale invariance of the spacetime, but we expect this symmetry to recover at energies well above the characteristic energy scale of the deformation. That is, in the UV-limit, we expect to obtain a scale-invariant theory again. In the language of general relativity, the spacetime should be asymptotically Anti-deSitter, thus ensuring scale-invariance on the boundary.
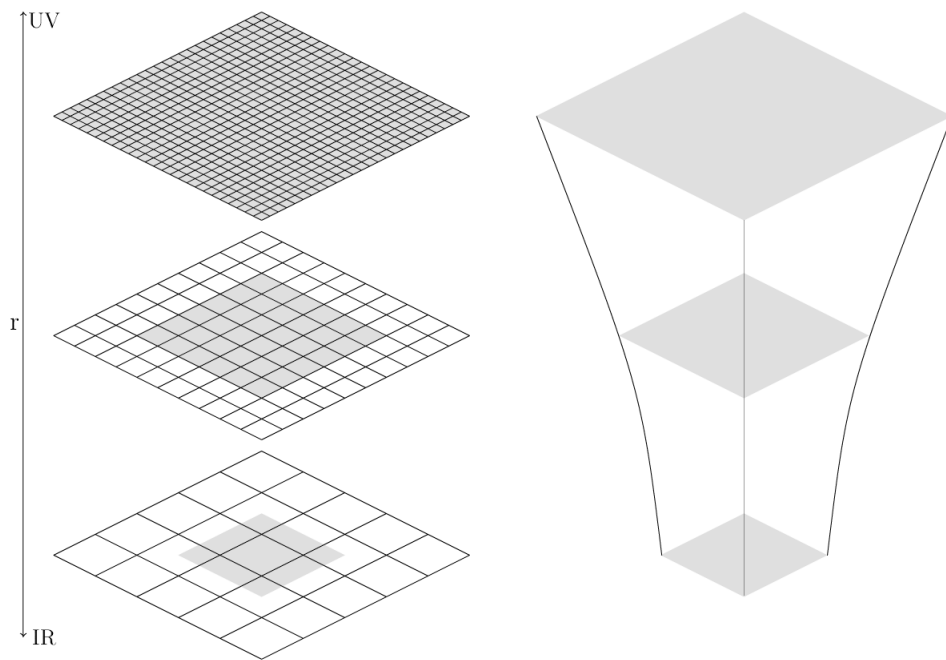
Figure 2.1: A sketch of the geometric realization of the QFT resolution scale. The resolution scale introduces a length scale in the QFT which is interpreted as an extra dimension. The total spacetime, including this extra dimension, is a curved spacetime, as depicted on the right. This figure is based on a figure from ref. [4].

The dictionary

As we have mentioned, the holographic duality entails a correspondence between events or quantities in the theories on both sides. In particular, there is a dictionary which translates between the physics of the boundary field theory and the bulk gravity theory. The core of this dictionary is the so-called GPKW-rule, which essentially tells us that the partition functions of the field theory and the gravity theory coincide. Let us consider this in more detail.

In the field theory one has the partition function, or the generating functional, given by

$$\mathcal{Z}_{\mathrm{QFT}}\left[\phi_0\right] = \int \mathcal{D}A \exp\left[i\left(S_{\mathrm{QFT}} + \int d^d x\, \phi_0 \mathcal{O}\left(A\right)\right)\right],$$

where A denotes all of the fundamental fields in the QFT, and where S_{QFT} is the action of the QFT. This generating functional is used to compute expectation values of the operator $\mathcal{O}\left(A\right)$, by differentiating with respect to ϕ_0. The field ϕ_0 is said to "source" the operator $\mathcal{O}\left(A\right)$.

In the context of the AdS/CFT correspondence, the source ϕ_0 is promoted from a fixed field on the boundary of AdS spacetime to a dynamical field in the bulk, which is governed by its own action. This field, $\phi_0\left(x,r\right)$, becomes $\phi_0\left(x\right)$ precisely on the boundary. The fundamental rule of holography, the GKPW rule (after Gubser, Klebanov, Polyakov, and Witten), then relates the partition functions by

$$\mathcal{Z}_{\mathrm{QFT}}\left[\phi_0\right] = \mathcal{Z}_{\mathrm{QG}}\left[\phi\big|_{\partial\mathrm{AdS}}\right],$$

where "QG" stands for quantum gravity. In the large N limit, the bulk partition function can be treated in a saddle point approximation, from which we find

$$\mathcal{Z}_{\mathrm{QFT}}\left[\phi_0\right] \approx e^{iS_c}\big|_{\phi\to\phi_0}, \tag{2.9}$$

where S_c is the classical, or "on-shell", bulk action providing the dominant contribution to the path integral.

In general, fields in the bulk correspond to sources of operators in the field theory. The simplest examples are scalar and fermionic fields

$$\phi, \psi \leftrightarrow \mathcal{O}_s, \mathcal{O}_f \tag{2.10}$$

which correspond to scalar and fermionic operators, respectively. In general, tensor fields correspond to tensor operators. For example

$$A_\mu \leftrightarrow J_\mu \tag{2.11}$$

and

$$g_{\mu\nu} \leftrightarrow T_{\mu\nu}. \tag{2.12}$$

This is the first example of a dictionary rule relating both sides of the duality. Another important dictionary rule concerns the symmetries of the gravity theory and the dual quantum field theory. The symmetry group of AdS_{d+1} is $\mathrm{SO}\left(d,2\right)$, as is clear from equation (2.1). This is precisely the symmetry group of a d dimensional CFT, as its generators satisfy the $\mathfrak{so}\left(d,2\right)$ algebra, see ref. [9]. The dictionary then relates *local* symmetries in the bulk to *global* symmetries on the boundary. For example, consider the $U\left(1\right)$ gauge field A_μ, dual to the current J^μ in the boundary field theory. Then the local $U\left(1\right)$ symmetry in the bulk implies the conservation $\partial_\mu J^\mu = 0$, by partial integration, hence a global $U\left(1\right)$ symmetry on the boundary. Similarly, invariance under local coordinate transformations implies the conservation $\partial_\mu T^{\mu\nu} = 0$ associated with global Poincaré symmetry on the boundary. Other dictionary rules are listed in Table 2.1.

Bulk	Boundary
Scalar field ϕ	Scalar operator $\mathcal{O}_s$
Fermionic field ψ	Fermionic operator $\mathcal{O}_\psi$
Vector field A_μ	Current operator J_μ
Spacetime metric $g_{\mu\nu}$	Energy-momentum tensor $T_{\mu\nu}$
Field boundary value (properly (re)normalized)	Source of operator
Local isometry/gauge symmetry	Global symmetry
Hawking temperature (black hole)	Temperature

Table 2.1: The AdS/CFT dictionary rules

2.1.3 Condensed matter

Although discovered in the context of string theory, the AdS/CFT correspondence has applications far beyond this field alone. One application is in quantum chromodynamics (QCD), under the banner "AdS/QCD". One physical system studied using this correspondence is the quark-gluon plasma, which is a phase of QCD consisting of free quarks and gluons. Especially in the case of a strongly coupled plasma, the idea is that the holographic duality can be used to gain insight.

A second example is the field of condensed-matter physics, which is the application we will focus on in this thesis. In order to motivate this application, we begin by investigating quantum phase transitions. By definition, these are (continuous) transitions between phases of matter that occur at zero temperature. In contrast, all non-zero temperature phase transitions are referred to as classical. In classical phase transition, the physical state of the system is changed by thermal fluctuations. The quantum phase transitions, on the other hand, are driven solely by quantum fluctuations. It is the occurrence of fluctuations at zero temperature that explains the nomenclature "quantum".
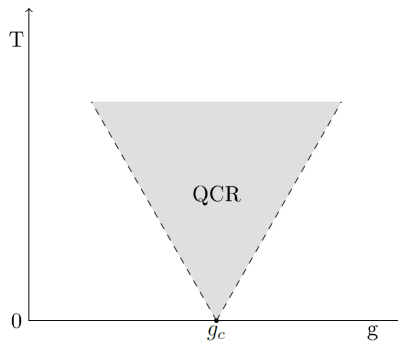

Figure 2.2: Sketch of a typical quantum phase diagram with a quantum phase transition driven by the parameter g. The quantum critical point is at g_c, above which the shaded quantum critical region (QCR) extends at non-zero temperature.

Just as their classical counterparts, quantum phase transitions are at a critical point, which is referred to as the quantum critical point (QCP). At this point, the system exhibits universal behavior; various quantities of interest diverge or vanish according to power laws, in terms of so-called critical exponents. These exponents can be identical for systems having completely different microscopic degrees of freedom, in which case the two systems are said to be in the same universality class.

A particularly important quantity in this respect is the correlation length ξ, which is a typical length scale in the system of interest. For example, this could the length scale determined by the

exponential decay of equal time correlations in the ground state. Another important quantity is the energy scale Δ, which could be given by the energy gap in the system. When tuning the driving parameter g towards the critical point g_c, these quantities typically exhibit the power law behavior [2]

$$\begin{aligned}\Delta &\sim |g - g_c|^{\nu} \\ \xi^{-1} &\sim |g - g_c|^{\nu},\end{aligned}$$

i.e. the energy gap vanishes while the correlation length diverges at the critical point. The latter implies that the system looks the same on all length scales; the system is said to be *scale invariant*. It is this scale invariance that causes the system to exhibit universal behavior, as it effectively averages over microscopic degrees of freedom.

At zero temperature, there are no thermal fluctuations, so any phase transition is purely driven by quantum fluctuations having a typical energy $\hbar\omega$. Here, ω the frequency associated with the correlation time, which is a typical time scale of the system. At non-zero temperature, there are thermal fluctuations with an energy scale $k_B T$. Any phase transition at a non-zero temperature is a classical phase transition because the thermal fluctuations always dominate close enough to the critical point. Again, the diverging correlation length washes out the microscopic quantum details, and the thermal fluctuations dominate on larger scales that control the critical behavior.

In the quantum critical region (QCR), see Figure 2.2, the energy scale of the quantum fluctuations $\hbar\omega$ is roughly less than the energy scale of the thermal fluctuations $k_B T$. In this region, $g \approx g_c$, but due to the non-zero temperature the system is not at the quantum critical point, see ref. [10]. Thus, the system prefers the quantum critical ground state, characterized by an absence of quasi-particle excitations, but is constantly thermally excited. Thus, the physics in the quantum critical region is unusual: the system can exhibit, for example, unusual finite-temperature properties or non-Fermi liquid behavior.

Scale invariance at the quantum critical point implies[3] that the theory governing the system becomes conformal. This is a natural place to start with the application of the AdS/CFT correspondence, as we have mentioned. Then, following our discussion in section 2.1.2, specifically the dictionary in table 2.1, one might consider deformations of the dual gravity theory in order to describe (the universal behavior of) a given system. By adding a charged black hole to the spacetime, for instance, one can aim at a dual description of a system at a non-zero temperature and chemical potential.

2.2 Lifshitz Holography

In this section, we will consider an important extension of the holographic duality applied to condensed matter. It is the generalization towards anisotropic scale invariance, providing a more realistic picture of condensed matter. We will be lead to the Lifshitz spacetime, after which we consider a specific model in the resulting Lifshitz holography.

2.2.1 Anisotropic scale invariance

In the previous section we have seen how the holographic duality can be applied to strongly coupled systems in condensed-matter physics. However, the focus was on a very specific class of systems. Namely, we considered systems in which the correlation time and the correlation length diverged with the same exponent, referred to as isotropic scale invariance. More often that not, systems in condensed

---

[2]This is not the most general power law behavior near the critical point. The more general case, where $\Delta \sim |g - g_c|^{z\nu}$ while $\xi^{-1} \sim |g - g_c|^{\nu}$, is discussed in the next section.

[3]Strictly speaking, scale invariance does not imply conformal invariance. However, we will not concern ourselves with the precise difference here, as counterexamples are generally exotic.

matter have an anisotropic scale invariance at the quantum critical point. That is, the energy scale typically vanishes as

$$\Delta \sim |g - g_c|^{z\nu},$$

while the length scale diverges as

$$\xi^{-1} \sim |g - g_c|^{\nu}$$

near the critical point $g = g_c$. This implies

$$\Delta \sim \xi^{-z},$$

which yields an anisotropy between time and space, measured by the so called dynamical critical exponent z. In particular, such systems have a scaling symmetry

$$t \to \lambda^z t, \qquad \mathbf{x} \to \lambda \mathbf{x}. \tag{2.13}$$

The case $z = 1$ corresponds to a conformal field theory which can be considered to live on the boundary of AdS spacetime, dual to a gravitational theory in the AdS bulk. These correspond to *relativistic* systems at a quantum critical point, as the dispersion relations of excitations there are linear in momentum; $E \sim \mathbf{p}$. The generalization to a general z takes us towards *non-relativistic systems*, in particular the case $z = 2$, where the dispersion relation becomes $E \sim \mathbf{p}^2$. Including such non-relativistic systems in the holographic duality necessitates a different bulk gravitational theory, which is called the **Lifshitz spacetime**.

By requiring the boundary field theory to be invariant under temporal and spatial translation, spatial rotations, spatial parity and time-reversal, one finds a metric

$$ds^2 = -\frac{r^{2z}}{\ell^{2z}} dt^2 + \frac{\ell^2}{r^2} dr^2 + \frac{r^2}{\ell^2} dx_i^2, \tag{2.14}$$

which is invariant under the anisotropic scaling

$$t \to \lambda^z t, \quad \mathbf{x} \to \lambda \mathbf{x}, \quad r \to \lambda^{-1} r.$$

This metric was first found in ref. [11]. From the expression for the metric, one sees that towards the boundary at $r = \infty$, the metric component g_{tt} diverges faster than the components g_{ii} when $z > 1$. Thus, the light-cones flatten out, yielding a diverging effective speed of light, as expected for non-relativistic theories. The case $z = 1$ corresponds to the AdS metric in r coordinates, equation (2.5), and corresponds to a relativistic system.

Having obtained the desired boundary scaling behavior, our goal is to find a bulk action S which is minimized by a Lifshitz metric. This action consists of an Einstein-Hilbert action with a negative cosmological constant and a matter action S_M coupled to gravity. It turns out, see refs. [12, 13], that the matter action

$$S_M = \frac{-1}{4\kappa^2} \int d^{d+1}x \sqrt{-g} \left[(\nabla_\mu \phi)^2 + \frac{1}{2} e^{\lambda \phi} F_{\mu\nu} F^{\mu\nu} \right],$$

in terms of a dilaton field ϕ and an antisymmetric field strength tensor $F_{\mu\nu}$, produces a vacuum Lifshitz spacetime. Note that the matter fields are not meant to have a physical interpretation. Instead, they are solely introduced to obtain the correct boundary scaling behavior. The full action is given by

$$S = \frac{1}{2\kappa^2} \int d^{d+1}x \sqrt{-g} \left[R - 2\Lambda - \frac{1}{2} (\nabla_\mu \phi)^2 - \frac{1}{4} e^{\lambda \phi} F_{\mu\nu} F^{\mu\nu} \right]$$

where $\kappa^2 = 8\pi G_{d+1}$ is proportional to the Newton constant in $d+1$ dimensions. The resulting equations of motion are

$$R_{\mu\nu} + \left(\Lambda - \frac{1}{2} R \right) g_{\mu\nu} = T_{\mu\nu} \tag{2.15}$$

$$\nabla_\mu \left(e^{\lambda \phi} F^{\mu\nu} \right) = 0 \tag{2.16}$$

$$\Box \phi - \frac{1}{4} \lambda e^{\lambda \phi} F_{\mu\nu} F^{\mu\nu} = 0. \tag{2.17}$$

with

$$T_{\mu\nu} = \frac{1}{2}\partial_\mu\phi\partial_\nu\phi - \frac{1}{4}\left(\partial\phi\right)^2 g_{\mu\nu} + \frac{1}{2}e^{\lambda\phi}\left[F_{\mu\sigma}F_\nu{}^\sigma - \frac{1}{4}F^2 g_{\mu\nu}\right].$$

2.2.2 The Lifshitz black brane

We turn to an important model for this thesis, the Lifshitz black brane. It is a model of a black hole with planar topology on top of a Lifshitz spacetime. Of course, the presence of the black hole distorts the curvature of the Lifshitz spacetime. As discussed in section 2.1.2, we are interested in a resulting spacetime with a metric that asymptotes the Lifshitz metric (2.14).

Of particular importance to us is the *charged* Lifshitz black brane, which we will study in more detail here, broadly following ref. [12]. The Lifshitz black brane has been used in the context of holography in refs. [14, 15]. In this model, the metric is given by

$$ds^2 = -\frac{V^2\left(r\right)r^{2z}}{\ell^{2z}}dt^2 + \frac{\ell^2}{V^2\left(r\right)r^2}dr^2 + \frac{r^2}{\ell^2}dx_i^2 \tag{2.18}$$

where $V\left(r\right)$ is referred to as the emblackening factor. The black hole has a horizon r_h where $V\left(r_h\right) \to 0$, while $V \to 1$ on the boundary at $r = \infty$. The action for the charged black brane is the Lifshitz action with an additional gauge field coupled to the dilaton, i.e.

$$S = \frac{1}{2\kappa^2}\int d^{d+1}x\,\sqrt{-g}\left[R - 2\Lambda - \frac{1}{2}\left(\nabla_\mu\phi\right)^2 - \sum_i \frac{1}{4}e^{\lambda\phi}F_{i,\mu\nu}F^{i,\mu\nu}\right], \tag{2.19}$$

where $F_{1,\mu\nu}$ is the (unphysical) gauge field of the Lifshitz action and $F_{2,\mu\nu}$ is a physical gauge field, to which other fields can couple. For simplicity, it is assumed that $A_{i,t}$ is the only non-zero component of $A_{i,\mu}$, and that it only depends on the radial coordinate r. The equations of motion for this model are given by

$$R_{\mu\nu} - \frac{2\Lambda}{d-1}g_{\mu\nu} - \frac{1}{2}\partial_\mu\phi\partial_\nu\phi - \frac{1}{2}\sum_i e^{\lambda_i\phi}\left[\left(F_i\right)_{\mu\sigma}\left(F_i\right)_\nu{}^\sigma - \frac{1}{2\left(d-1\right)}F_i^2 g_{\mu\nu}\right] = 0 \tag{2.20}$$

$$\nabla_\mu\left(e^{\lambda_i\phi}F_i^{\mu\nu}\right) = 0 \tag{2.21}$$

$$\Box\phi - \frac{1}{4}\sum_i \lambda_i e^{\lambda_i\phi}F_i^2 = 0, \tag{2.22}$$

where the first equation is obtained by tracing (2.15), eliminating R. We proceed to solve these equations exactly, following ref. [12].

In the following, we denote Einstein's equation by $E_{\mu\nu}$. We begin by subtracting E_r^r from E_t^t, which leaves only

$$R_t^t - R_r^r + \frac{1}{2}g^{rr}\partial_r\phi\partial_r\phi = 0.$$

This particular linear combination is useful as several Riemann tensor components cancel. One finds

$$R_t^t - R_r^r = g^{tt}R^i{}_{tit} - g^{rr}R^i{}_{rir}$$
$$= \frac{\left(d-1\right)\left(1-z\right)V^2\left(r\right)}{\ell^2},$$

and hence

$$r^2\phi'^2 = 2\left(d-1\right)\left(z-1\right) \Rightarrow e^\phi = \alpha r^{\sqrt{2(d-1)(z-1)}}$$

where α is an integration constant. Next, setting $\nu = t$ in Maxwell's equation,

$$
\begin{aligned}
0 &= \lambda_i \partial_r \phi F_i^{rt} + \partial_\mu F_i^{\mu t} + \Gamma_{\mu\alpha}^\mu F_i^{\alpha t} \\
&= \partial_r F_i^{rt} + F_i^{rt} \left(\lambda_i \partial_r \phi + \frac{z + d - 2}{r} \right).
\end{aligned}
$$

Substituting the solution for ϕ, one finds

$$
(F_i)_{rt} = \rho_i r^{z-d} e^{-\lambda_i \phi},
$$

where the ρ_i are integration constants.

Having solved the matter fields, we determine the emblackening factor and the cosmological constant Λ. By entering the solutions for ϕ and F_i, E_{ii} becomes

$$
R_{ii} - \frac{r^2}{\ell^4} \left(\frac{2\Lambda\ell^2}{d-1} + \frac{r^{2(1-d)}\ell^{2z}}{2(d-1)} \sum_i \rho_i^2 r^{-\lambda_i\sqrt{2(d-1)(z-1)}} \right) = 0
$$

Then, one easily computes $R_{ii} = \frac{r^2}{\ell^4}\left((1-d-z)V^2 - 2rVV' \right)$ and substitutes it in the above equation to find a differential equation solved by

$$
V^2(r) = -\frac{2\Lambda\ell^2}{(d-1)(1-z-d)} - Mr^{1-z-d} + \frac{\ell^{2z}}{2(d-1)} \sum_i \frac{\rho_i^2 \alpha^{-\lambda_i} r^{2(1-d)-\lambda_i\sqrt{2(d-1)(z-1)}}}{d-z-1+\lambda_i\sqrt{2(d-1)(z-1)}}.
$$

Here, M is yet another integration constant. The final equation of motion is a combination of the dilaton equation of motion and the remaining Einstein equations, cast in the form

$$
4\Lambda\sqrt{2(d-1)(z-1)} = \ell^{2(z-1)} r^{-2(d-1)} \sum_i \rho_i^2 r^{-\lambda_i\sqrt{2(d-1)(z-1)}} \alpha^{-\lambda_i} \left[(d-1)\lambda_i - \sqrt{2(d-1)(z-1)} \right].
$$

If we pick

$$
\lambda_1 = -\sqrt{2\frac{d-1}{z-1}}, \quad \rho_1^2 = -4\Lambda\alpha^{-\lambda_1}\ell^{2(1-z)}\frac{z-1}{d+z-2},
$$

the first term in the sum will equal the left hand side, which in turn implies that the second term on the right hand side must vanish. This happens when

$$
\lambda_2 = \sqrt{2\frac{z-1}{d-1}}.
$$

Note that while ρ_1 is fixed, ρ_2 is still a free parameter, interpreted as the charge density of the black brane - see [12]. Requiring an asymptotically Lifshitz space, we take the limit $r \to \infty$ of the emblackening factor V

$$
\lim_{r\to\infty} V^2(r) = \frac{2\Lambda\ell^2}{(d-1)(1-z-d)} - \frac{2\Lambda\ell^2(z-1)}{(d-1)(d+z-2)(1-z-d)}
$$

and require it to be unity. This yields

$$
\Lambda = -\frac{(d+z-1)(d+z-2)}{2\ell^2}. \tag{2.23}
$$

The solution for $V^2(r)$ can now be written

$$
V^2(r) = 1 - Mr^{1-z-d} + \frac{\ell^{2z}\rho_2^2\alpha^{\sqrt{\frac{d-1}{2(z-1)}}}}{2(d-1)(d+z-3)} r^{-2(d+z-2)}. \tag{2.24}
$$

It is interesting to consider the special case of $z = 1$, $\phi = 0$. In this case, we retrieve the asymptotically Anti-deSitter Reissner-Nordström (AdS-RN) solution. The emblackening factor is given by

$$V^2(r) = 1 - Mr^{-d} + \frac{\ell^2 \rho_2^2 r^{2(1-d)}}{2(d-1)(d-2)}, \tag{2.25}$$

while the gauge field A_2 satisfies

$$A'_{2,t} = \rho_2 r^{1-d}. \tag{2.26}$$

This is a solution of a charged black hole which asymptotes Anti-deSitter spacetime far away from the origin.

As mentioned above, when fermions are added to the bulk spacetime, they can couple to the gauge field $A_{2,\mu}$ of the black brane. In particular, the covariant derivative for the fermions[4] becomes

$$\nabla_\mu \to \nabla_\mu - iqA_{2,\mu}$$

via a minimal coupling scheme. Upon a Fourier transform, this means

$$\begin{aligned} \mathbf{k} &\to \mathbf{k} \\ \omega &\to \omega + qA_{2,t}(r), \end{aligned}$$

assuming $A_{2,i} = 0$ as above. On the boundary, this means that

$$\omega \to \omega + \lim_{r \to \infty} qA_{2,t}(r),$$

where the second term is interpreted as a chemical potential. Thus, charging the black brane and adding charged fermions to the bulk corresponds to a chemical potential of the boundary. Considering table 2.1, this makes sense, as a chemical potential μ is associated to a global $U(1)$ symmetry, while $A_{2,\mu}$ is associated to a local $U(1)$ symmetry.

The black brane versus the electron star

This brings us to a distinction between the Lifshitz black brane model and the electron-star model we will study in this thesis. In the black brane model, the fermions couple to the gauge field but they do not backreact onto the metric, i.e. they are treated in a probe limit. Thus, one can still use the expression (2.18) for the metric, as the fermions do not affect it in this limit. In the electron-star model, the backreaction of the fermions *is* taken into account - albeit in a fluid approximation to be explained in the next chapter - so we will go beyond the probe limit. The reason for doing this is the fact that the Lifshitz black brane model has non-zero entropy at zero temperature, see ref. [3], which is unwanted from the point of view of field theory. By invoking the fermion fluid approximation, a vanishing entropy at absolute zero is guaranteed.

We will focus mainly on the electron star in an Anti-deSitter spacetime, rather than a Lifshitz spacetime. This means that our model will not produce a dual description of critical points with anisotropic scale invariance. Although we will build towards the Lifshitz electron star, discussing the equations of motion of this model in Appendix C, we will leave the full generalization for future work.

---

[4]We will mention the precise definition of the covariant derivatives for spinors in Chapter 4

Chapter 3

The electron star

In this chapter we study a holographic model called the electron star, which is an Einstein-Maxwell-Dirac theory in which the fermions are treated in a fluid limit. In light of the AdS/CFT correspondence, we will be interested in finding a spacetime that asymptotes Anti-deSitter spacetime, but which is deformed in the bulk due to the backreaction of the fermion fluid onto the geometry.

We begin by addressing the origin of this model, and study the fluid limit of the fermions. Next, we derive the equations of motion pertaining to the electron star, where we will find one of them to be solved trivially. The remaining equations are solved numerically and the subsequent results are discussed. In this chapter, we will broadly follow ref. [16], generalizing the discussion to an arbitrary spacetime dimension.

3.1   The model

Our goal is to study, by means of the holographic duality, quantum field theories with fermionic degrees of freedom at a non-zero charge density, becoming strongly coupled near a quantum critical point. As we have seen in the previous chapter, this desired additional structure necessitates a deformation of the dual spacetime geometry. In particular, the dictionary rules (2.1) hint at a model of charged fermions in an Anti-deSitter background. Thus, we start our investigation from the model

$$\mathcal{Z} = \int \mathcal{D}\left[g, A, \Psi\right] e^{i(S_g + S_A + S_\Psi)}$$

where

$$
\begin{aligned}
S_g &= \frac{1}{2\kappa^2} \int d^{d+1}x \sqrt{-g}\,(R - 2\Lambda) \\
S_A &= -\frac{1}{4e^2} \int d^{d+1}x \sqrt{-g}\,F_{\mu\nu}F^{\mu\nu},
\end{aligned}
$$

are the Anti-deSitter and Maxwell actions. In these actions, $\kappa^2 = 8\pi G_{d+1}$ is the gravity coupling in $d + 1$ dimensions, while e is the Maxwell coupling. Finally, S_Ψ is the Dirac action for fermions in curved spacetime, which describes fermions coupled to gravity as well as the gauge field A. We will postpone an in-depth discussion of this action to Chapter 4, as we will not need it explicitly here.

In the large N limit, classical gravity suffices, allowing us to approximate the path integral by employing a saddle-point approximation applied to the metric g and the Maxwell gauge field A. This yields

$$\mathcal{Z} \approx \int \mathcal{D}\psi e^{i\left(S_g^{\text{cl}} + S_A^{\text{cl}} + S_\Psi\right)},$$

where the gravity and the Maxwell actions S_g and S_A are taken on-shell. This way we only retain the full quantum nature of the fermionic field. This model is referred to as the quantum electron star [17]. Even this simplified model is quite hard to solve[1], so we invoke an approximation called the *fluid approximation*. In this approximation, the model is referred to as the **electron star** and it is this model we will study intensively here. The fluid approximation consists of taking a limit in which the number of fermions per AdS radius ℓ is infinite, while ϵ_F/m is held fixed, ϵ_F being the Fermi energy - see ref. [18]. This implies that the length scale set by the variations of the fermionic fields is very small compared to the length scale set by the curvature of the space, so that

$$m\ell \gg 1.$$

Each fermion "sees" a flat spacetime, which means we can invoke the flat space expressions for an ideal Fermi gas. The effect of gravity is only noticeable by comparing different points, and is subsumed in some parameter. This approximation mirrors the Local-Density Approximation (LDA) familiar in statistical field theory, used to describe atoms in a spatially slowly varying trapping potential. In this approximation, the spatially varying nature of the trapping potential can be subsumed in a *local* chemical potential, see ref. [19]. Other quantities describing the particles can then be calculated from their ordinary expressions with a constant trapping potential, where only the chemical potential is replaced by the local chemical potential. In our case, the metric itself plays the role of the trapping potential, and the effects of the curvature are subsumed in the chemical potential describing the fermion fluid. The local-density approximation and its application to our curved spacetime is discussed in more detail in appendix A .

In the fluid approximation, the Dirac action S_D is replaced by an effective action

$$S_\Psi^{\text{eff}} = \int d^{d+1}x \sqrt{-g}\, p,$$

where p is the pressure of the fermion fluid. We will show shortly that this action can yield a perfect fluid energy-momentum tensor when varied with respect to the metric. It is this action, together with S_A and S_g, that will provide the equations of motion which are solved throughout the rest of this chapter.

3.1.1   The perfect fluid

We describe the perfect fluid of fermions in the local-density approximation, at zero temperature. We will focus on the zero-temperature case throughout this thesis, although we will mention the generalization to non-zero temperature in section *3.2*. The parameters of the fermion fluid are the pressure p, the energy density ρ, and the charge density σ. In **flat** space, the energy and charge densities are given by the familiar expressions

$$\rho_f = \int_m^\mu E g(E)\, dE, \quad \sigma_f = \int_m^\mu g(E)\, dE,$$

where $g(E)$ is the density of states, m is the mass of the fermion, and μ is the chemical potential. In these expressions, we integrate from the minimal energy m to the Fermi energy ϵ_F which is given by the chemical potential at zero temperature. The density of states for a relativistic fermion gas in $(d+1)$-dimensional spacetime

$$g(E) = \beta_{d+1} E \left(E^2 - m^2\right)^{(d-2)/2}, \tag{3.1}$$

---

[1]The reason is that the dominant contribution (via the on-shell actions) of this path integral involves solving the equations of motion, which in this case involve a fermionic energy-momentum tensor and a current which are non-local functionals. It is possible to solve these numerically, again referring to [17], but this falls outside of the scope of this thesis.

see ref. [20] also Appendix A, where β_{d+1} is a constant given by

$$\beta_{d+1} = \frac{1}{\pi^{d/2}2^{d-2}\Gamma\left(\frac{d}{2}\right)} \tag{3.2}$$

for electrons. The fluid pressure is related to the other parameters by means of an equation of state. In our case, we will invoke the thermodynamical identity $\Omega = H - \mu N$ (at zero temperature) and the ideal fluid relation $\Omega = -pV$ to obtain the equation of state

$$-p_f = \rho_f - \mu\sigma_f.$$

In the local-density approximation applied to our curved space, the global chemical potential μ is replaced by the local chemical potential

$$\mu_{\text{loc}} = u^t A_t, \tag{3.3}$$

where u^t is the temporal component of the four-velocity u^μ. It acts as a vielbein[2], so the local chemical potential is nothing but the tangent frame value of the global chemical potential μ. In turn, the global chemical potential is nothing but the temporal component of the gauge field, from the dictionary rules in table 2.1 - see also section 2.1.3. The four-velocity u^μ satisfies $u^\mu u_\mu = -1$, and in the rest frame of the gas one finds

$$u^t = \frac{1}{\sqrt{-g_{tt}}}.$$

Thus, the fluid parameters take the form

$$\rho = \beta_{d+1} \int_m^{\mu_{\text{loc}}} E\,g\left(E\right) dE \tag{3.4}$$

$$\sigma = \beta_{d+1} \int_m^{\mu_{\text{loc}}} g\left(E\right) dE \tag{3.5}$$

$$-p = \rho - \mu_{\text{loc}}\sigma. \tag{3.6}$$

The backreacting effect of the fermions to the metric, in the fluid approximation, is then captured by the associated energy-momentum tensor which appears in Einstein's equations. Realizing that the pressure depends on the local chemical potential and using equation (3.3), we determine the energy momentum tensor by varying the effective action with respect to the metric. One finds

$$\frac{-2}{\sqrt{-g}}\frac{\delta S_\psi^{\text{eff}}}{\delta g^{tt}} = pg_{tt} + A_t\frac{\partial p}{\partial \mu_{\text{loc}}}\frac{1}{\sqrt{-g^{tt}}}$$

$$= pg_{tt} + \mu_{\text{loc}}\frac{\partial p}{\partial \mu_{\text{loc}}}u_t u_t$$

$$\frac{-2}{\sqrt{-g}}\frac{\delta S_\psi^{\text{eff}}}{\delta g^{ii}} = pg_{ii}.$$

Invoking the equation of state, the energy-momentum tensor is seen to take the form

$$T_{\mu\nu} = \frac{-2}{\sqrt{-g}}\frac{\delta S}{\delta g^{\mu\nu}}$$

$$= \left(\rho + p\right)u_\mu u_\nu + pg_{\mu\nu}$$

in a general frame. We will, however, be mainly interested in the local rest frame of the fermions.

---

[2]We will introduce the notion of a vielbein more precisely in the next chapter, where we need it to construct the fermionic action in curved spacetime.

3.2   Equations of motion

We determine the equations of motion for the electron-star model. It is important to realize that these equations of motion will provide differential equations from which the metric and the gauge field are solved, as these are unknown to us at this point due to the backreaction of the fermion fluid. As in the Lifshitz black brane case, we will require a spacetime which is asymptotically Anti-deSitter, thus retrieving a scale invariant quantum field theory at high-energies. We parametrize the metric by

$$ds^2 = -\ell^2 \left(f\left(u\right) dt^2 + g\left(u\right) du^2 + \frac{1}{u^2} dx_i^2 \right), \tag{3.7}$$

where $i = 1, ..., d$, and where[3] $f\left(u\right)$ and $g\left(u\right)$ are the unknown functions, depending only on u through the requirement of spherical symmetry. Demanding an asymptotically Anti-deSitter spacetime translates into the asymptotic behavior

$$f, g \sim u^{-2}$$

near the boundary $u \to 0$, as is seen by comparing the metric above to the Poincare metric (2.3). This requirement is automatically satisfied by letting

$$\Lambda = -\frac{d\left(d-1\right)}{2\ell^2}$$

as in the Lifshitz black brane case, see equation (2.23) with $z = 1$. Further, we will consider the case where the gauge field A_μ has vanishing spatial components. Thus only A_t is non-zero, and we write it down as

$$A_t\left(u\right) = \frac{e\ell}{\kappa} h\left(u\right),$$

where h is an unknown function as well. As a result, the only non-trivial component of the field strength tensor is $F_{ut} = \frac{e\ell}{\kappa} h'$. We stress that the total charge of the bulk theory is carried by the charged fermions, rather than by the black hole horizon as in the previous chapter.

As described in the previous section, the action of the model is

$$ S \;=\; \int d^{d+1}x \sqrt{-g} \left[\frac{1}{2\kappa^2}\left(R - 2\Lambda\right) - \frac{1}{4e^2} F_{\mu\nu}F^{\mu\nu} - p\left(\mu_{\mathrm{loc}}\right) \right], \tag{3.8}$$

which yields the equations of motion that we need to solve. They are given by

$$R_{\mu\nu} + \left(\Lambda - \frac{1}{2}R \right) g_{\mu\nu} \;=\; \kappa^2 T_{\mu\nu} \tag{3.9}$$

$$\nabla_\mu F^{\nu\mu} \;=\; e^2 \sigma u^\nu \tag{3.10}$$

$$\nabla_\mu T^{\mu\nu} \;=\; 0. \tag{3.11}$$

The last equation of motion is the covariant conservation of the energy-momentum tensor, and replaces what would be the fermion equation of motion when allowing the full fermion backreaction. Here, the energy-momentum tensor $T_{\mu\nu}$ of the charged fluid is given by

$$T_{\mu\nu} = \left(\rho + p\right) u_\mu u_\nu + p g_{\mu\nu} + \frac{1}{e^2} F_{\mu\sigma} F_\nu{}^\sigma - \frac{1}{4e^2} g_{\mu\nu} F^2.$$

---

[3]Note that both the determinant of the metric as well as the "radial" metric component g_{uu} are denoted by g. In principle, this should not lead to any confusion.

It will be convenient to scale out the parameters e, κ and ℓ and to work with dimensionless fluid parameters. For this, we note that in $(d+1)-$dimensional spacetime

$$
\begin{aligned}
{[p]} = [\rho] &= [\text{length}]^{-1-d} \\
[\sigma] &= [\text{length}]^{-d} \\
[\kappa]^2 &= [\text{length}]^{d-1} \\
[e]^2 &= [\text{length}]^{d-3},
\end{aligned}
$$

from which we find the dimensionless fluid parameters

$$
\hat{\rho}\left(u\right) = \kappa^2 \ell^2 \rho\left(u\right), \quad \hat{p}\left(u\right) = \kappa^2 \ell^2 p\left(u\right), \quad \hat{\sigma}\left(u\right) = e\ell^2 \kappa \sigma\left(u\right).
$$

In terms of the dimensionless quantities, the equations of motion can be cast in the form

$$
\begin{aligned}
\hat{p}' + \left(\hat{\rho} + \hat{p}\right)\frac{f'}{2f} - \frac{h'\hat{\sigma}}{\sqrt{f}} &= 0 \qquad [\nabla_\mu T^{\mu r} = 0] \\
\frac{(d-1)}{2u}\left(\frac{4}{u} + \frac{g'}{g} + \frac{f'}{f}\right) + g\left(\hat{\rho} + \hat{p}\right) &= 0 \qquad \left[R^r_r - R^t_t = \kappa^2 T^r_r - \kappa^2 T^t_t\right] \\
\frac{f'}{fz} - \frac{(d-2)}{u^2} - \frac{h'^2}{(d-1)f} + g\left(\frac{d\left(d-1\right) + 2\hat{p}}{d-1}\right) &= 0 \qquad \left[R_{ii} + \left(\Lambda - \frac{1}{2}R\right)g_{ii} = \kappa^2 g_{ii}\left(p - \frac{1}{4e^2}F^2\right)\right] \\
h'' - \frac{h'}{2}\left(\frac{f'}{f} + \frac{g'}{g} + \frac{2\left(d-1\right)}{u}\right) - g\sqrt{f}\hat{\sigma} &= 0 \qquad \left[\nabla_\mu F^{t\mu} = e^2 \sigma u^t\right],
\end{aligned}
$$

where we have indicated the specific equation of motion used in square brackets. For a detailed derivation of the equations, see Appendix B.

At this point, we mention that upon inserting the fermion equation of state and the expressions for the charge and energy density of the fluid, **the first equation of motion is solved trivially**, for arbitrary h and f. We proceed to show this explicitly. Inserting the form of the metric into (3.3), (3.4) and (3.5), one finds

$$
\mu_{\text{loc}} = \frac{e}{\kappa}\frac{h}{\sqrt{f}}, \tag{3.12}
$$

while the fluid parameters take the form

$$
\rho = \beta_{d+1}\int_m^{\mu_{\text{loc}}} E^2 \left(E^2 - m^2\right)^{(d-2)/2} dE, \quad \sigma = \beta_{d+1}\int_m^{\mu_{\text{loc}}} E\left(E^2 - m^2\right)^{(d-2)/2} dE.
$$

Scaling out dimensionful parameters $m \to \frac{e}{\kappa}\hat{m}$ and $E \to \frac{e}{\kappa}\epsilon$, one finds the dimensionless expressions

$$
\hat{\rho} = \hat{\beta}_{d+1}\int_{\hat{m}}^{h/\sqrt{f}} \epsilon^2 \left(\epsilon^2 - \hat{m}^2\right)^{(d-2)/2} d\epsilon \tag{3.13}
$$

$$
\hat{\sigma} = \hat{\beta}_{d+1}\int_{\hat{m}}^{h/\sqrt{f}} \epsilon\left(\epsilon^2 - \hat{m}^2\right)^{(d-2)/2} d\epsilon \tag{3.14}
$$

where $\hat{\beta}_{d+1} = \frac{e^{d+1}\ell^2}{\kappa^{d-1}}\beta_{d+1}$. These quantities are related to the dimensionless pressure via the equation of state (3.6), which now reads

$$
-\hat{p} = \hat{\rho} - \frac{h}{\sqrt{f}}\hat{\sigma}. \tag{3.15}
$$

By differentiating with respect to the upper limit, one the easily verifies that these expression solve the first equation of motion trivially. Then, substituting the second equation of motion in the last, we

are left with the set of equations

$$\frac{d-1}{2u}\left(\frac{4}{u}+\frac{g'}{g}+\frac{f'}{f}\right)+\frac{gh}{\sqrt{f}}\hat{\sigma} = 0 \tag{3.16}$$

$$\frac{f'}{fu}-\frac{d-2}{u^2}-\frac{h'^2}{(d-1)f}+g\left(\frac{d(d-1)+2\hat{p}}{(d-1)}\right) = 0 \tag{3.17}$$

$$h''-\frac{h'(d-3)}{u}+\frac{g\hat{\sigma}}{\sqrt{f}}\left(\frac{zhh'}{d-1}-f\right) = 0, \tag{3.18}$$

with $\hat{p}$ and $\hat{\sigma}$ as given above. Clearly, these equations constitute a set of non-linear and highly coupled differential equations, which are too complex to be solved analytically. Thus, in the next section, we will proceed by solving these equations numerically.

Intermezzo: non-zero temperature

It is important to stress that the electron star model considered here is at zero temperature. Let pause for a moment to consider the case of a non-zero temperature. According to Table (2.1), in order to introduce a temperature scale in the boundary field theory, we are required to introduce of black hole in the bulk spacetime. Then, the Hawking temperature of the black hole would coincide with the temperature in the boundary field theory.

Precisely this addition of a black hole was studied in ref. [21]. While one would expect the bulk fluid to have a different equation of state due to a non-zero temperature, the equation of state was kept the same in this case. That is, the fluid is treated as if at zero temperature. It was argued that the thermalization of the bulk fluid with thermal Hawking radiation of the black hole is suppressed. The resulting model at non-zero temperature becomes an electron shell, or an electron cloud, suspended over the black hole, while the zero-temperature limit coincides with the electron star considered here. See also ref. [22].

It is interesting to see what happens when the fermion fluid is treated at a non-zero temperature. Introducing a temperature means that the thermodynamical identity used to determine the equation of state for the fermions picks up an extra term. Namely,

$$\Omega = H - \mu N - TS,$$

where S is the entropy of a Fermi gas. Thus, the equation of state for the fermions becomes

$$-p = \rho - \mu\sigma - Ts,$$

where $s = S/V$ is the entropy density. The integral expressions for the fluid parameters also change, as we now have to integrate over the Fermi-Dirac distribution

$$n_E = \left[\exp\left[\beta\left(E-\mu\right)\right]+1\right]^{-1}$$

as well, where $\beta = T^{-1}$. Scaling out the couplings, the expressions become

$$\hat{\rho} = \hat{\beta}_{d+1}\int_{\hat{m}}^{\infty}\epsilon^2\left(\epsilon^2-\hat{m}^2\right)^{(d-2)/2}n_\epsilon d\epsilon$$

$$\hat{\sigma} = \hat{\beta}_{d+1}\int_{\hat{m}}^{\infty}\epsilon\left(\epsilon^2-\hat{m}^2\right)^{(d-2)/2}n_\epsilon d\epsilon, \tag{3.19}$$

with the distribution

$$n_\epsilon = \left[\exp\left[\beta\frac{e}{\kappa}\left(\epsilon-\frac{h\ell}{\sqrt{f}}\right)+1\right]\right]^{-1}.$$

Taking the limit $T \to 0$, the Fermi-Dirac distribution becomes a Heaviside step function, and the above expressions reduce to the expressions (3.13) and (3.14). The entropy follows from the continuum limit of the ideal gas entropy

$$S = -k_B \sum_k \left(n_k \log n_k + (1 - n_k) \log (1 - n_k) \right),$$

which, after some algebra - see Appendix B, yields

$$\hat{s} = -\hat{\beta}_{d+1} \int_{\hat{m}}^{\infty} \epsilon \left(\epsilon^2 - \hat{m}^2 \right)^{(d-2)/2} \left(n_\epsilon \log n_\epsilon + (1 - n_\epsilon) \log (1 - n_\epsilon) \right)$$

with $\hat{s} = e\ell^2 \kappa\, s$.

If we substitute these expressions in the first equation of motion, however, one finds they do not constitute a solution. For this, the temperature needs to have a radial profile

$$T(u) = \frac{T_0}{\sqrt{f(u)}},$$

which can be interpreted as a local temperature for the fermion fluid, or as a redshift due to gravitational effects. One can check that this profile indeed solves the first equation of motion.

Even better, this temperature profile as well as the profile of the local chemical potential can be derived without using the specific expressions for the fluid parameters. This is worked out in more detail in Appendix B. By using the equation of state and

$$\Omega = -pV \Rightarrow -p = \frac{\Omega}{V} \equiv \omega,$$

the equation of motion can be cast in the form

$$\frac{\partial \omega}{\partial \mu} \left(-\frac{\partial \mu}{\partial r} - \mu \frac{f'}{2f} + \frac{e}{\kappa} \frac{h'}{\sqrt{f}} \right) = \frac{\partial \omega}{\partial T} \left(\frac{\partial T}{\partial r} + T \frac{f'}{2f} \right).$$

Setting both sides equal to zero, one finds the desired radial profiles

$$\mu_{\text{loc}} = \frac{e}{\kappa} \frac{h}{\sqrt{f}}, \quad T = \frac{T_0}{\sqrt{f}}.$$

The problem with the non-zero temperature description of the fermion fluid is the divergence of T towards the infrared. If we add a black hole to the spacetime, this divergence will appear at the horizon of the black hole. If we do not add a black hole, this divergence will occur in the deep interior of the electron star.

If we insist on adding the "thermal" term to the equation of state, one needs to make sense of the infinitely red-shifted temperature in the interior of the star and the resulting divergences of the fluid parameters. Indeed, one can easily verify that the fluid parameters given in equation (3.19) as functions of u diverge in the infrared limit. These complications fall outside the scope of this thesis and are left for future work.

3.3 Solving the equations of motion

Having solved the first equation of motion, we now focus on solving the remaining equations

$$\frac{d-1}{2u}\left(\frac{4}{u}+\frac{g'}{g}+\frac{f'}{f}\right)+\frac{gh}{\sqrt{f}}\hat{\sigma} = 0$$

$$\frac{f'}{fu}-\frac{d-2}{u^2}-\frac{h'^2}{(d-1)f}+g\left(\frac{d\,(d-1)+2\hat{p}}{(d-1)}\right) = 0$$

$$h''-\frac{h'\,(d-3)}{u}+\frac{g\hat{\sigma}}{\sqrt{f}}\left(\frac{uhh'}{d-1}-f\right) = 0,$$

where $\hat{\sigma}$ and $\hat{p}$ are given by (3.14) and (3.15). These equations have to be solved numerically, due to the fact that they are highly coupled and non-linear. Although finding an exact solution for all u is futile, there are two regimes in which an **exact** solution can be found:

1. For $u \to \infty$, the set of equations are solved by an emergent scaling solution, which is a Lifshitz solution.

2. For small u, the equations are solved by the asymptotically Anti-deSitter Reissner-Nordström (AdS-RN) solutions, given in equations (2.25) and (2.26). For small u, namely, the fluid parameters vanish because the local chemical potential becomes smaller than the mass of the fermions[4]. As the fluid parameters vanish, the fermion backreaction is being turned off. Thus, the resulting action is an Einstein-Maxwell action, which is solved by a charged black hole solution.

The numerical integration of the equations of motion interpolates between these two exact solutions. We begin with the Lifshitz solution in the infrared limit, perturbing it in order to generate initial conditions in the deep interior of the spacetime. The equations of motion are then numerically integrated, using these initial conditions, down to the point $u = u_s$ where the local chemical potential is equal to the mass of the fermion. At this value, the numerical solution is matched onto the AdS-RN solution.

3.3.1   The numerical calculation

In the limit $u \to \infty$, which is the deep infrared of the spacetime, one finds a Lifshitz metric (2.14) as an exact solution to the above equations of motion. Intuitively, this can be explained by the screening of the electric field due to the local charge density, which serves to decrease the range of the electric field. Hence, the electric field can be thought of as being "massive", and actions of negatively curved spaces with massive vector fields are known to yield Lifshitz solutions, see ref.s [23]. Here, the Lifshitz solution takes the form

$$f=\frac{1}{u^{2z}}; \quad g=\frac{g_\infty}{u^2}; \quad h=\frac{h_\infty}{u^z}, \tag{3.20}$$

where z is the dynamical exponent - one can check that this solution indeed yields the Lifshitz metric (2.14) by transforming back to the r coordinates.

By substituting these expressions into the equations of motion, one finds

$$g_\infty^2 = \frac{z^{d-1}\,(z-1)\,d^2\,(d-1)^2}{\hat{\beta}_{d+1}^2\,((1-\hat{m}^2)\,z-1)^d} \quad h_\infty^2 = \frac{z-1}{z},$$

while the equation of motion (3.17) yields a complicated relation between $\hat{m}$, z and $\hat{\beta}_d$. For completeness, it is given by

$$2-d-2z-\frac{z\,(z-1)}{d-1}+\frac{z^{(d+1)/2}\sqrt{z-1}d\,(d-1)}{\hat{\beta}_{d+1}\,((1-\hat{m}^2)\,z-1)^{d/2}}\left(d+\frac{2}{d-1}\hat{p}\right)=0. \tag{3.21}$$

---

[4]This is because both the electron star model and the AdS-RN solutions asymptote to Anti-deSitter space on the boundary. Far away from the origin, therefore, the local chemical potential becomes the local chemical potential as determined from the AdS-RN solution, which vanishes as u towards the boundary as we will see.

This relation can be solved for $\hat{\beta}_{d+1}$ in terms of the parameters z and $\hat{m}$. Thus, the Lifshitz solution is fixed completely if we pick a mass $\hat{m}$ and a Lifshitz parameter z; these are therefore the free parameters of this model. The dependence of $\hat{\beta}_5$ is shown in Figure 3.1, for the case $d+1=5$.
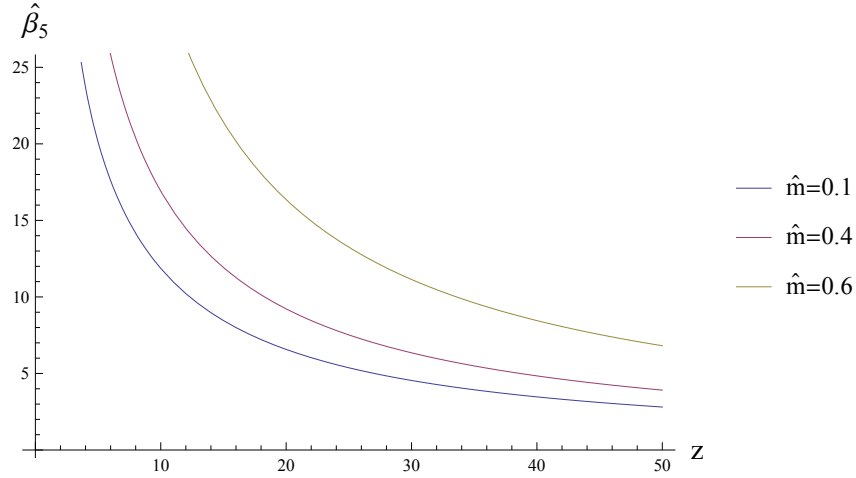

Figure 3.1:   The parameter $\hat{\beta}_5$ as a function of the Lifshitz scaling parameter z, for fixed fermion mass $\hat{m} = 0.1,\ 0.4,\ 0.6$.

Following ref. [16], we then consider the limits $\hat{m} \to 1$ from below with $\hat{\beta}_{d+1}$ fixed, and $\hat{\beta}_{d+1} \to 0$. From the expressions (3.13) and (3.14), it is immediately clear that the fermion backreaction is turned off in the limit $\hat{\beta}_{d+1} \to 0$. The same holds for the first limit, as $z \to \infty$ in this limit, from (3.21). This implies $h_\infty \to 1$, and thus, as $\hat{m} \to 1$, the integrals in (3.13) and (3.14) vanish. In order to stay in the backreacting regime, therefore, the dimensionless mass thus satisfy the bounds

$$0 \leq \hat{m} < 1.$$

From the relation (3.21), it turns out that by dialing $\hat{\beta}_{d+1}$ at a fixed $\hat{m}$ we can achieve all z such that

$$z \geq \frac{1}{1 - \hat{m}^2} \geq 1.$$

Perturbing the IR scaling solution

As described above, we use the exact solution in the infrared limit to numerically integrate the equations of motion down to of u. For this, however, initial conditions are required at a large infrared cut-off u_{IR}. In order to generate these initial conditions, we perturb the infrared solutions by an irrelevant deformation

$$
\begin{aligned}
f &= \frac{1}{u^{2z}} \left(1 + f_1 u^\alpha\right) \\
g &= \frac{g_\infty}{u^2} \left(1 + g_1 u^\alpha\right) \\
h &= \frac{h_\infty}{u^z} \left(1 + h_1 u^\alpha\right),
\end{aligned}
\tag{3.22}
$$

where we require that this deformation vanishes in the IR, but grows in the UV limit. Thus, we are looking for $\alpha < 0$.

Entering these expressions in the equations of motion, one finds zeroth order equations that are solved by the Lifshitz scaling solutions, while the first order corrections yield a set of equations that can be used to find expressions for α in terms of z and m, and g_1 and h_1 in terms of f_1. In $d+1$ dimensions, the solutions for α are

$$
\begin{aligned}
\alpha_0 &= d - 1 + z \\
\alpha_\pm &= \frac{d-1+z}{2} \pm \frac{1}{2\sqrt{(1-\hat{m}^2)z-1}} \left[-9 + 14\,(d-2) - 5\,(d-2)^2 \right. \\
&\qquad \left. -z\left(-19 - 16\,(d-2) - 5\,(d-2)^2 + \hat{m}^2\,(d-1-3z)^2 + (19 + 2\,(d-2) - 9z)\,z \right) \right]^{1/2}.
\end{aligned}
$$

For the allowed values for $\hat{m}$ and z determined in the previous section, α_- is negative. Hence, this is the exponent we are looking for. Next, g_1 and h_1 are found to be of the form

$$
\begin{aligned}
g_1 &= f_1 \gamma_g\,(z, \hat{m}, \alpha_-) \\
h_1 &= f_1 \gamma_h\,(z, \hat{m}, \alpha_-),
\end{aligned}
$$

where γ_g, γ_h are some functions of $z, \hat{m}$ and $\alpha_-\,(z,m)$. That is, g_1 and h_1 are proportional to f_1. Having used all equations, f_1 remains undetermined. However, this factor can be set to any value after an appropriate rescaling of the coordinates. Its sign is important, however. It should be taken negative in order to appropriately match the numerical solution onto the Reissner-Nordström solution later - see Appendix B. Thus, we set $f_1 = -1$ in our numerical calculation.

Having obtained the perturbed solutions, we introduce a large cut-off u_{IR} at which the solutions of equation and their derivatives are computed. These serve as initial conditions to the numerical integration of the equation of motion, which is carried out - using Mathematica's NDSolve - until

$$
\frac{h}{\sqrt{f}} = \hat{m}
$$

for a certain value $u = u_s$, at which point the integration is stopped. It is at this point that the fluid parameters vanish, and the solutions becomes the AdS-RN solution. The value u_s can be interpreted as the (inverse) radius of the star, separating the perfect fluid from empty space.

Thus, one obtains numerical solutions f, g and h on the interval $[u_{IR}, u_s]$. Of course, one should check that these solutions do not depend on the choice of u_{IR}, which is the case if the WorkingPrecision of NDSolve is chosen large enough, around 50-60 digits. For those values, the solutions indeed do not depend on the infrared cut-off.

We now turn to the results of the numerical calculation, for $d+1 = 5$. A typical result for the fluid parameters as function of inverse dimensionless radial distance is shown in Figure 3.2.
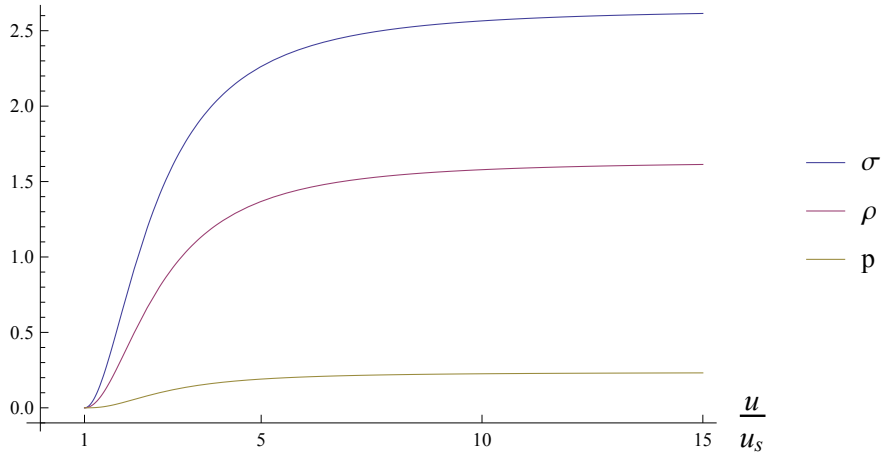
Figure 3.2: The fermion fluid energy density ρ, charge density σ and pressure p as functions of the radial coordinate u, in units of the star "radius" u_s. In this figure, the fermion mass is $\hat{m} = 0.4$, and the Lifshitz scaling parameter is $z = 2$.

One can see that the fluid parameters indeed go to zero at the radius u_s, while they tend to their constant values in the infrared limit at large u. These values are simply the Lifshitz values, found by combining equations (3.20) and (3.13)-(3.15). These radial profiles are very similar to the fluid profiles of neutron stars, which are determined from TOV equations very similar to our equations of motion.

We also plot the fluid parameters separately for various masses at a fixed IR Lifshitz parameter z, in Figure 3.3.

3.3.2 Matching onto Reissner-Nordström

As mentioned before, the equations of motion have exact solutions in the regime $u \leq u_s$. In this region, namely, the fluid parameters vanish as the local chemical potential μ_l is smaller than the fermion mass $\hat{m}$. Hence, from the integral expressions (3.13) and (3.14), the pressure, energy density and charge density of the fluid become zero. In this case, the equations of motion simplify greatly and can be solved exactly. The resulting solutions are the Anti-deSitter Reissner-Nordström (AdS-RN) solutions, which for our choice of metric can be written

$$
\begin{aligned}
f_{\mathrm{RN}}(u) &= \frac{c^2}{u^2} - Mu^{d-2} + \frac{Q^2 u^{2d-4}}{(d-1)(d-2)}. \\
g_{\mathrm{RN}}(u) &= \frac{c^2}{u^4 f(u)} \\
h_{\mathrm{RN}}(u) &= \mu - \frac{Q}{d-2} u^{d-2}.
\end{aligned}
\tag{3.23}
$$

Thus the metric outside the electron star is given by the AdS-RN solutions, which are parametrized by integration constants M, Q, μ and c. By parametrizing the functions f, g and h in this way throughout the spacetime, the first two parameters can be given analytically by integrating over the fermions in the electron star, as in ref. [16]. They are interpreted as the mass and the charge of the black hole, respectively. The integration constant μ is simply the boundary value of the gauge field, and is hence referred to as the chemical potential of the black hole. Finally, the parameter c is related to our choice $f_1 = -1$ and can be freely set to one by rescaling the time coordinate.
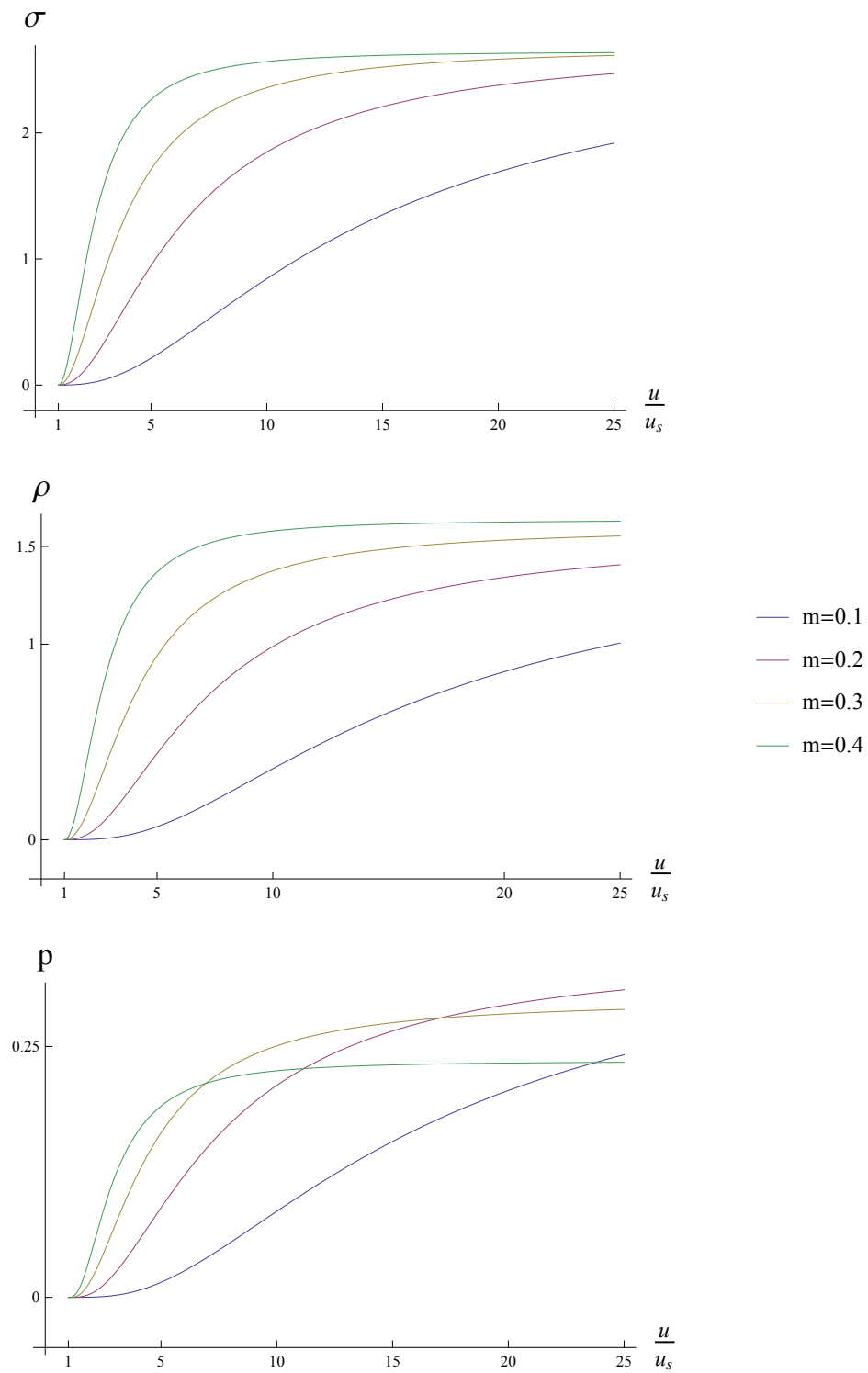
Figure 3.3: The radial profiles of the fermion fluid for a fixed Lifshitz scaling parameter $z = 2$, and varying fermion masses $\hat{m}$.

These solutions are equivalent to the AdS black brane solution in section 2.2.2. Indeed, by transforming $f(u), g(u) \rightarrow \tilde{f}(r), \tilde{g}(r)$ using equation (2.8) and setting $c = 1$, one finds

$$
\begin{aligned}
\tilde{f}(r) &= 1 - M\ell^{2d}r^{-d} + \frac{Q^2\ell^{4(d-1)}r^{2(1-d)}}{(d-1)(d-2)} \\
\tilde{g}(r) &= \frac{1}{\tilde{f}(r)},
\end{aligned}
$$

which corresponds to equation (2.25). Further, one finds

$$
A_t' = \frac{e\ell^{2d-3}Q}{\kappa}r^{1-d},
$$

which corresponds to equation (2.26). In order to completely map these solutions onto those in Chapter 2, however, note that the convention for the energy-momentum tensor here is slight different. By letting

$$
F = \frac{e}{\kappa\sqrt{2}}\tilde{F},
$$

one can identify $\tilde{F}$ with the energy-momentum tensor used in Chapter 2. Proceeding this way, one can map the above solutions to the solutions in Chapter 2.

The numerical solutions for f, g, h and h' are matched at the "radius" u_s. That is, we equate the numerical solutions for f, g, h and h' and the Reissner-Nordström solutions (3.23) at u_s, thus providing equations that are solved for μ, c, Q and M. The full solutions f, g and h that determine the metric and the gauge field in the electron-star spacetime, are simply the numerical solutions for $u > u_s$, and the matched Reissner-Nordström solutions for $u < u_s$. They are shown in Figure 3.4, along with the infrared scaling solution as well as the Reissner-Nordström solution for $u > u_s$. In the last figure, we clearly see that the numerical solutions for f and g converge towards their inverse relation as in equation (2.25)
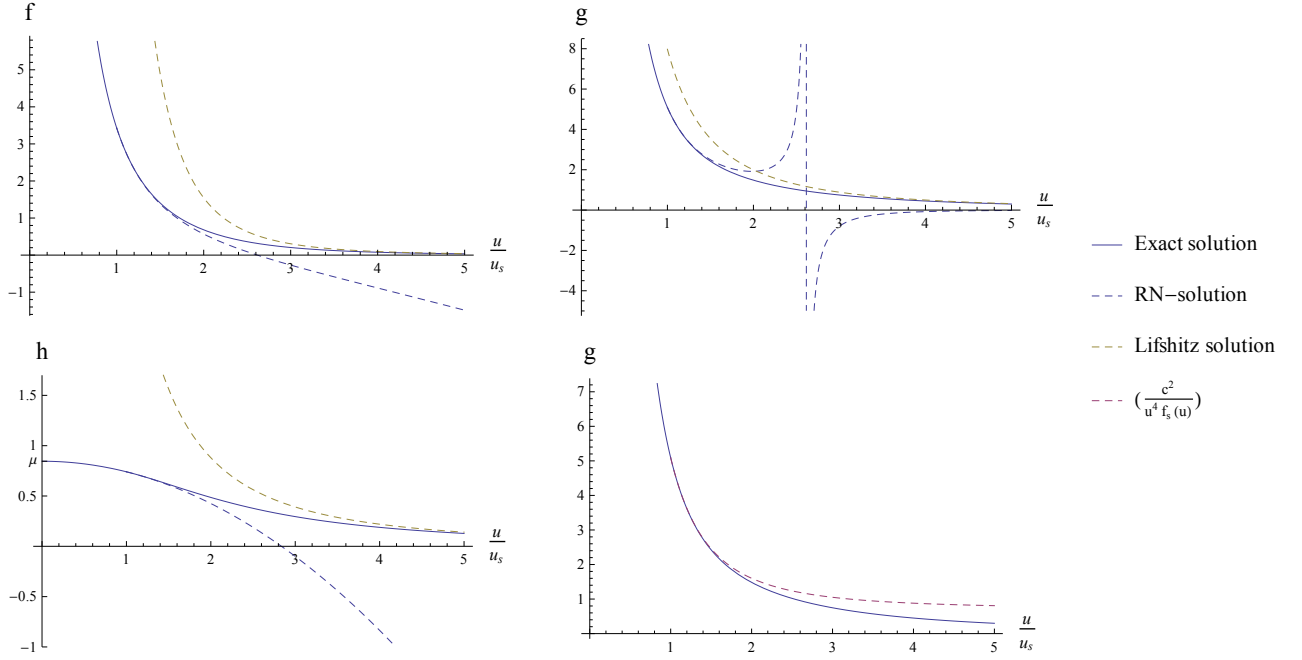
Figure 3.4: The radial profiles of the metric functions f and g and the gauge field h, with the radial coordinate u units of the star "radius" u_s. Notice that the gauge field tends to the chemical potential μ on the boundary at $u = 0$. The solid line indicates the exact solutions, which is the Reissner-Nordström (RN) solution for $u < u_s$ and the numerical solution for $u > u_s$. The dotted lines indicate the RN-solution outside the domain of validity (blue and red), and the infrared Lifshitz solution (yellow). Here, the fermion mass is $\hat{m} = 0.4$ and the Lifshitz scaling parameter is $z = 2$.

Next, we study the dependence on the parameters $\hat{m}$ and z. As discussed before, when these parameters are fixed, $\hat{\beta}_{d+1}$ is known. With these values at hand, the equations of motion are solved and matched onto the Reissner-Nordström solution. Repeating this procedure, one finds the dependence of u_s, μ, Q and M on the parameters $\hat{m}$ and z. This dependence in shown in Figure 3.5, and will be important in later numerical calculations. Through this dependence, by fixing a mass $\hat{m}$ and requiring a certain value of the chemical potential μ, one can find a z which generates the required solution.

It is clear from the first figure that the inverse radius of the star increases upon an increase of the mass $\hat{m}$. Thus, the actual radius of the star - identified with u_s^{-1} - decreases, which makes sense as the larger mass deepens the gravitational potential well, pulling the electrons together. This effect explains the other figures as well: a smaller star implies a Reissner-Nordström black hole of smaller radius, and hence a smaller total mass and charge. The chemical potential also decreases when mass is increased, which can be explained by the smaller total charge Q. Finally, an increase in z is directly related to a decrease in $\hat{m}$ via the relation (3.21).
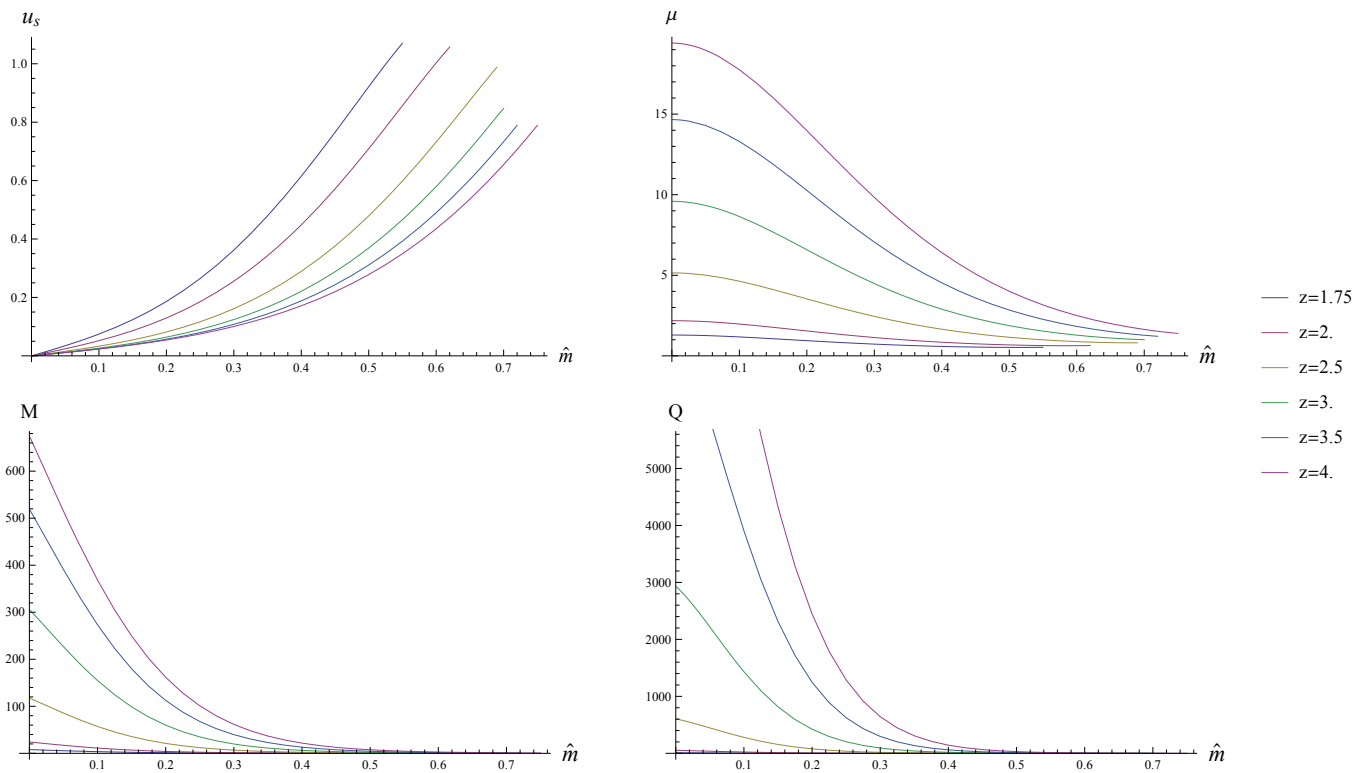
Figure 3.5: The dependence of the star "radius" u_s and the Reissner-Nordström parameters μ, M, Q of the fermion mass $\hat{m}$ at fixed Lifshitz scaling parameters z.

Chapter 4

The fermion correlator

In this chapter, we add probe-fermion to the electron star model by constructing the Dirac action in curved spacetime. Having obtained the geometry of the electron-star spacetime within the fluid approximation. These fermions are not treated in the fluid approximation, and they do not backreact onto the geometry found in the previous chapter. From the Dirac action, we compute the retarded Green's function and the spectral function by numerically solving the Dirac equation.

We start by constructing the Dirac action in flat spacetime, after which we will generalize the discussion to curved spacetime by using the vielbein formalism. The resulting action is not complete, however, as it does not satisfy the variation principle when employed in a holographic manner. In order to solve this problem, we add counter terms to the action. The spinors in the action are then split up in chiral components and one of them is integrated out to yield an effective action for a chiral fermion. From this, we will be able to construct the fermion correlator and the spectral function.

Here, we broadly follow ref. [14] where the Dirac action is built in a different background, namely that of the Lifshitz black brane, section 2.2.2. We will generalize this discussion to the case of the electron-star background which was determined in Chapter 3. In order to do so, however, it will be convenient to transform to the r coordinate system by letting $u = \frac{\ell^2}{r}$, as discussed in section 2.1.1.

4.1   The Dirac action in curved spacetime

In order to add additional fermions to the electron-star model, a Dirac action for charged fermions in curved spacetime is required. It will be convenient to study the construction of such an action in more detail, as the concepts required to do so will be important later. For this, we begin by writing down the Dirac action for flat $d+1$-dimensional spacetime and subsequently generalize it to a curved spacetime. This is done by employing the vielbein formalism, which essentially maps flat space to curved space.

The final action, however, needs an additional term in order to satisfy the variational principle, due to fact that variations at spatial infinity do not vanish. Instead, they source operators, see section 2.1.2. Moreover, an extra term is added by hand, for reasons explained in the next section.

4.1.1   Flat spacetime

We will begin with the Dirac action in a flat spacetime, after which we will generalize our discussion using vielbeins which translate between locally-flat space and curved spacetime. We will consider a flat spacetime both of dimension d and $d+1$, in order to generalize to the $(d+1)$-dimensional AdS-like bulk and the d dimensional boundary in the curved spacetime[1].

---

[1]Note that we cannot speak of a flat $d+1$ dimensional spacetime and its flat d dimensional boundary; Minkowski spacetime does not have a boundary like the Anti-deSitter spacetime does.

In d dimensional flat spacetime, the Dirac equation takes the form

$$\left(\gamma^{\underline{a}}\partial_{\underline{a}} - m\right)\psi = 0$$

with $\underline{a} \in \{\underline{t}, \underline{i}\}$, where $\underline{i} \in \{1, ..., d-1\}$, and where the underlines indicate that we are working in flat space. In one higher dimension, i.e. in a flat $d+1$ dimensional spacetime, we have the Dirac equation

$$\left(\Gamma^{\underline{a}}\partial_{\underline{a}} - m\right)\Psi = 0,$$

where we denote the gamma matrices by Γ and where Ψ is the Dirac spinor. In this case, the indices $\underline{a} \in \{\underline{r}, \underline{t}, \underline{i}\}$, where again $i \in \{1, ..., d-1\}$.

The matrices $\gamma^{\underline{a}}$ and $\Gamma^{\underline{a}}$ form representations of the Clifford algebra, of dimensions d and $d+1$ respectively[2], which means they satisfy the relations

$$\left\{\gamma^{\underline{a}}, \gamma^{\underline{b}}\right\} = 2\eta^{\underline{ab}}\mathbf{1} \quad \text{and} \quad \left\{\Gamma^{\underline{a}}, \Gamma^{\underline{b}}\right\} = 2\eta^{\underline{ab}}\mathbf{1}.$$

The matrices themselves have dimensions $2^{\lfloor \frac{d}{2} \rfloor}$ and $2^{\lfloor \frac{d+1}{2} \rfloor}$, respectively. We now make an important distinction between the case that d is even, and the case that d is odd. First, we mention the fact that any even-dimensional representation of the Clifford algebra is *reducible*[3] [24]. In flat four-dimensional spacetime ($d+1 = 4$), one can define the matrix γ^5 which satisfies

$$\left\{\gamma^5, \gamma^\mu\right\} = 0, \quad \left(\gamma^5\right)^2 = \mathbf{1}.$$

The last property implies that the operators

$$L = \frac{1}{2}\left(\mathbf{1} - \gamma^5\right), \quad R = \frac{1}{2}\left(\mathbf{1} + \gamma^5\right)$$

are projection operators acting on spinors, which can then be split up as

$$\Psi = \Psi_L + \Psi_R$$

with

$$\Psi_L = L\Psi, \quad \Psi_R = R\Psi.$$

For more information, we refer to ref. [25]. The spinors Ψ_L and Ψ_R are called the *chiral components* of the Dirac spinor Ψ. These components behave independently of each other under the action of the Lorentz group, indicating reducibility.

We first consider the case that d is **even**, which is the relevant case in this thesis. Generalizing the above, one can define a matrix $\gamma^{\underline{d+1}}$ and the associated projection operators and chiral components. Meanwhile, the Γ matrices have the same dimension as the γ matrices. One can easily check that the matrices

$$\begin{aligned}
\Gamma^{\underline{r}} &= \gamma^{\underline{d+1}} \\
\Gamma^{\underline{i}} &= \gamma^{\underline{i}} \\
\Gamma^{\underline{t}} &= \gamma^{\underline{t}}
\end{aligned} \tag{4.1}$$

with

$$\gamma^{\underline{d+1}} = \begin{pmatrix} \mathbf{1} & 0 \\ 0 & \mathbf{1} \end{pmatrix}, \quad \gamma^{\underline{t}} = \begin{pmatrix} 0 & -\mathbf{1} \\ \mathbf{1} & 0 \end{pmatrix}, \quad \gamma^{\underline{i}} = \begin{pmatrix} 0 & \sigma^i \\ \sigma^i & 0 \end{pmatrix}$$

---

[2]The dimensionality of the representation is equal to the dimension of the spacetime.

[3]This means that the matrices assigned to the abstract elements of the Clifford algebra are of block-diagonal form. Equivalently, reducibility of the representation means that there is a non-identity matrix in the algebra which commutes with all the generators.

form a $(d+1)$-dimensional representation of the Clifford algebra. In the $(d+1)$-dimensional spacetime, the spinor Ψ can not be split into chiral components[4]. On a constant radius hyper-surface, however, this is possible. There, we define

$$\Psi_{R,L} = \frac{1}{2}\left(\mathbf{1} \pm \Gamma^{\underline{r}}\right)\Psi. \tag{4.2}$$

For future reference, we also define the fields $\Psi_{\pm}$ by

$$\Psi_R = \left(\begin{array}{c} \Psi_+ \\ 0 \end{array}\right), \quad \Psi_L = \left(\begin{array}{c} 0 \\ \Psi_- \end{array}\right). \tag{4.3}$$

These components and fields satisfy the relations

$$\Gamma^{\underline{r}}\Psi_{R,L} = \pm\Psi_{R,L} \tag{4.4}$$
$$\Gamma^{\underline{r}}\Psi_{\pm} = \pm\Psi_{\pm}. \tag{4.5}$$

For completeness, we also consider the case when d is **odd**. In this case, the Γ matrices have twice the dimension of the γ matrices. Further, since $d+1$ is even, the Γ matrices constitute a reducible representation. One can then choose

$$\Gamma^{\underline{r}} = \mathbf{1}_{\lfloor\frac{d}{2}\rfloor} \otimes \mathbf{1}_{\lfloor\frac{d}{2}\rfloor}$$
$$\Gamma^{\underline{t}} = \mathbf{1}_{\lfloor\frac{d}{2}\rfloor} \otimes \gamma^{\underline{t}}$$
$$\Gamma^{\underline{i}} = \mathbf{1}_{\lfloor\frac{d}{2}\rfloor} \otimes \gamma^{\underline{i}},$$

assuming that the γ matrices constitute a representation of the Clifford algebra.

4.1.2   Curved spacetime

We now generalize our discussion to curved spacetime. In particular, we are interested in the setup of a bulk $(d+1)$-dimensional spacetime with a d-dimensional boundary. In accordance with our previous notation, we denote the bulk gamma matrices by Γ and the boundary gamma matrices by γ.

Describing the spinors coupled to gravity turns out to be rather intricate, however. The reason is that while bosons transform according to tensor representations of the general covariance group, this group does not admit finite-dimensional spinor representations. Thus, it is not clear how spinors are to transform under general coordinate transformations.

The Lorentz group, however, *does* admit finite-dimensional spinor representations. This opens up the possibility of describing spinor gravity by employing a *local* Lorentz representation at each spacetime point, and connecting these covariantly.

The vielbein basis

The natural basis for the tangent space T_x at the spacetime point x is given by the set of coordinate vectors $\hat{e}_\mu(x) = \partial_\mu$. The dual basis for the cotangent space T_x^* is then given by the set $\hat{e}^\mu = \theta^\mu$, which satisfy $\hat{e}^\mu(\hat{e}_\nu) = \delta^\mu_\nu$. However, we are free to choose any basis for T_x, and the convenient basis for this discussion is the *vielbein basis*. It is a basis, denoted $\hat{e}_{\underline{a}} \in T_x$, chosen such that

$$g\left(\hat{e}_{\underline{a}}, \hat{e}_{\underline{b}}\right) = \eta_{\underline{ab}},$$

---

[4]Of course, one can split Ψ into components Ψ_+ and Ψ_-, but these components do not transform independently under the action of the Lorentz group. Hence, they are not chiral components.

i.e. they constitute an orthonormal basis in which the space looks *flat*. The dual basis for T_x^* is denoted by $\hat{e}^{\underline{a}}$, and satisfies $\hat{e}^{\underline{a}}\left(\hat{e}_{\underline{b}}\right) = \delta_{\underline{b}}^{\underline{a}}$. At each spacetime point, then, we have two bases, which are therefore related by invertible linear transformations:

$$\hat{e}_\mu\left(x\right) = e_\mu^{\underline{a}}\left(x\right)\hat{e}_{\underline{a}}, \quad \hat{e}_{\underline{a}} = e_{\underline{a}}^\mu\left(x\right)\hat{e}_\mu.$$

The matrix $e_\mu^{\underline{a}}\left(x\right)$ is referred to as the *vielbein*, and $e_{\underline{a}}^\mu\left(x\right)$ as the *inverse vielbein*. They are related to each other via the relations

$$e_\nu^{\underline{a}}\left(x\right)e_{\underline{a}}^\mu\left(x\right) = \delta_\nu^\mu \qquad e_\mu^{\underline{a}}\left(x\right)e_{\underline{b}}^\mu\left(x\right) = \delta_{\underline{b}}^{\underline{a}}$$
$$g_{\mu\nu}e_{\underline{a}}^\mu e_{\underline{b}}^\nu = \eta_{\underline{ab}} \qquad e_\mu^{\underline{a}}e_\nu^{\underline{b}}\eta_{\underline{ab}} = g_{\mu\nu},$$

which can be derived in a straightforward manner from the above relations.

We still have remaining freedom when choosing the vielbein basis at each point x. Indeed, the above relations are still satisfied when transforming

$$\hat{e}_{\underline{a}} \to \Lambda_{\underline{a}}^{\underline{b}}\hat{e}_{\underline{b}},$$

where $\Lambda_{\underline{a}}^{\underline{b}}$ is a *local* Lorentz transformation. These transformations correspond to rotations and boosts applied to the tetrad basis in the tangent space at x.

The Latin indices $\underline{a}, \underline{b}, \ldots$ are referred to as local Lorentz indices, as they label tensor representations of the local Lorentz group. These indices are raised and lowered by the flat metric η. The Greek indices label tensorial objects on the manifold, and are raised and lowered by the Lorentzian metric g, as usual.

The relation between the coordinate basis and the vielbein basis implies the following relations between (co)vector components

$$\begin{aligned} V^{\underline{a}} &= e_\mu^{\underline{a}}V^\mu, \quad V^\mu = e_{\underline{a}}^\mu V^{\underline{a}} \\ W_{\underline{a}} &= e_{\underline{a}}^\mu W_\mu, \quad W_\mu = e_\mu^{\underline{a}}W_{\underline{a}}. \end{aligned}$$

In general, any (k, l) tensor can be expressed as a linear combination of tensor products of the vielbein and dual vielbein basis. Moreover, we can define the "curved" gamma matrices by

$$\gamma^\mu = e_{\underline{a}}^\mu\gamma^{\underline{a}}, \quad \Gamma^\mu = e_{\underline{a}}^\mu\Gamma^{\underline{a}},$$

with respect to the coordinate basis. One easily verifies that

$$\{\gamma^\mu, \gamma^\nu\} = 2g^{\mu\nu}\mathbb{1}, \quad \{\Gamma^\mu, \Gamma^\nu\} = 2g^{\mu\nu}\mathbb{1}.$$

The spin connection

We turn to parallel transport of vectors in the vielbein formalism, thus covariantly connecting the local Lorentz representations. The parallel transport of a vector in coordinate based general relativity is described by

$$\frac{D}{d\lambda}V^\mu \equiv \frac{dx^\nu}{d\lambda}\nabla_\nu V^\mu = 0,$$

with $\nabla_\nu V^\mu = \partial_\nu V^\mu + \Gamma_{\nu\sigma}^\mu V^\sigma$ the covariant derivative in terms of the Levi-Civita connection. In the vielbein formalism, the role of the Levi-Civita connection is played by the *spin connection*:

$$\nabla_\mu V^{\underline{a}} = \partial_\mu V^{\underline{a}} + \omega_{\mu\underline{b}}^{\underline{a}}V^{\underline{b}}.$$

One can regard the spin connection as a gauge field, introduced as a correction to the ordinary derivative, with the purpose of causing the covariant derivative of vectors to transform properly under local

Lorentz transformations. Indeed, the spacetime dependence of the Lorentz transformations spoils the transformation behavior of the ordinary derivative.

In order for the introduction of the vielbein formalism to not affect the ordinary formalism, the covariant derivative of vectors expressed in both the coordinate and the vielbein basis should agree. After some algebra - see Appendix B, one finds

$$\omega_{\mu\underline{b}}^{\underline{a}} = e_\nu^{\underline{a}}e_{\underline{b}}^\lambda \Gamma_{\mu\lambda}^\nu - e_{\underline{b}}^\lambda \partial_\mu \left(e_\lambda^{\underline{a}} \right)$$

in terms of the Levi-Civita connection.

The formalism derived up to this point allows us to define a covariant derivative for spinors, denoted again by Ψ. The covariant derivative takes the general form

$$\nabla_\mu \Psi = \partial_\mu \Psi + \Omega_\mu \Psi,$$

in terms of the connection Ω_μ. Recall that the bilinears $\bar{\Psi}\Psi$ and $\bar{\Psi}\gamma^{\underline{a}}\Psi$, with $\bar{\Psi} = \Psi^\dagger \Gamma^{\underline{t}}$ transform as a scalar and a vector under local Lorentz transformations, respectively. Requiring these combinations to transform in the same way under parallel transport, one finds the relations

$$
\begin{aligned}
\Gamma^{\underline{t}}\Omega_\mu^\dagger \Gamma^{\underline{t}} &= -\Omega_\mu \\
[\Gamma^a, \Omega_\mu] &= \omega_{\mu b}^a \Gamma^b
\end{aligned}
$$

have to be satisfied. This is solved by taking $\Omega_\mu = \frac{1}{8}\omega_{\mu ab}\left[\Gamma^{\underline{a}}, \Gamma^{\underline{b}}\right]$, which implies

$$\nabla_\mu \Psi = \left(\partial_\mu + \frac{1}{8}\omega_{\mu\underline{ab}}\left[\Gamma^{\underline{a}}, \Gamma^{\underline{b}}\right] \right) \Psi. \tag{4.6}$$

This is the definition of the covariant derivatives for spinors we will use.

In the following, we will consider the spacetime with the electron-star metric, which we will take to be of the form as in equation (2.5), namely

$$ds^2 = -\frac{r^2}{\ell^2}\tilde{f}(r)\,dt^2 + \tilde{g}(r)\frac{\ell^2}{r^2}dr^2 + \frac{r^2}{\ell^2}dx_i^2. \tag{4.7}$$

Here, the functions $\tilde{f}(r), \tilde{g}(r)$ are related to the electron-star solutions $f(u), g(u)$ as in equation (2.8). We will write $\tilde{f} \to f$ in the following, for simplicity. For the electron-star metric, the vielbeins take the form

$$
\begin{aligned}
e_{\underline{r}}^r &= \frac{r}{\ell\sqrt{g}} \\
e_{\underline{i}}^i &= \frac{\ell}{r} \\
e_{\underline{t}}^t &= \frac{\ell}{r\sqrt{f}}.
\end{aligned}
\tag{4.8}
$$

from which one derives (see Appendix B) the covariant derivatives

$$
\begin{aligned}
\nabla_r &= \partial_r \\
\nabla_i &= \partial_i + \frac{1}{2}\frac{r}{\ell^2\sqrt{g}}\Gamma^{\underline{i}}\Gamma^{\underline{r}} \\
\nabla_t &= \partial_t - \frac{1}{2}\frac{r}{\ell\sqrt{g}}\partial_r\left(\frac{r}{\ell}\sqrt{f}\right)\Gamma^{\underline{t}}\Gamma^{\underline{r}}.
\end{aligned}
\tag{4.9}
$$

4.1.3 The Dirac action

We turn to the Dirac action for the fermions in the electron-star spacetime, where we focus on the case that d is odd. With the discussion of the previous section at hand, our point of departure is the action

$$S_D = -ig_f \int d^{d+1}x \sqrt{-g}\, \bar{\Psi} \left[\frac{1}{2} \overset{\leftrightarrow}{\slashed{\nabla}} - i\slashed{A} - m \right] \Psi,$$

where a coupling g_f for the fermions has been introduced. Further, we have included a minimal coupling $\nabla_\mu \to \nabla_\mu - iA_\mu$ as the fermions are charged. Note that the charge of the fermions has been absorbed in the gauge field, as in Chapter 3. Finally, m is the mass of the fermions, which can be made dimensionless by scaling out e and κ. The dimensionless mass $\hat{m}$ then ranges between $\hat{m} \in [0, 1]$. As mentioned above, the spinor Ψ has the same dimensions in the bulk as it has on the boundary when d is odd, and can be written

$$\begin{aligned} \Psi &=& \Psi_R + \Psi_L \\ &=& \begin{pmatrix} \Psi_+ \\ 0 \end{pmatrix} + \begin{pmatrix} 0 \\ \Psi_- \end{pmatrix}. \end{aligned}$$

The components $\Psi_\pm$ are chiral components only when Ψ is restricted to $(d-1)$-dimensional space and satisfy equation (4.5).

We use the above action by introducing a cut-off radius r_0, which we later take to infinity.

$$\delta_{\Psi,\bar{\Psi}} S_D \;=\; \text{terms} - \frac{ig_f}{2} \int d^{d+1}x \sqrt{-g}\, \left[\bar{\Psi}\Gamma^r \nabla_r \left(\delta\Psi\right) - \nabla_r \left(\delta\bar{\Psi}\right) \Gamma^r \Psi \right].$$

We note that the contribution of the spinor connection vanishes on the surface $r = r_0$ due to our choice of gamma matrices, equation (4.1). One then finds

$$\begin{aligned} \delta_{\Psi,\bar{\Psi}} S_D &=& \text{EOM} - \frac{ig_f}{2} \int d^d x \sqrt{-h} e^r_{\underline{r}} \left[\bar{\Psi}\Gamma^{\underline{r}} \delta\Psi - \delta\bar{\Psi}\Gamma^{\underline{r}}\Psi \right] \\ &=& \text{EOM} - \frac{ig_f}{2} \int d^d x \sqrt{-h} e^r_{\underline{r}} \left[\bar{\Psi}_R \Psi_L \right] \end{aligned}$$

by splitting up $\Psi = \Psi_R + \Psi_L$ and using (4.4). Here EOM denotes a collection of terms that are to become the equations of Ψ and $\bar{\Psi}$. Explicitly, the Ψ contribution is

$$\Gamma^\mu \left(\nabla_\mu - iA_\mu \right) \Psi - m\Psi \;=\; 0 \tag{4.10}$$

as one would expect: this is simply the Dirac equation for Ψ, coupled to the gauge field A_μ. In order for these terms to become the equations of motion, however, the rest of the action needs to vanish under variations. We can specify a Dirichlet boundary condition at the cut-off surface, namely either $\delta\Psi_L = 0$ or $\delta\Psi_R = 0$, but we are always left with additional terms that do not vanish. Thus, we need to add a counter-term, which we take to be

$$S_\partial = \mp i\frac{g_f}{2} \int d^d x \sqrt{-h} e^r_{\underline{r}} \left[\bar{\Psi}_L \Psi_R + \bar{\Psi}_R \Psi_L \right] \tag{4.11}$$

with the choice of signs $-$ for picking $\delta\Psi_R = 0$, $+$ for picking $\delta\Psi_L = 0$. With this counter term, the total action indeed has zero variations. However, we are going to be interested in obtain the *retarded* Green's function, which means we have to drop one of the terms in this boundary action as in ref. [14], depending on the Dirichlet boundary condition. It turns out that keeping both terms yields a real propagator, instead of a retarded or advanced Green's function. Choosing the Dirichlet condition $\delta\Psi_R = 0$ ($\delta\Psi_L = 0$) means we have to drop the first (second) term. In the following, we will choose $\delta\Psi_R = 0$ without loss of generality.

We are free to add additional terms, as long as we keep satisfying this requirement. A necessary additional term is

$$S_{UV} = -iZ \int d^d x \sqrt{-g} \bar{\Psi}_R \left[\overset{\rightarrow}{\nabla} - i\slashed{A} \right] \Psi_R \tag{4.12}$$

which will describe the free dynamics of a chiral fermion Ψ_R on the boundary. We will indicate why this term is necessary in section 4.2.2.

The total action, then, is given by

$$
\begin{aligned}
S &= -ig_f \int d^{d+1} x \sqrt{-g}\, \bar{\Psi} \left[\frac{1}{2} \overset{\leftrightarrow}{\slashed{\nabla}} - i\slashed{A} - m \right] \Psi - ig_f \int d^d x \sqrt{-h} \left(e_r^r \right) \left[\bar{\Psi}_R \Psi_L \right] \\
&\quad -iZ \int d^d x \sqrt{-g} \left[\bar{\Psi}_R \left[\overset{\rightarrow}{\nabla} - i\slashed{A} \right] \Psi_R \right].
\end{aligned}
\tag{4.13}
$$

4.2 The chiral fermion

Having obtained the Dirac action, we turn our attention to the description of the chiral fermion on the spacetime boundary. For this, we consider the Dirac equation (4.10) and derive an equivalent equation. This equation is used to integrate out one of the chiral components of the Dirac spinor, leaving us with an effective action for a chiral fermion on the boundary, described by the remaining chiral component. From this effective action, we derive the retarded Green's function and the spectral density of this chiral fermion.

In the previous discussions, we had assumed d to be odd, but otherwise arbitrary. In the following, we will explicitly consider the case $d + 1 = 5$.

4.2.1 The Dirac equation

Our first goal will be to rewrite the Dirac equation, obtained from the action S, as a different equation. For this, we first note that the Dirac equation (4.10) itself implies the relation

$$\Psi_- = -i\xi \Psi_+ \tag{4.14}$$

in momentum space between the chiral components of Ψ, where ξ is a 2×2 matrix. Indeed, the Dirac equation in terms of the chiral components becomes two equations of the form

$$\eta_+ \Psi_+ + \eta_- \Psi_- = 0$$

where $\eta_\pm$ are 2×2 matrices. This clearly relates the two chiral components by a 2×2 matrix as in (4.14). Moreover, if we rotate our axes such that $\mathbf{k} = (0, 0, k_3)$, the matrices $\eta_\pm$ involved are sums of diagonal matrices, as only the identity matrix and σ^3 are involved in gamma-matrix expansion in the Dirac equation. Thus, the matrix ξ will be diagonal, providing the relation

$$\left(\begin{array}{c} u_- \\ d_- \end{array} \right) = -i \left(\begin{array}{cc} \xi_+ & 0 \\ 0 & \xi_- \end{array} \right) \left(\begin{array}{c} u_+ \\ d_+ \end{array} \right), \tag{4.15}$$

where $u_\pm$, $d_\pm$ are the components of $\Psi_\pm$. Then, one can read off

$$\xi_+ = i \frac{u_-}{u_+}, \quad \xi_- = i \frac{d_-}{d_+}. \tag{4.16}$$

We now turn to the bulk Dirac equation, writing a plane-wave ansatz for Ψ. From equations (4.10), (4.8) and (4.9) we find

$$
\begin{aligned}
0 &= \left(\slashed{\nabla} - i\slashed{A} - m \right) \Psi\left(r\right) e^{ikx} \\
&= \left(\Gamma^{\underline{r}} e^r_{\underline{r}} \partial_r + \Gamma^{\underline{t}} e^t_{\underline{t}} \left(\partial_t - \frac{r}{2\ell\sqrt{g}} \partial_r \left(\frac{r}{\ell}\sqrt{f} \right) \Gamma^{\underline{t}}\Gamma^{\underline{r}} - iA_t \right) + \Gamma^{\underline{i}} e^i_{\underline{i}} \left(\partial_i + \frac{r}{2\ell^2\sqrt{g}} \Gamma^{\underline{i}}\Gamma^{\underline{r}} \right) - m\mathbf{1} \right) \Psi\left(r\right) e^{ikx} \\
&= \left(\Gamma^{\underline{r}} \frac{r}{\ell\sqrt{g}} \partial_r + i\frac{\ell}{r} \left(\Gamma^{\underline{i}} k_i - \frac{(\omega + A_t)}{\sqrt{f}} \Gamma^{\underline{t}} \right) + \frac{1}{2} \frac{1}{\ell\sqrt{fg}} \partial_r \left(r\sqrt{f} \right) \Gamma^{\underline{r}} + \frac{(d-1)}{2\ell\sqrt{g}} \Gamma^{\underline{r}} - m\mathbf{1} \right) \Psi\left(r\right) e^{ikx}
\end{aligned}
$$

Introducing new notation, let $\tilde{k} = (-\tilde{\omega}, \mathbf{k})$ and $\Gamma \cdot \tilde{k} = \Gamma^{\underline{i}} k_i + \tilde{\omega}\Gamma^{\underline{t}}$, with $\tilde{\omega} = \frac{-(\omega + A_t)}{\sqrt{f}}$. Next, define $p_z\left(r\right) = \frac{1}{\ell\sqrt{fg}} \partial_r \left(r^z \sqrt{f} \right) + \frac{(d-1)}{\ell\sqrt{g}}$. In terms of these, the above equation becomes

$$
\begin{aligned}
0 &= \left(\Gamma^{\underline{r}} \frac{r}{\ell\sqrt{g}} \partial_r + i\frac{\ell}{r}\Gamma \cdot \tilde{k} + \frac{1}{2} p_z\left(r\right) \Gamma^{\underline{r}} - m\mathbf{1} \right) \Psi\left(r\right) e^{ikx} \\
&= \left(\Gamma^{\underline{r}} \frac{r^2}{\ell\sqrt{g}} \partial_r + i\ell\Gamma \cdot \tilde{k} - rm\mathbf{1} \right) \Phi,
\end{aligned}
$$

where in the last line we have defined $\Phi\left(r\right) = e^{\frac{\ell}{2} \int^r d\tilde{r} \sqrt{g(\tilde{r})} p_z(\tilde{r})/\tilde{r}} \Psi\left(r\right)$. The components of Φ, which we denote $\tilde{u}_\pm$ and $\tilde{d}_\pm$, are then easily shown to satisfy the set of equations

$$
\begin{aligned}
A\left(m\right) \tilde{u}_+ = i\ell \left(\tilde{\omega} - k_3 \right) \tilde{u}_- \qquad & A\left(-m\right) \tilde{u}_- = i\ell \left(k_3 + \tilde{\omega} \right) \tilde{u}_+ \\
A\left(m\right) \tilde{d}_+ = i\ell \left(\tilde{\omega} + k_3 \right) \tilde{d}_- \qquad & A\left(-m\right) \tilde{d}_- = i\ell \left(\tilde{\omega} - k_3 \right) \tilde{d}_+,
\end{aligned}
\tag{4.17}
$$

where $A\left(m\right) \equiv r \left(\frac{r}{\ell\sqrt{g}} \partial_r - m \right)$. Finally, from the definition of the function Φ, we have

$$
\begin{aligned}
\xi_+ &= i\frac{u_-}{u_+} = i\frac{\tilde{u}_-}{\tilde{u}_+} \\
\xi_- &= i\frac{d_-}{d_+} = i\frac{\tilde{d}_-}{\tilde{d}_+},
\end{aligned}
$$

which we use to write down an equation for $\xi_\pm$. From the set of equations (4.17), we find

$$
\begin{aligned}
\frac{r^2}{\ell\sqrt{g}} \partial_r \xi_+ &= \frac{ir^2}{\ell\sqrt{g} u_+} \left[\partial_r u_- - \frac{u_-}{u_+} \partial_r u_+ \right] \\
&= -\ell \left(k_3 + \tilde{\omega} \right) - 2mr\xi_+ - \ell\xi_+^2 \left(\tilde{\omega} - k_3 \right)
\end{aligned}
$$

and a similar equation for ξ_-. Combining these equations, we obtain

$$
\frac{r^2}{\ell\sqrt{g}} \partial_r \xi_\pm + 2mr\xi_\pm = \ell \left(\frac{\omega + A_t}{\sqrt{f}} \mp k_3 \right) + \ell\xi_\pm^2 \left(\frac{\omega + A_t}{\sqrt{f}} \pm k_3 \right).
\tag{4.18}
$$

In order to solve this equation, we need to specify a boundary condition. Because we are ultimately interested in finding the retarded Green's function, we have to take in-falling boundary conditions. We will take

$$
\xi_\pm\left(0, \omega, k_3\right) = i
\tag{4.19}
$$

for $\omega \neq 0$. This follows from the above equation by considering the limit $r \to 0$, entering the exact Lifshitz solutions in the r coordinate frame. This yields

$$
\xi_\pm^2 = -1
$$

and hence $\xi_+ = \pm i$ and $\xi_- = \pm i$. The sign can be fixed by looking at the equations for the components $u_\pm, d_\pm$. In order to get in-falling boundary conditions, we should pick the plus sign.

Further, equation (4.18) for $\xi_\pm$ exhibits the symmetry

$$\xi_+(k_3) = \xi_-(-k_3), \tag{4.20}$$

which will simplify our numerical calculation.

4.2.2   Green's function

We turn to a description of a chiral fermion on the boundary of spacetime. For this, we invoke equation (4.14) to integrate out one of the chiral components of the Dirac spinor Ψ, obtaining an effective boundary action S_{eff}.

Using the Fourier transform

$$\Psi_\pm(r, x) = \int \frac{d^d k}{(2\pi)^d} \Psi_\pm(r, p) e^{ikpx^\mu},$$

and integrating out Ψ_-, one obtains

$$S_{\text{eff}}[\Psi_+] = \int \frac{d^d k}{(2\pi)^d} \sqrt{-g}\, \Psi_+^\dagger \left[g_f \sqrt{g^{rr}} \xi(\omega, \mathbf{k}) - Z\sigma^{\underline{a}} e_{\underline{a}}^\mu (k_\mu - A_\mu) \right] \Psi_+,$$

where $\sigma^{\underline{a}} = \left(1, \sigma^{\underline{i}}\right)$. Here, the second term originates from the S_{UV} action we have introduced by hand, while the first is a result of the boundary term S_∂ which introduces a coupling between Ψ_+ and Ψ_-. Explicitly entering the expressions for the vielbeins (4.8) and the metric (4.7), we find

$$S_{\text{eff}}[\Psi_+] = \int \frac{d^d k}{(2\pi)^d} \sqrt{fg}\frac{r^{d-1}}{\ell^{d-1}} \Psi_+^\dagger \left[\frac{r_0^2 g_f}{\ell^2 \sqrt{g}} \xi(\omega, \mathbf{k}) + \frac{Z}{\sqrt{f}} (\omega + e\, h) - Z\boldsymbol{\sigma} \cdot \mathbf{k} \right] \Psi_+.$$

Now we perform a rescaling of the fields

$$\Psi_+ \to Z^{-1/2} g^{-1/4} \left(\frac{r_0}{\ell}\right)^{(1-d)/2} \Psi_+$$

to get

$$S_{\text{eff}}[\Psi_+] = \int \frac{d^d k}{(2\pi)^d} \Psi_+^\dagger \left[\omega + e\, h - \sqrt{f}\boldsymbol{\sigma} \cdot \mathbf{k} + \frac{g_f}{Z} \sqrt{\frac{f}{g}} \frac{r_0^2}{\ell^2} \xi(r_0, \mathbf{k}) \right] \Psi_+. \tag{4.21}$$

The spectral function

From the effective action (4.21), one finds the inverse retarded Green's function G_R^{-1} as the term within brackets, so that

$$G^{-1}(\omega, \mathbf{k}, r_0) = \left[\omega + eh(r_0) - \sqrt{f(r_0)}\boldsymbol{\sigma} \cdot \mathbf{k} + \frac{g_f}{Z} \sqrt{\frac{f(r_0)}{g(r_0)}} \frac{r_0^2}{\ell^2} \xi(r_0, \mathbf{k}) \right].$$

This describes the propagation of a chiral fermion associated with Ψ_+ on the UV-slice at r_0. Now, our goal is to consider this description on the boundary of the spacetime, so we now considering a limiting procedure with $r_0 \to \infty$. From equation (3.23), it is clear that

$$\begin{aligned} \sqrt{f} &\to c \\ \sqrt{g} &\to 1. \end{aligned}$$

Next, we use the fact that $\xi \sim r_0^{-2m}$ as $r_0 \to \infty$ which is clear from the large r behavior of equation (4.18). See also ref. [14]. Therefore,

$$r_0^{2m}\xi\left(r_0, \mathbf{k}\right) \to \text{constant}.$$

In order to keep the retarded Green's function finite on the boundary when taking the limit, we require

$$g \equiv c\frac{g_f}{Z}\frac{r_0^{2-2m}}{\ell^{2-2m}} \to \text{constant}.$$

After taking these limits, the inverse retarded Green's function takes the form

$$G_R^{-1}\left(\omega, \mathbf{k}\right) = \left[\omega + \mu - c\boldsymbol{\sigma} \cdot \mathbf{k} - \Sigma\left(\omega, \mathbf{k}\right)\right]. \tag{4.22}$$

The final term, defined by

$$\Sigma\left(\omega, \mathbf{k}\right) \equiv -g \lim_{r_0 \to \infty} r_0^{2m}\xi\left(r_0, \omega, \mathbf{k}\right),$$

follows from the boundary action S_∂, while the first three terms follow from the free boundary action S_{UV}. This is why we had to add this term to the action: without it, the retarded Green's function would not have a free part. Further, as we will see in the next section, without this part the associated spectral function will not satisfy a certain sum rule to be introduced in the next section. We now invert equation 4.22, in the case $\mathbf{k} = (0, 0, k_3)$. Invoking the symmetry (4.20), the matrix ξ as in equation (4.15) can be written as

$$
\begin{aligned}
\xi &= \begin{pmatrix} \xi_+\left(\omega, k_3\right) & 0 \\ 0 & \xi_-\left(\omega, k_3\right) \end{pmatrix} \\
&= \frac{1}{2}\xi_+^{\mathrm{sym}}\left(\omega, k_3\right)\mathbf{1} + \frac{1}{2}\xi_+^{\mathrm{asym}}\left(\omega, k_3\right)\sigma^3
\end{aligned}
$$

where

$$
\begin{aligned}
\xi_+^{\mathrm{sym}} &= \xi_+\left(k_3\right) + \xi_+\left(-k_3\right) & (4.23) \\
\xi_+^{\mathrm{asym}} &= \xi_+\left(k_3\right) - \xi_+\left(-k_3\right). & (4.24)
\end{aligned}
$$

Since the self-energy is proportional to the matrix ξ, we can expand it in terms of the same matrices

$$\Sigma\left(\omega, \mathbf{k}\right) = \Sigma_0\mathbf{1} + \Sigma_3\sigma^3,$$

from which one can read off

$$
\begin{aligned}
\Sigma_0 &= -\frac{g}{2}\lim_{r_0 \to \infty} r_0^{2m}\xi_+^{\mathrm{sym}}\left(\omega, k_3\right) & (4.25) \\
\Sigma_3 &= -\frac{g}{2}\lim_{r_0 \to \infty} r_0^{2m}\xi_+^{\mathrm{asym}}\left(\omega, k_3\right). & (4.26)
\end{aligned}
$$

With this, one writes 4.22 in matrix form, and finds the retarded Green's function

$$
\begin{aligned}
G_R\left(\omega, k_3\right) &= \begin{pmatrix} \omega + \mu - \Sigma_0 - \Sigma_3 - k_3 & 0 \\ 0 & \omega + \mu - \Sigma_0 + \Sigma_3 + k_3 \end{pmatrix}^{-1} \\
&= \frac{\left(\omega + \mu - \Sigma_0\right)\mathbf{1} + \left(k_3 + \Sigma_3\right)\sigma^3}{\left(\omega + \mu - \Sigma_0\right)^2 - \left(\Sigma_3 + k_3\right)^2}.
\end{aligned}
$$

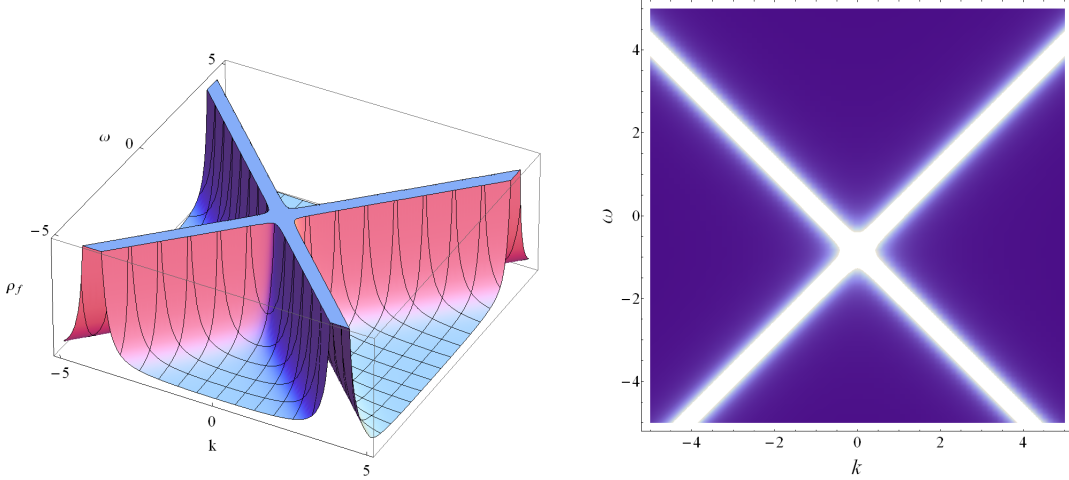The retarded Green's function in turn defines the spectral weight function ρ, by

Figure 4.1: The free spectral function (4.28) as a function of the energy ω and momentum k_3 of a chiral fermion. The bands have been broadened via $\omega \to \omega + i\epsilon$, with $\epsilon = 10^{-10}$, and shifted down via $\omega \to \omega + \mu$ with $\mu = 1$.

$$
\begin{aligned}
\rho\left(\omega, k_3\right) & \equiv -\frac{1}{2\pi} \text{Im}\left[\text{Tr}\left[G_R\left(\omega, k_3\right)\right]\right] \\
& = -\frac{1}{\pi} \text{Im}\left[\frac{\omega + \mu - \Sigma_0}{\left(\omega + \mu - \Sigma_0\right)^2 - \left(k_3 + \Sigma_3\right)^2}\right].
\end{aligned}
\tag{4.27}
$$

The spectral function gives information about the states accessible to the particles; it can be interpreted as a single particle density of states. It is incredibly important as it can be directly measured using angle-resolved photo-emission spectroscopy (ARPES) in solid-state systems, and radio-frequency spectroscopy in ultra cold atoms. Clearly, from (4.23) and (4.24) and the definition of Σ_0 and Σ_3, the spectral weight function is symmetric in k_3.

Another important property of spectral functions is the so-called ARPES sum rule

$$
\int_{-\infty}^{\infty} \rho\left(\omega, k\right) d\omega = 1,
$$

valid for any k. This rule follows directly from the anti-commutation relations of the fermionic single particle operators, see ref. [26]. It is this sum rule that necessitates the addition of the action S_{UV}, equation (4.12). Without it, the retarded Green's function would not have a free part, and would not satisfy this rule.

An important simple case to consider is the free fermion case with a chemical potential, i.e. when the self-energy Σ vanishes. In this case, the spectral weight function takes the form

$$
\rho_f\left(\omega, k_3\right) = -\frac{1}{\pi} \text{Im}\left[\frac{\omega + i\epsilon + \mu}{\left(\omega + i\epsilon + \mu\right)^2 - k_3^2}\right],
\tag{4.28}
$$

where a small imaginary part is added to avoid the poles on the real axis. This function is plotted in Figure 4.1 and will also serve as a comparison to the interacting spectral function we will plot later.

In the figure, the spectral function has a distinct cross-like shape, which is due to the linear dispersion of the chiral fermion. This shape consists of narrow peaks which would be delta peaks, were

it not for the small imaginary part of ω, broadening the peaks uniformly. The addition of the chemical potential shifts the structure down on the ω axis. By integrating the free spectral function, it can be shown easily it satisfies the ARPES sum rule.

In the interacting case, we would expect roughly the same picture, except that the broadening of the peaks will be nonuniform: the self-energy is a function of ω and k_3 as well. Further, we also expect the interacting spectral function to satisfy the sum rule.

4.3   Numerical calculation

We now turn to the numerical calculation. The goal is to plot the spectral weight function, equation (4.27), as a function of ω and k_3, for various values of $\hat{m}$ and z. For this, we numerically solve the differential equation (4.18), in the form

$$\frac{r^2}{\sqrt{g}}\partial_r\xi_\pm + 2\hat{m}r\xi_\pm = \left(\frac{\hat{\omega}+h}{\sqrt{f}}\mp\hat{k}_3\right) + \xi_\pm^2\left(\frac{\hat{\omega}+h}{\sqrt{f}}\pm\hat{k}_3\right)$$

where we have scaled out $\frac{e}{\kappa}$ and put $\ell = 1$. This equation is to be solved with the initial condition

$$\xi_\pm\left(0,\hat{\omega},\hat{k}_3\right) = i$$

for $\hat{\omega} \neq 0$. To this end, we invoke the solutions for f, g and h from Chapter 3, transformed to the r coordinate system. Further, we can simplify the calculation by focusing on $\hat{k}_3 \geq 0$ only, due to the symmetry $\xi_+\left(-\hat{k}_3\right) = \xi_-\left(\hat{k}_3\right)$, equation (4.20).

The above equation is first solved in the interior of the star, where f, g, h are given by the numerical solutions. We introduce a cutoff ϵ close to zero, at which we start numerically integrating using the initial condition. Of course, one needs to check if ϵ is small enough by calculating ρ at various choices for ϵ.
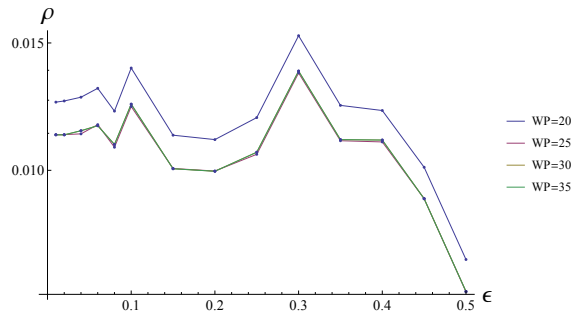

Figure 4.2: A plot of the spectral function ρ at fixed $\hat{\omega} = 0.5$, $\hat{k}_3 = 1$, $\hat{m} = 0.4$ and Lifshitz parameter $z = 2$, for various infrared cut-off values ϵ and values for the Working Precision WP of the numerical integration. There is a clear convergence with respect to both a smaller value of ϵ and a larger value of the Working Precision.

The behavior of the spectral function for various ϵ at fixed parameter values is shown in Figure 4.2. A degree of convergence of the spectral function is seen for small values of ϵ. Unfortunately, the stiffness of equation (4.18) for small r yields a enormous increase of computational time for even smaller ϵ. The convergence exhibited by the spectral function is well enough to trust the results considered here at at choice of $\epsilon = 10^{-2}$, but for precise analysis of the behavior of the spectral function requires a better numerical computational scheme. One possibility is consider only the dominant terms in the
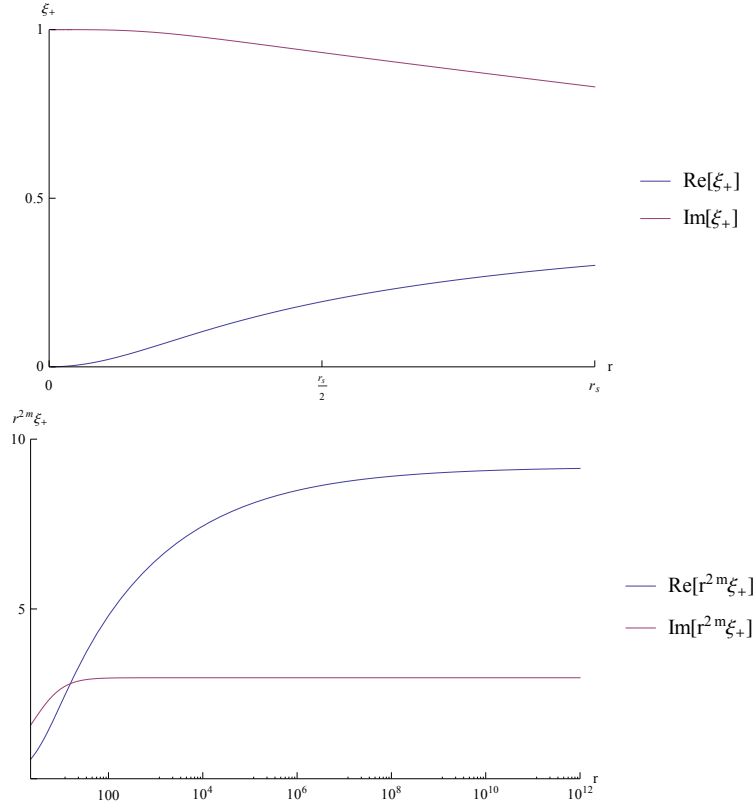
Figure 4.3:   A plot of ξ_+ inside the star $r \leq r_s$ (left) and a log-plot of $r^{2m}\xi_+$ outside the star $r \geq r_s$ (right). Here, the fermion mass is $\hat{m} = 0.4$, the Lifshitz scaling parameter is $z = 2$, while the fermion energy and $z-$momentum are given by $\left(\hat{\omega}, \hat{k}_3\right) = (1, 0)$. The ultraviolet cut-off is $r_0 = 10^{12}$, while the infrared cut-off is $\epsilon = 10^{-2}$. A convergence of $r^{2m}\xi_+$ for large r is seen.

differential equations at small r, yielding a differential equation that may be solved analytically. The resulting exact solution can then be used to start the numerical integration closer to $r = 0$. However, such a computational scheme falls outside the scope of this thesis.

Next, after having introduced the cutoff, we integrate up to the radius of the star $r_s = u_s^{-1}$, after which we continue solving the same equation outside the star, starting from an initial condition at r_s calculated from the solution inside the star. Then, we integrate up to a large value r_0, taken such that

$$r_0^{2m}\xi\left(r_0, \hat{\omega}, \hat{k}_3\right) = \text{const.}$$

We plot the real and imaginary parts of $r^{2m}\xi_\pm$ in Figure 4.3, both inside and outside the star.

After having solved the differential equations for $\xi_\pm$, we simply calculate Σ_0 and Σ_3 from (4.25) and (4.26), and hence the spectral function from the formula (4.27). This procedure is repeated for a range of values $\left(\hat{\omega}, \hat{k}_3\right)$ with $\omega \neq 0$. The spectral weight functions for various masses $\hat{m}$ and IR Lifshitz parameters z are shown in Figure 4.4.
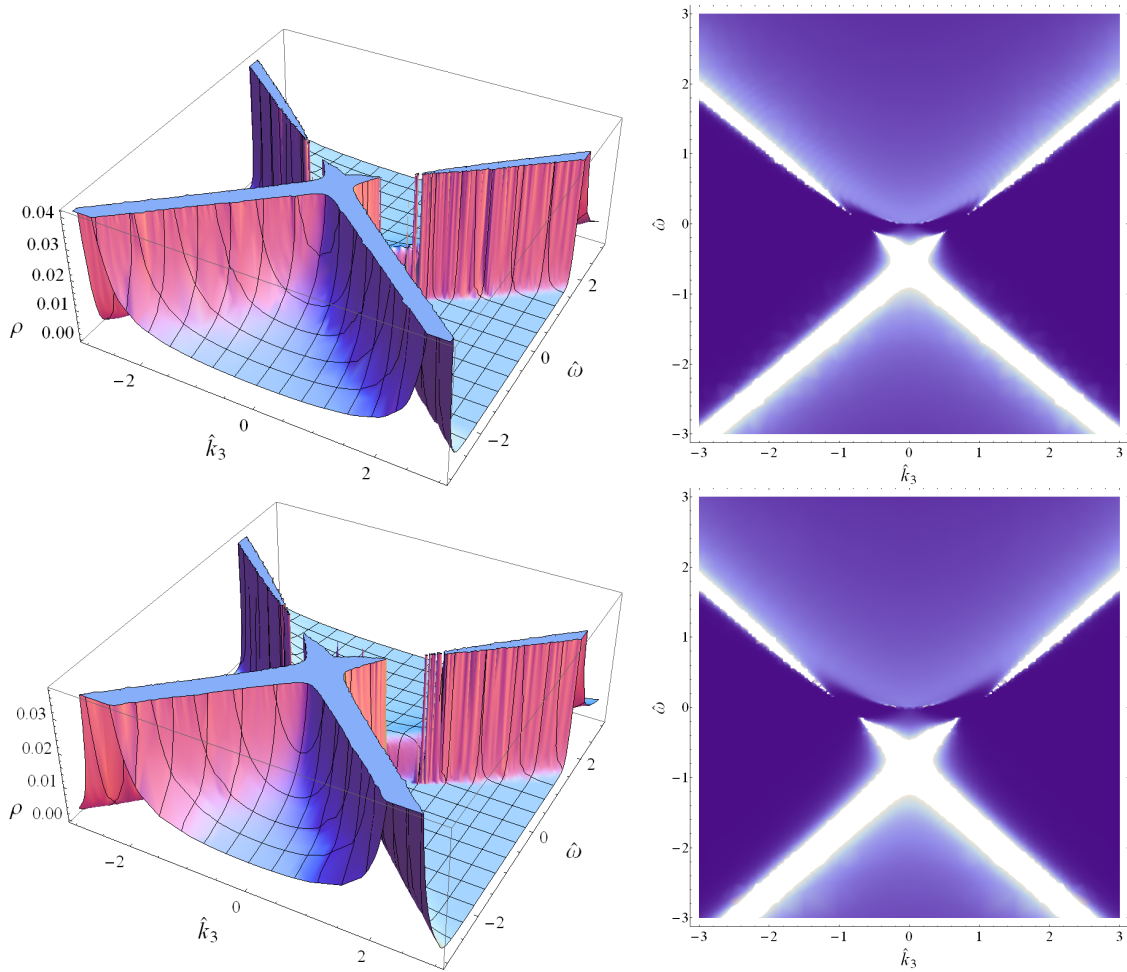
Figure 4.4: The interacting spectral function (4.27) as a function of the energy $\hat{\omega}$ and $z-$momentum $\hat{k}_3$ of a chiral fermion. Here, the Lifshitz parameter is $z = 1.75$ (top) and $z = 2$ (bottom) while $\hat{m} = 0.4$.

In these figures, several properties of the interacting spectral function can be seen. First of all, a clear cross-like shape as in Figure 4.1 is visible, indicating relativistic scaling for high energies. This relativistic scaling is, of course, a consequence of the asymptotically Anti-deSitter structure of the electron-star spacetime. Further, the presence of a chemical potential μ, which is the boundary value of the gauge field in the bulk, shifts the bands down.

Near $\hat{\omega} = 0$ the spectral function appears to vanish, visible by a gap in the cross. In this region, the imaginary part of the self-energy becomes zero. As in the free case, we would expect a delta peak to be present at $\hat{\omega} = 0$, as there is no imaginary part in the Green's function to produce a broadening of the lines. This is indicative of a Fermi surface, as a peak corresponds to a pole in the Green's function G_R. However, the nature of this Fermi surface is still unknown - for this, we would need to find how precisely the spectral function vanishes near zero energy.

Also visible in these figures is the presence of a plateau at low energies $\hat{\omega}$, resulting purely from the self-energy of the chiral fermion. These plateaus are seen to be bounded by $\hat{\omega} \sim k_3^z$. The explanation for this scaling behavior is that the low energy excitations correspond to the infrared of the electron-star spacetime, by the geometric realization of the renormalization group as discussed in section 2.1.2. As we have seen, the anisotropic scaling in the infrared Lifshitz geometry of the electron-star spacetime implies the given relation between the energy and momentum of the chiral fermion, see section 2.2.1.
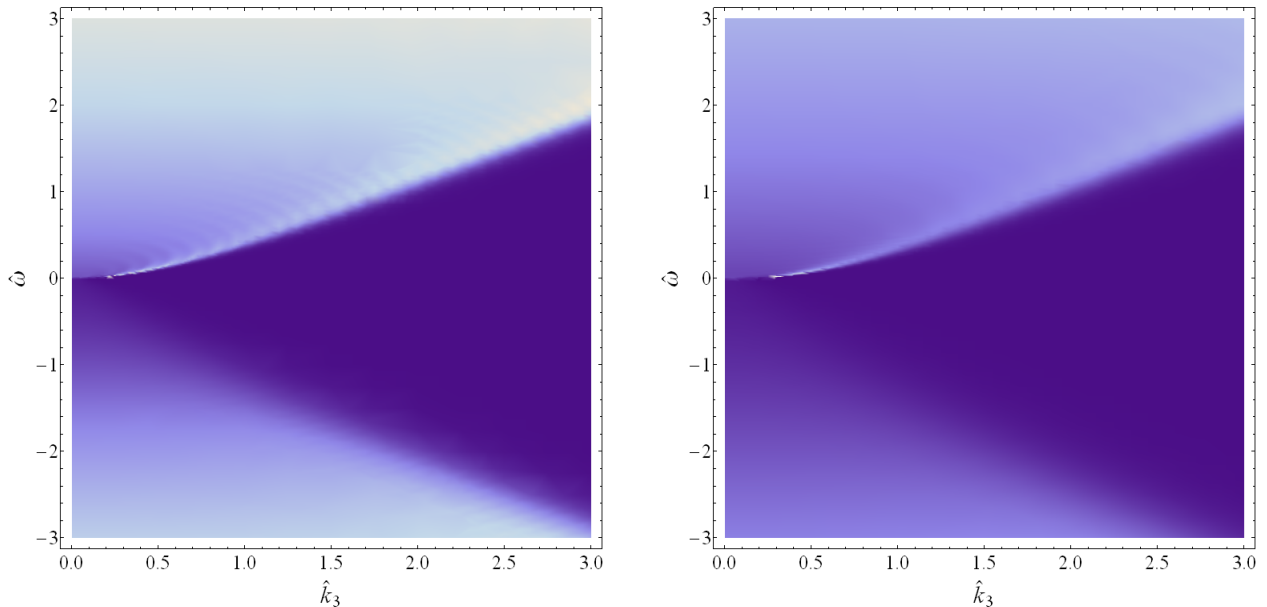
Figure 4.5: The spectral function ρ_{aq} (4.29) in the alternative quantization scheme as a function of energy $\hat{\omega}$ and $z-$momentum $\hat{k}_3$. Here, $\hat{m} = 0.4$ and $z = 1.75$ (left) and $z = 2$ (right).

The scaling behavior for low energies was also found in ref. [27], where the probe-fermions are treated in a WKB-limit.

We can also plot the results of purely holographic computation, i.e. without the free part of the Green's function that was added by hand. For comparison with ref. [27], we determine this Green's function in an alternative quantization scheme. In this scheme, the Dirichlet condition $\delta\Psi_- = 0$ is chosen on the boundary, rather than the condition $\delta\Psi_+ = 0$ that we have used. Effectively, this means the matrix ξ is inverted everywhere, which results in

$$
\begin{aligned}
\rho_{\mathrm{aq}} &\equiv -\frac{1}{2\pi}\mathrm{Im}\left[\mathrm{Tr}\left[G_R\right]\right] \\
&= \frac{1}{\pi}\mathrm{Im}\left[\Sigma_0\right].
\end{aligned}
\tag{4.29}
$$

This spectral function is plotted in Figure 4.5, for the same mass and Lifshitz parameters as before.

Finally, it is interesting to see the effect of the fermion backreaction in comparing the results found here with the results of the AdS-RN model. In the AdS-RN, the fermion backreaction is turned off, but the same computation as considered here can be done. In the latter model, multiple Fermi surfaces appeared at a large chemical potential, see ref. [15]. In particular, this behavior was found at values of the chemical potential larger than at least $\mu = 2\sqrt{2}$. By tuning the parameter z, invoking Figure 3.5, we can achieve such values of the chemical potential in the electron-star model as well. Unfortunately, the resulting numerical calculation is much slower. Hence, in Figure 4.6, we plot the interacting spectral function as a function of $\hat{\omega}$ at fixed values of $\hat{k}_3$. As $\hat{k}_3$ increases, we see the two peaks - corresponding to the free part of the Green's function - growing further apart. In this figure, just as in the previous figures of the spectral function, only one Fermi surface is present. Thus, the electron-star model appears to solve the issue of the emergence of multiple Fermi surfaces at large chemical potentials by taking into account the fermion backreaction. This can be traced back to the fact that the Reissner-Nordström black hole has a non-zero entropy at zero temperature. Because of

this we would not expect this model to yield the ground state. Instead, the electron star does have a zero entropy at absolute zero, as its constituent ideal fermion fluid satisfies this property.
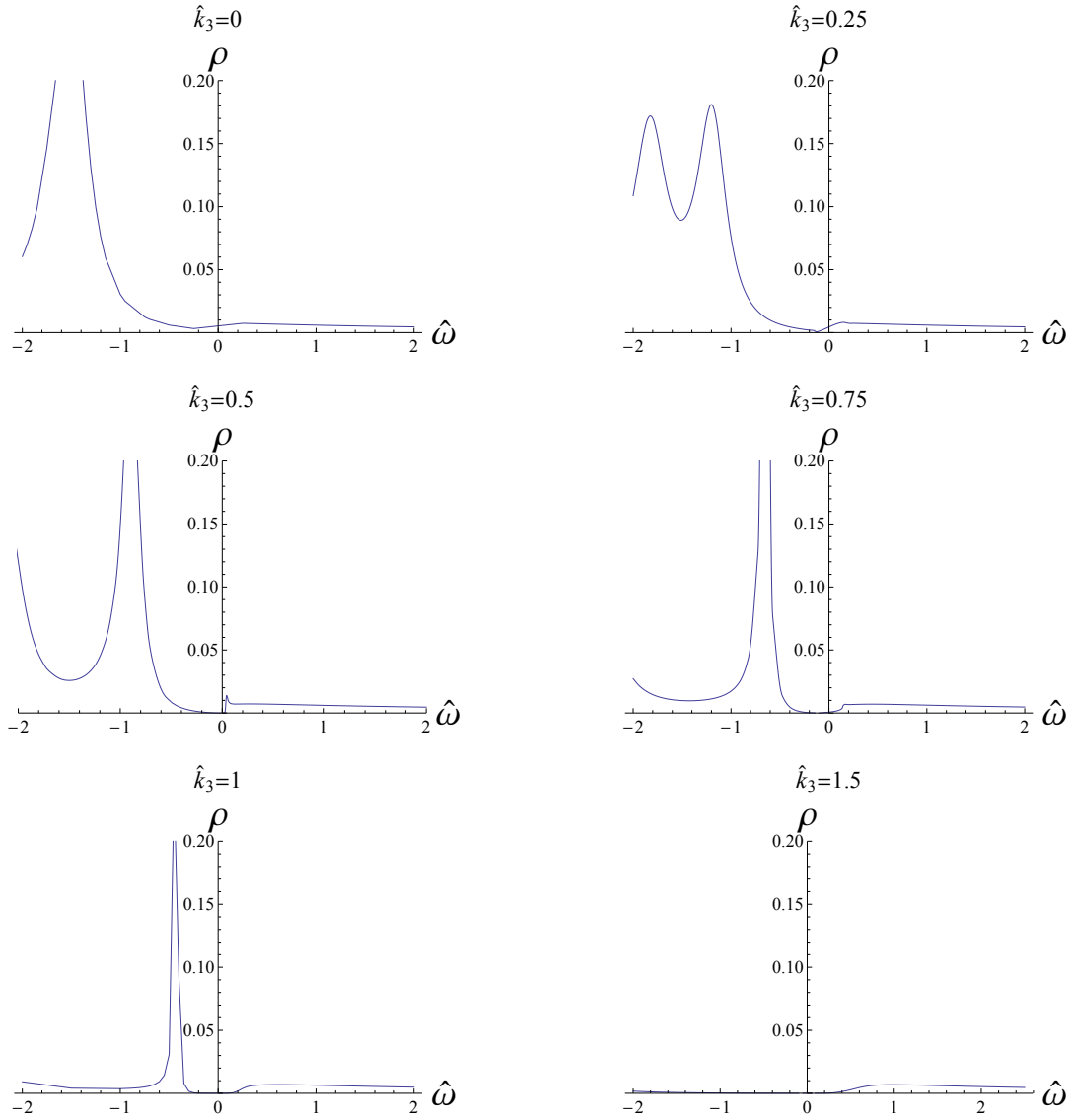

Figure 4.6: The spectral function at fixed values of $\hat{k}_3$ as a function of $\hat{\omega}$. Here, the Lifshitz parameter is $z = 2.5$, which corresponds to a chemical potential of $\mu \approx 1.6$.

Chapter 5

Conclusion and outlook

Conclusion

The holographic duality is a powerful tool which can be used to gain insight into the universal behavior of strongly coupled systems in condensed-matter physics. This is incredibly useful, as conventional theoretical investigations are generally not successful in these cases. The electron-star model is a relatively simple model within this framework, but still allows insight into a general class of strongly coupled systems The goal of this thesis was to study the electron star as a holographic dual for strongly coupled systems at a non-zero density. We have done so by first solving the electron-star model and subsequently adding additional fermions to determine the fermion correlator and the spectral function of a chiral spinor on the boundary of the electron-star spacetime.

In Chapter 2, we provided a brief introduction to the holographic duality and considered its application to condensed-matter physics. We discussed the generalization to Lifshitz spacetimes as a way of obtaining models dual to systems at anisotropic criticality. We discussed the Lifshitz black brane model in more detail, solving the equations of motion exactly.

With this introduction at hand, we introduced the electron-star model in Chapter 3. By taking the fluid limit of the fermions we were able to take the fermion backreaction into account. The equations of motion were then derived and solved numerically. Although we were able to derive and solve the equations of motion in any spacetime dimension, we focused on the case $d+1 = 5$, since this corresponds to a four-dimensional field theory on the boundary. In principle, our analysis can be carried out for higher spacetime dimensions.

Once the electron-star background was found, additional probe-fermions governed by the full Dirac action were added to the electron-star model Chapter 4. We introduced the Dirac action and added a free part by hand. The Dirac equation was used to integrate out one of the components of the fermion, thus obtaining an effective action of a chiral fermion. From this, we were able to determine the retarded Green's function in terms of the chiral fermion self-energy. By solving the Dirac equation, we were able to determine the self-energy, allowing us to compute the spectral function from the retarded Green's function. It would be interesting to add yet another chiral fermion to the boundary, and an additional mass term, to obtain a massive Dirac spinor on the boundary.

The main result of this thesis is the calculation of the spectral function for a chiral fermion, obtained by solving the Dirac equation in the presence of the electron-star geometry. From this calculation, we have seen

- The occurrence of a Fermi surface at $\omega = 0$. This is indicated by the gap in the spectral function due to the vanishing of the imaginary part of the self-energy. However, the precise nature of this Fermi surface is not known at this point. This requires the behavior of the spectral function near zero energy to be determined more precisely, which in turn necessitates an improvement of the numerical computational scheme presented here.

- A plateau for small ω bounded by $\omega \sim k_3^z$, confirming analytical results that were found by treating the fermions in a WKB limit. Here, no such limit was taken, but the fermion equation of motion was solved numerically in the presence of the electron star geometry.

- No occurrence of multiple Fermi surfaces, even at large chemical potential μ. Because multiple Fermi surfaces do occur in the AdS-RN model, this suggests that the fermion backreaction present in the electron star has solved this unphysical trait. This can be traced back to the fact that the AdS-RN model has non-zero entropy at zero temperature, while the electron star does not.

Outlook

There are many different ways in which the presented research can be extended. A first extension would be to use the setup presented here to compute transport properties of the dual boundary system, such as charge transport. This is done by perturbing the gauge field and capturing the effects on the charge current by linear response.

Next, the electron-star model can be extended towards Lifshitz spacetime. In that case, one would start from an Einstein-Maxwell-Dilaton-Dirac action, again treating the fermions in a fluid limit. This would generalize the model considered here by introducing anisotropic scaling symmetry on the boundary. It appears - see Appendix B - that the IR geometry is again Lifshitz, which asymptotes to another Lifshitz geometry on the boundary. It would be interesting to see, after adding additional fermions as we have done here, how the spectral weight function behaves in this case. Of course, having obtained this solution, it would be interesting to revisit the previous extensions in the Lifshitz case.

Another interesting extension is the extension towards the thermal electron star. By turning on the temperature, the fermion equation of state is changed, which in turn affects the equations of motion as we have seen in the intermezzo 3.2 in Chapter 3. Although the first equation of motion is still trivially solved, as is shown in Appendix B, the fluid parameters suffer from divergences due to the infinitely red-shifted local temperature in the interior of the electron star. It would be interesting to see if one can get rid of these divergences. One possible way to do this is by studying the quantum electron star discussed in Chapter 3. Assuming a solution to these problems, it would be interesting to compute the heat transport in the boundary field theory and to consider the effect on the spectral function.

Yet another interesting possibility concerns adding a scalar field to the action (3.8) in the thermal case to obtain the characteristics of superconductivity. This model would fall in the category of the holographic superconductors, which are theories of gravity dual to strongly coupled field theories undergoing a superconducting phase transition below a critical temperature. A non-zero scalar field is dual to a non-zero condensate, so one would look for the scalar field becoming non-zero below the critical temperature. Especially interesting will be the interplay between this bosonic field and the fermion fluid.

Bibliography

[1] D. Musso, *Introductory notes on holographic superconductors*, [arXiv:1401.1504 [hep-th]]

[2] J. Zaanen, Y. Sun, Y. Liu and K. Schalm, *The AdS/CMT manual for plumbers and electricians*, [adscmtreview.pdf]

[3] S. Hartnoll, *Lectures on holographic methods for condensed matter physics*, [arXiv:0903.3246 [hep-th]]

[4] A. Ramallo, *Introduction to the AdS/CFT correspondence*, [arXiv:1310.4319 [hep-th]]

[5] S. Carroll, *Spacetime and Geometry: An Introduction to General Relativity*, (Pearson Education, San Fransisco, 2004)

[6] C. Bayona and N. Braga, *Anti-deSitter boundary in Poincare coordinates*, [arXiv:hep-th/0512182]

[7] J. Malcadena, *The Large N Limit of Superconformal Field Theories and Supergravity*, [arXiv:hep-th/9711200]

[8] D. Tong, *Lectures on Holographic Conductivity*, [zakopane.pdf]

[9] R. Blumenhagen and E. Plauschinn, *Introduction to Conformal Field Theory: With Applications to String Theory*, (Springer-Verlag Berlin Heidelberg, Heidelberg, 2009)

[10] M. Vojta, *Quantum phase transitions*, [arXiv:cond-mat/0309604]

[11] S. Kachru, X. Liu and M. Mulligan, *Gravity Duals of Lifshitz-Like Fixed Points*, [arXiv:0808.1725 [hep-th]]

[12] J. Tarrio and S. Vandoren, *Black holes and black branes in Lifshitz spacetimes*, [arXiv:1105.6335 [hep-th]]

[13] M. Taylor, *Non-relativistic Holography*, [arXiv:0812.0530 [hep-th]]

[14] U. Gursoy, E. Plauschinn, H. Stoof and S. Vandoren, *Holography and ARPES sum-rules*, [arXiv:1112.5074 [hep-th]]

[15] P. Borman, *Holographic Fermions: From Black Branes Towards Cold Atoms*, [Master thesis]

[16] S. Hartnoll and A. Tavanfar, *Electron stars for holographic metallic criticality*, [arXiv:1008.2828 [hep-th]]

[17] A. Allais and J. McGreevy, *How to construct a gravitating quantum electron star*, [arXiv:1306.6075 [hep-th]]

[18] V. Parente and R. Roychowdhury, *A study on Chared Neutron Star in AdS$_5$*, [arXiv:1011.5362 [hep-th]]

[19] H.Stoof, K Gubbels and D. Dickerscheid, *Ultracold Quantum Fields*, (Springer Science+Business Media B.V., Dordrecht, 2009)

[20] G. Horowitz, *Black holes in higher dimensions*, (Cambridge University Press, Cambridge, 2012)

[21] V. Giangreco, M. Puletti, S. Nowling, L. Thorlacius and T. Zingg, *Holographic metals at finite temperature*, [arXiv:1011.6261 [hep-th]]

[22] S. Hartnoll and P. Petrov, *Electron star birth: A continuous phase transition at nonzero density*, [arXiv:1011.6469 [hep-th]]

[23] R. Mann and R. McNees, *Holographic Renormalization for Asymptotically Lifshitz Spacetimes*, [arXiv:1107.5792 [hep-th]]

[24] M. Rausch de Traubenberg, *Clifford Algebras in Physics*, [arXiv:hep-th/0506011]

[25] P. Pal, *Dirac, Majorana and Weyl fermions*, [arXiv:1006.1718 [hep-ph]]

[26] H. Bruus and K. Flensberg, *Many-Body Quantum Theory in Condensed Matter Physics*, (Oxford University Press, 2004)

[27] S. Hartnoll, D. Hofman and D. Vegh, *Stellar spectroscopy: Fermions and holographic Lifshitz criticality*, [arXiv:1105.3197 [hep-th]]

Appendix A

The local-density approximation

In this appendix, we will more closely investigate the local-density approximation, which is applied to the fermions in the electron-star spacetime. The physical idea of the approximation is that the length scale associated with the fermions, such as the Compton wavelength, is small compared to the length scale ℓ - the AdS radius - set by the curvature.

In the following, we assume a diagonal metric $ds^2 = g_{tt}dt^2 + g_{ii}dx^i dx^i$. The Klein-Gordon equation - see ref. [5] - reads

$$\left(\Box - m^2 \right) \phi = 0, \quad \Box \phi = \frac{1}{\sqrt{-g}} \partial_\mu \left(\sqrt{-g} g^{\mu\nu} \partial_\nu \phi \right),$$

and becomes

$$-m^2 = g_{\mu\nu} p^\mu p^\nu$$

in momentum space when neglecting the derivatives on the metric tensor. Of course, the Dirac spinor fields also obey this equation. Solving for p^0, we obtain

$$\begin{aligned} p^t &= \sqrt{-g^{tt} \left(m^2 + g_{ii} \left(p^i \right)^2 \right)} \\ &= E_{\text{loc}} \left(p^i \right), \end{aligned}$$

which we refer to as the *local* energy, as $p^t = u^t E \left(p^i \right)$ with $E \left(p^i \right)^2 = m^2 + p_i p^i$. Here u^μ is the four-velocity of the gas, $u_\mu u^\mu = -1$. In the rest frame of the gas, u^t is the only non-zero component, which then satisfies

$$u^t = \frac{1}{\sqrt{-g_{tt}}}, \quad u_t = -\sqrt{-g_{tt}}.$$

We now write down the grand-canonical partition function for fermions in the local-density approximation. In the grand canonical ensemble

$$\mathcal{Z} = \operatorname{Tr} \exp \left[-\beta \left(\hat{H} - \mu \hat{N} \right) \right],$$

which we now write down in a covariant form.

The single-particle energy in the rest frame of the gas, ignoring the chemical potential, is given by $E \left(p^i \right) = -u^t p_t$, and hence is generalized to a general frame as $-u^\mu p_\mu$. Realizing that $A_t = \mu \left(x \right)$, we can invoke a minimal coupling scheme to obtain the full covariant single-particle energy, which takes the form $-u^\mu \left(p_\mu + A_\mu \right)$. In the rest frame, this becomes $-u_t p^t - u^t A_t = \sqrt{m^2 + p_i p^i} - \mu_{\text{loc}}$ where we have defined the local chemical potential

$$\begin{aligned} \mu_{\text{loc}} &= u^t A_t \\ &= \frac{\mu}{\sqrt{-g_{tt}}}. \end{aligned}$$

Then,

$$\mathcal{Z} = \prod_{p^i} \sum_{N(p^i)} \exp\left[\beta_{\text{loc}}\left(u_t p^t + \mu_{\text{loc}}\right) N\left(p^i\right)\right],$$

replacing the trace by a sum over energy eigenstates, with $N\left(p^i\right)$ the occupation number of an energy state labeled by p^i. In this expression, we to use the *local* inverse temperature β_{loc}, since in the local-density approximation the time integral - related to the temperature in the usual way - becomes

$$\int_0^\beta dt\sqrt{-g_{tt}} = \int_0^{\sqrt{-g_{tt}}\beta} dt',$$

so $\beta_{\text{loc}} = -\sqrt{g_{tt}}\beta$, or $T_{\text{loc}} = \frac{T}{\sqrt{-g_{tt}}}$. For the Fermi gas, the occupation numbers are 0 or 1, leaving

$$\begin{aligned}
\mathcal{Z} &= \prod_{p^i}\left[1 + \exp\left[\beta_{\text{loc}}\left(u_t p^t + \mu_{\text{loc}}\right)\right]\right] \\
&= \exp\left[\sum_{p^i}\log\left[1 + \exp\left[\beta_{\text{loc}}\left(u_t p^t + \mu_{\text{loc}}\right)\right]\right]\right].
\end{aligned}$$

The grand potential Ω is then defined as $-\beta_{\text{loc}}\Omega = \log\mathcal{Z}$, which implies

$$\Omega = -\frac{1}{\beta_{\text{loc}}}\sum_{p^i}\log\left[1 + \exp\left[\beta_{\text{loc}}\left(u_t p^t + \mu_{\text{loc}}\right)\right]\right].$$

Continuum limit

We now wish to take the continuum limit, in which the energy levels of the fermions form a continuum. The proposition is to use the following;

$$\sum_{p^i} \to V_{\text{flat}}\prod_i^d\int\frac{dp_i}{2\pi}$$

where the flat d-volume is given by $V_{\text{flat}} = \prod_{i=1}^d\int dx^i$. Now we can define "flat" momentum variables $\tilde{p}_i$ by $p_i = \sqrt{g_{ii}}\tilde{p}_i$, in terms of which the single-particle energy looks like the flat energy. This leads to the continuum limit

$$\begin{aligned}
\sum_{p^i} &\to \prod_i\int dx^i\int\frac{dp_i}{2\pi} \\
&= \prod_i\int dx^i\sqrt{g_{ii}}\int\frac{d\tilde{p}_i}{2\pi} \\
&= V_{\text{cov}}\int\frac{d^d\tilde{p}}{(2\pi)^d}
\end{aligned}$$

where $V_{\text{cov}} = \int dx^i\sqrt{-h}$ and where $\sqrt{h} = \prod_i\sqrt{g_{ii}}$.

In this continuum limit, the thermodynamical potential becomes

$$\begin{aligned}
-\beta_{\text{loc}}\Omega &= \int d^d x\sqrt{h}\int\frac{d^d\tilde{p}}{(2\pi)^d}\log\left(1 + \exp\left[-\beta_{\text{loc}}\left(-u_0 E_{\text{loc}}\left(\tilde{p}_i\right) - \mu_{\text{loc}}\left(x\right)\right)\right]\right) \\
&= \int d^d x\sqrt{h}\int\frac{d^d\tilde{p}}{(2\pi)^d}\log\left(1 + \exp\left[-\beta_{\text{loc}}\left(E\left(\tilde{p}_i\right) - \mu_{\text{loc}}\left(x\right)\right)\right]\right).
\end{aligned}$$

The pressure of the ideal Fermi gas, then, is given by

$$\Omega = -\int d^d x \sqrt{h} p_{\text{flat}}\left(x\right),$$

and so

$$p_{\text{flat}}\left(x\right) = \frac{1}{\beta_{\text{loc}}} \int \frac{d^d \tilde{p}}{\left(2\pi\right)^d} \log\left(1 + \exp\left[-\beta_{\text{loc}}\left(E\left(\tilde{p}_i\right) - \mu_{\text{loc}}\left(x\right)\right)\right]\right).$$

Thus, we conclude that we need to use the flat pressure p_{flat} as a function of the local chemical potential μ_{loc}. Another way in which we can see that we have to use the local chemical potential is by studying the Dirac action directly. It takes the form

$$S = -\int d^{d+1} x \sqrt{-g} \bar{\Psi}\left(i\Gamma^\mu \nabla_\mu - m\right) \Psi.$$

By performing a coordinate transformation to locally-flat coordinates,

$$d^{d+1} x \sqrt{-g} \rightarrow d^{d+1} x'$$

we find $\frac{d}{dt'} = \frac{1}{\sqrt{-g_{tt}}} \frac{d}{dt}$, which implies

$$E_{\text{locally flat}} = \frac{E}{\sqrt{-g_{tt}}},$$

which is the local energy. Thus, the local energy E_{loc} appears when using the Dirac action in locally-flat coordinates. In thermodynamical calculations, therefore, we integrate over E_{loc}, so the locally-flat pressure depends on the local chemical potential μ_{loc}. Performing a Wick rotation, one obtains

$$\begin{aligned} \tau' &= \sqrt{-g_{tt}}\tau \\ &= \sqrt{-g_{tt}}\hbar\beta \\ &= \hbar\beta_{\text{loc}}. \end{aligned}$$

Thus, we obtain the local inverse temperature in flat expressions. Indeed,

$$\begin{aligned} \frac{i}{\hbar}S &= \frac{i}{\hbar} \int d^{d+1} x \sqrt{-g} p_{\text{flat}} \\ &= \frac{i}{\hbar} \int dt \sqrt{-g_{tt}} \int d^d x \sqrt{h} p_{\text{flat}} \\ &= -\beta_{\text{loc}}\Omega. \end{aligned}$$

Note that p_{flat} depends on position through β_{loc} and μ_{loc}. Invoking ordinary thermodynamical relations, this implies

$$p_{\text{flat}} = -\rho_{\text{flat}} + \mu_{\text{loc}}\left(x\right)\sigma + T_{\text{loc}}s.$$

In the case of zero temperature, the Fermi sphere is defined by

$$E\left(\tilde{p}_i\right) - \mu_{\text{loc}} < 0,$$

in which case the above expression for the flat pressure becomes

$$\begin{aligned} p_{\text{flat}}\left(x\right) &= \frac{1}{\beta_{\text{loc}}} \int \frac{d^d \tilde{p}}{\left(2\pi\right)^d}\left[-\beta_{\text{loc}}\left(E\left(\tilde{p}_i\right) - \mu_{\text{loc}}\left(x\right)\right)\right] \\ &= \int_m^{\mu_{\text{loc}}\left(x\right)} dE\, g\left(E\right)\left(-E + \mu_{\text{loc}}\left(x\right)\right). \end{aligned}$$

In this expression, $g(E)$ is the density of states, calculated from

$$
\begin{aligned}
g(\mathbf{p}) \frac{d\mathbf{p}}{(2\pi)^d} &= (2\pi)^{-d} p^{d-1} \sin^{d-2}(\phi_1) \sin^{d-3}(\phi_2) \cdots \sin(\phi_{d-2}) \, dp \, d\phi_1 \cdots d\phi_{d-1} \\
&\to \beta_{d+1} E \left(E^2 - m^2\right)^{(d-2)/2} dE \\
&\equiv g(E) \, dE,
\end{aligned}
\tag{A.1}
$$

where we have used $p^2 = E^2 - m^2$ and where we have integrated over angular variables. Here, β_d given by equation (3.2) for electrons, having spin $\frac{1}{2}$. For fermions of arbitrary spin s, there is a multiplicative factor of $2s+1$, rather than the factor 2 implicit in the above equation.

This is the essence of the expressions use in equations (3.4), (3.5), and (3.6). It is the flat pressure, depending on the local chemical potential, that is used in the action (3.8).

Appendix B

Details on calculations

In this appendix we provide details on several calculations in the main text. First, we provide the derivation of the equations of motion in Chapter 3 as well as details concerning the numerical calculation. Next, we discuss the derivation of the spinor covariant derivative in Chapter 4.

Chapter 3

We provide the details of deriving the equations of motion for the electron star. The metric takes the form

$$ds^2 = -\ell^2 f(u) \, dt^2 + \ell^2 g(u) \, du^2 + \ell^2 u^{-2} dx_i^2$$

while the action is given by

$$S = \int d^{d+1}x \sqrt{-g} \left[\frac{1}{2\kappa^2} \left(R + \frac{6}{\ell^2} \right) - \frac{1}{4e^2} F_{\mu\nu} F^{\mu\nu} + p(\mu_{\mathrm{loc}}) \right]$$

as explained in the text. The dimensions of relevant quantities are

$$
\begin{aligned}
[\ell] = [x^\mu] &= [\mathrm{length}] & [p] = [\rho] &= [\mathrm{length}]^{-1-d} \\
[f] = [g] &= [\mathrm{length}]^{-2} & [\sigma] &= [\mathrm{length}]^{-d} \\
[A] = [h] &= [\mathrm{length}]^{-1} & [\kappa]^2 &= [\mathrm{length}]^{d-1} \\
& & [e]^2 &= [\mathrm{length}]^{d-3} .
\end{aligned}
$$

In particular,

$$\left[\frac{e}{\kappa} \right] = [\mathrm{length}] = [\mathrm{energy}]^{-1}$$

and the fluid parameters can be made dimensionless by scaling out the couplings

$$\rho = \frac{\hat{\rho}}{\ell^2 \kappa^2}, p = \frac{\hat{p}}{\ell^2 \kappa^2}, \sigma = \frac{\hat{\sigma}}{e\ell^2 \kappa}.$$

The metric components are given by

$$g_{tt} = -\ell^2 f(u), \quad g_{uu} = \ell^2 g(u), \quad g_{ii} = \frac{\ell^2}{u^2},$$

and the resulting non-zero Christoffel symbols are

$$
\begin{aligned}
\Gamma^i_{iu} &= -\frac{1}{u}, & \Gamma^t_{tu} &= \frac{f'}{2f}, & \Gamma^u_{uu} &= \frac{g'}{2g}; \\
\Gamma^u_{ii} &= \frac{1}{gu^3}, & \Gamma^u_{tt} &= \frac{f'}{2g}.
\end{aligned}
$$

From this, we calculate the relevant Riemann tensor components

$$R^u_{\ tut} = \frac{f''}{2g} - \frac{f'g'}{4g^2} - \frac{f'^2}{4gf} \qquad R^u_{\ iui} = \frac{-1}{gr^3}\left(\frac{2}{r} + \frac{g'}{2g}\right)$$

$$R^t_{\ utu} = g_{uu}g^{tt}R^u_{\ tut} \qquad R^t_{\ iti} = \frac{f'}{2fgr^3}. \tag{B.1}$$

EOM1

The first equation of motion is the covariant conservation of the energy-momentum tensor

$$\begin{aligned}
\nabla_\mu T^{\mu\nu} &\equiv& \partial_\mu T^{\mu\nu} + \Gamma^\mu_{\mu\alpha}T^{\alpha\nu} + \Gamma^\nu_{\mu\alpha}T^{\mu\alpha} \\
&=& 0,
\end{aligned}$$

where the energy-momentum tensor is given by

$$\begin{aligned}
T_{\mu\nu} &=& (\rho + p)u_\mu u_\nu + pg_{\mu\nu} + \frac{1}{e^2}F_{\mu\sigma}F_\nu^{\ \sigma} - \frac{1}{4e^2}g_{\mu\nu}F^2 \tag{B.2} \\
&=& T^f_{\mu\nu} + T^A_{\mu\nu}.
\end{aligned}$$

In the last line, we have split up the EM-tensor in a fluid part and a part due to the gauge field. Now $A_t = \frac{e\ell}{\kappa}h(u)$ implies that $F_{ut} = \frac{e\ell}{\kappa}h'$ is the only independent non-zero component of $F_{\mu\nu}$. Further, we will invoke Maxwell's equation

$$\nabla_\mu F^{\nu\mu} = \sigma e^2 u^\nu$$

with $u^t = \left(\ell\sqrt{f}\right)^{-1}$.

First of all, it is easy to show that the only non-zero component of the equation of motion will be the u component. Thus, we focus on writing out $\nabla_\mu\left(T^{u\mu}_f + T^{u\mu}_A\right) = 0$. Using Maxwell's equation, we find

$$\begin{aligned}
\nabla_\mu T^{u\mu}_A &=& \frac{1}{e^2}\nabla_\mu\left(F^{u\alpha}F^\mu_{\ \alpha} - \frac{1}{4}g^{u\mu}F^2\right) \\
&=& \sigma F^{u\alpha}u_\alpha + \frac{1}{e^2}F^\mu_{\ \alpha}\nabla_\mu\left(F^{u\alpha}\right) - \frac{1}{4}g^{u\mu}\nabla_\mu\left(F^2\right) \\
&=& \frac{eh'}{\ell^2\kappa g\sqrt{f}},
\end{aligned}$$

since the last two terms in the second line cancel. Next, expanding the covariant derivatives in terms of the Christoffel symbols, one shows

$$\nabla_\mu T^{u\mu}_f = \frac{p'}{\ell^2 g} + (\rho + p)\frac{f'}{2fg\ell^2}.$$

Thus, the total equation becomes

$$p' + (p + \rho)\frac{f'}{2f} - \frac{e}{\kappa}\frac{h'\sigma}{\sqrt{f}} = 0.$$

Multiplying by $\ell^2\kappa^2$, one finds the desired equation of motion.

EOM 2

The second equation of motion is a linear combination of the (uu) and (tt) components of Einstein's equation

$$R_{\mu\nu} + \left(\Lambda - \frac{1}{2}R\right) g_{\mu\nu} = \kappa^2 T_{\mu\nu}.$$

Given the form of the energy-momentum tensor (B.2), one finds

$$R^u_u - R^t_t = \kappa^2 (\rho + p)$$
$$g^{uu} R^i_{\ uiu} - g^{tt} R^i_{\ tit} = \kappa^2 (\rho + p),$$

and hence, by virtue of the Riemann tensor components (B.1),

$$\frac{d-1}{g\ell^2 u} \left(-\frac{2}{u} - \frac{g'}{2g} - \frac{f'}{2f}\right) - \kappa^2 (\rho + p) = 0.$$

Thus, multiplying by $-2g\ell^2$, we obtain the second equation of motion

$$\frac{(d-1)}{2u} \left(\frac{4}{u} + \frac{g'}{g} + \frac{f'}{f}\right) + g (\hat{\rho} + \hat{p}) = 0.$$

EOM 3

The third equation of motion uses the ii components of the Einstein equation

$$R_{ii} + \left(\Lambda - \frac{1}{2}R\right) g_{ii} = \kappa^2 p g_{ii} - \frac{\kappa^2}{4e^2} g_{ii} F^2.$$

This becomes

$$\left(\frac{f'}{2fu} - \frac{g'}{2gu} - \frac{d}{u^2}\right) - g \left(-\Lambda \ell^2 + \hat{p}\right) - \frac{1}{2}g\ell^2 R - \frac{h'^2}{2f} = 0.$$

Next, substitute the second equation of motion to eliminate g', resulting in

$$\frac{f'}{fu} - \frac{d-2}{u^2} - \frac{h'^2}{2f} + g \left(\Lambda \ell^2 - \hat{p} - \frac{1}{2}\ell^2 R + \frac{\hat{\rho}}{d-1} + \frac{\hat{p}}{d-1}\right) = 0.$$

Then, by tracing the general form of Einstein's equation, one finds the expression

$$-\frac{1}{2}R\ell^2 = \frac{-\Lambda \ell^2 (d+1) - \hat{\rho} + \hat{p}d + \frac{\kappa^2 \ell^2}{e^2} F^2 \left(1 - \frac{1}{4}(d+1)\right)}{d-1}$$

for the Ricci scalar. Entering this into the result found earlier, eliminating R, one finds

$$\frac{f'}{fu} - \frac{d-2}{u^2} - \frac{h'^2}{2f} + g \left(\frac{d(d-1) + 2\hat{p} - \frac{2h'^2}{gf} \left(1 - \frac{1}{4}(d+1)\right)}{d-1}\right) = 0.$$

Finally, this is rewritten to yield the third equation of motion

$$\frac{f'}{fu} - \frac{d-2}{u^2} - \frac{h'^2}{(d-1)f} + g \left(\frac{d(d-1) + 2\hat{p}}{(d-1)}\right) = 0.$$

EOM 4

The final equation of motion is Maxwell's equation

$$\nabla_\mu F^{\nu\mu} = e^2 J^\nu$$

with $J^\nu = \sigma u^\nu$, and where $u^t = \left(\ell\sqrt{f}\right)^{-1}$ is the only non-zero component of u^ν. It is easy to show that the only non-zero component of Maxwell's equation is the $\nu = t$ component. Then,

$$\partial_\mu F^{\mu t} + \Gamma^\mu_{\mu\alpha} F^{\alpha t} + \cancel{\Gamma^t_{\mu\alpha} F^{\mu\alpha}} + \frac{e^2\sigma}{\ell\sqrt{f}} = 0$$

$$-\frac{e}{\ell^3\kappa}\partial_u\left(\frac{h'}{fg}\right) - \frac{e\ell h'}{\kappa fg}\left((d-1)\Gamma^i_{iu} + \Gamma^t_{ut} + \Gamma^u_{uu}\right) + \frac{e^2\sigma}{\ell\sqrt{f}} = 0$$

$$h'' - h'\left(\frac{f'}{2f} + \frac{g'}{2g} + \frac{d-1}{u}\right) - g\sqrt{f}\hat{\sigma} = 0,$$

Finally, one invokes the second equation of motion to eliminate $\frac{f'}{2f} + \frac{g'}{2g}$ and uses the equation of state $\hat{p} + \hat{\rho} = \frac{h}{\sqrt{f}}\hat{\sigma}$ to find the fourth equation of motion

$$h'' - \frac{h'(d-3)}{u} + \frac{g\hat{\sigma}}{\sqrt{f}}\left(\frac{uhh'}{d-1} - f\right) = 0.$$

The constant f_1

As mentioned in the text, the constant f_1 appearing in the perturbed Lifshitz scaling solution

$$f = \frac{1}{u^{2z}}\left(1 + f_1 u^\alpha\right)$$

is undetermined from the equations of motion. However, it can be set to any value by an appropriate rescaling of the coordinates. Indeed, letting $u \to f_1^{-1/\alpha} u$,

$$f \to \frac{f_1^{2z/\alpha}}{u^{2z}}\left(1 + u^\alpha\right),$$

after which we can absorb the remaining factor in the coordinate t. Similarly, one absorbs such a factor in x_i as well. Yet, this does not determine the sign of f_1, which turns out to be crucial.

In order to determine the sign of f_1, we simply solve the equations of motion using either sign. A good way to see which sign should be used is to realize that f should interpolate between the Lifshitz and AdS-RN solutions. We write

$$f = \frac{1}{u^{\gamma(u)}}$$

for which $\gamma(\infty) = 2z$ and $\gamma(0) = 2$ from the AdS-RN solution. We can get a measure for γ by assuming it is slowly varying and taking the derivative of f:

$$\gamma \simeq -u\frac{f'(u)}{f(u)}.$$

By numerically solving the equations of motion with $f_1 = \pm 1$, we plot both associated γ functions. The result is shown in Figure B.1.

Clearly, when $f_1 = 1$, γ does not converge to 2 for small u, meaning that we cannot match it onto the Reissner-Nordström solutions properly. This solution simply does not become Reissner-Nordström for small u. This is why $f_1 = -1$ is chosen in the numerical calculation.
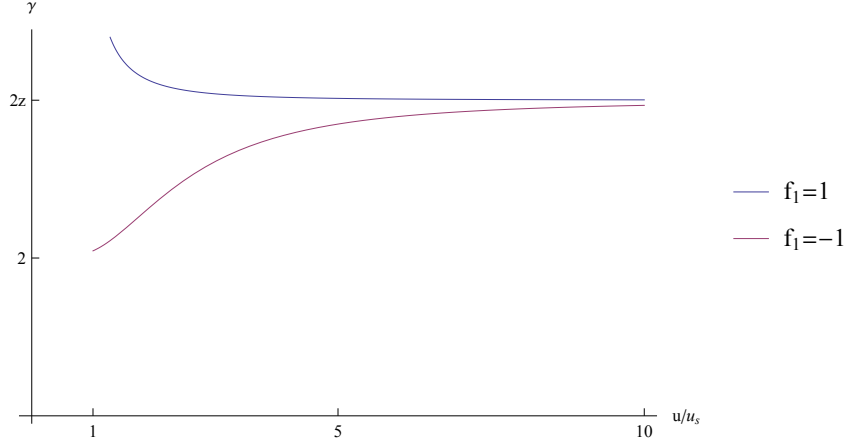
Figure B.1: The radial dependence of the measure of γ in units of the star "radius" u_s, for the two choices of signs of the perturbation away from the exact infrared Lifshitz solution. Clearly, the perturbation with a negative sign converges towards a black hole solution - for which $\gamma = 2$ - at $u = u_s$.

Non-zero temperature

We consider the extension to a non-zero temperature perfect fluid. In this case, the fluid parameters are given by

$$\rho = \int_m^\infty E g\left(E\right) n_E dE, \quad \sigma = \int_m^\infty g\left(E\right) n_E dE, \quad -p = \rho - \mu\sigma - Ts$$

in terms of the density of states (A.1) and the Fermi-Dirac distribution

$$n_E = \left[1 + \exp\left[\beta\left(E - \mu_{\text{loc}}\right)\right]\right]^{-1}.$$

The entropy of an ideal fluid of fermions is given by

$$S = -\sum_k n_k \log n_k + \left(1 - n_k\right)\log\left(1 - n_k\right),$$

where $n_k \equiv n_{E(k)}$. Taking the continuum limit $\sum_k \to \frac{V_{\text{cov}}}{(2\pi)^d}\int d^d k$ as in Appendix A and changing integration variables,

$$
\begin{aligned}
s &= -\beta_{d+1}\int_m^\infty dE\, E\left(E^2 - m^2\right)^{(d-2)/2}\left(n_E \log\left(n_E\right) + \left(1 - n_E\right)\log\left(1 - n_E\right)\right)\\
&= -\beta_{d+1}\left(\frac{e}{\kappa}\right)^d\int_{\hat{m}}^\infty d\epsilon\,\epsilon\left(\epsilon^2 - \hat{m}^2\right)^{(d-2)/2}\left(n_\epsilon \log\left(n_\epsilon\right) + \left(1 - n_\epsilon\right)\log\left(1 - n_\epsilon\right)\right)
\end{aligned}
$$

with

$$n_\epsilon = \left[1 + \exp\left[\frac{e\beta}{\kappa}\left(\epsilon - \frac{\ell h}{\sqrt{f}}\right)\right]\right]^{-1}.$$

Thus,

$$\hat{s} = -\hat{\beta}_{d+1}\int_{\hat{m}}^\infty d\epsilon\,\epsilon\left(\epsilon^2 - \hat{m}^2\right)^{(d-2)/2}\left(n_\epsilon \log\left(n_\epsilon\right) + \left(1 - n_\epsilon\right)\log\left(1 - n_\epsilon\right)\right),$$

with $\hat{s} = e\kappa\ell^2 s$, implying that s has the same dimension as σ.

The first equation of motion is still given by

$$\hat{p}' + (\hat{\rho} + \hat{p})\frac{f'}{2f} - \frac{h'\hat{\sigma}}{\sqrt{f}} = 0,$$

where we now substitute the equation of state

$$\hat{p} = -\hat{\rho} + \frac{h}{\sqrt{f}}\hat{\sigma} + \frac{\hat{T}_0}{\ell\sqrt{f}}\hat{s}$$

in terms of the local temperature $T = \hat{T}_0/\ell\sqrt{f}$. One then obtains

$$-\hat{\rho}' + \frac{h}{\sqrt{f}}\hat{\sigma}' + \frac{\hat{T}_0}{\ell\sqrt{f}}\hat{s}' = 0.$$

Entering the integral expressions, the left hand side becomes

$$
\begin{aligned}
-\hat{\rho}' + \frac{h}{\sqrt{f}}\hat{\sigma}' + \frac{\hat{T}_0}{\ell\sqrt{f}}\hat{s}' &= \hat{\beta}_{d+1}\int_{\hat{m}}^{\infty} d\epsilon\,\epsilon\left(\epsilon^2 - \hat{m}^2\right)^{(d-2)/2}\left[-\epsilon n'_\epsilon + \frac{h}{\sqrt{f}}n'_\epsilon - \frac{\hat{T}_0}{\ell\sqrt{f}}n'_\epsilon \log\left(\frac{n_\epsilon}{1-n_\epsilon}\right)\right] \\
&= \hat{\beta}_{d+1}\int_{\hat{m}}^{\infty} d\epsilon\,\epsilon\left(\epsilon^2 - \hat{m}^2\right)^{(d-2)/2}\left[-\epsilon n'_\epsilon + \frac{h}{\sqrt{f}}n'_\epsilon - \frac{\hat{T}_0}{\ell\sqrt{f}}n'_\epsilon \times \left(-\frac{\ell\sqrt{f}}{\hat{T}_0}\left(\epsilon - \frac{h}{\sqrt{f}}\right)\right)\right] \\
&= 0.
\end{aligned}
$$

Next, we derive the radial profiles of μ and T purely on thermodynamical grounds. without entering an explicit equation of state. Consider the grand potential Ω, and define $\omega = \Omega/V$;

$$
\begin{aligned}
\Omega &= H - \mu N - TS \\
\omega &= \rho - \mu\sigma - Ts.
\end{aligned}
$$

Then, $\Omega = -pV$ for an ideal fluid, which implies $p = -\omega$. The first equation of motion reads

$$p' + (p+\rho)\frac{f'}{2f} - \frac{h'\sigma e}{\kappa\sqrt{f}} = 0.$$

Now enter

$$
\begin{aligned}
\rho &= \omega + \mu\sigma + Ts \\
\sigma &= -\frac{\partial\omega}{\partial\mu} \\
s &= -\frac{\partial\omega}{\partial T}
\end{aligned}
$$

to find

$$-\omega' - \left(\mu\frac{\partial\omega}{\partial\mu} + T\frac{\partial\omega}{\partial T}\right)\frac{f'}{2f} + \frac{h'e}{\kappa\sqrt{f}}\frac{\partial\omega}{\partial\mu} = 0.$$

Writing $\omega' = \frac{\partial\omega}{\partial T}\frac{\partial T}{\partial u} + \frac{\partial\omega}{\partial\mu}\frac{\partial\mu}{\partial u}$, one finds

$$\frac{\partial\omega}{\partial\mu}\left(-\frac{\partial\mu}{\partial r} - \mu\frac{f'}{2f} + \frac{e}{\kappa}\frac{h'}{\sqrt{f}}\right) = \frac{\partial\omega}{\partial T}\left(\frac{\partial T}{\partial r} + T\frac{f'}{2f}\right).$$

Thus, we find the required radial profiles:

$$T' + T\frac{f'}{2f} = 0 \quad\Rightarrow\quad T = \frac{T_0}{\sqrt{f}}$$

$$\mu' + \mu\frac{f'}{2f} = \frac{e}{\kappa}\frac{h'}{\sqrt{f}} \quad\Rightarrow\quad \mu = \frac{e}{\kappa}\frac{h}{\sqrt{f}}.$$

Chapter 4

Spinor covariant derivative

We provide some details regarding the derivation of the spinor covariant derivatives for the electron-star metric

$$ds^2 = -\frac{r^2}{\ell^2} f\left(r\right) dt^2 + \frac{\ell^2}{r^2} g\left(r\right) dr^2 + \frac{r^2}{\ell^2} dx_i^2.$$

From the defining equation $g_{\mu\nu} e_{\underline{a}}^\mu e_{\underline{b}}^\nu = \eta_{\underline{ab}}$, labeling the locally-flat coordinates with $\underline{t}, \underline{r}, \underline{i}$, the vielbeins become

$$e_{\underline{r}}^r = \frac{r}{\ell\sqrt{g}}, \quad e_{\underline{i}}^i = \frac{\ell}{r}, \quad e_{\underline{t}}^t = \frac{\ell z}{r^z \sqrt{f}}.$$

As discussed in the text, the vielbeins define the spin connection in terms of the Christoffel symbols, which take the form

$$
\begin{aligned}
\Gamma_{ir}^i &= \frac{1}{r}, \quad \Gamma_{tr}^t = \frac{f'}{2f} + \frac{1}{r}, \quad \Gamma_{rr}^r = -\frac{1}{r} + \frac{g'}{2g} \\
\Gamma_{ii}^r &= -\frac{r^3}{g\ell^4}, \quad \Gamma_{tt}^r = \frac{r^3}{g\ell^4}\left(\frac{f'r}{2} + f\right)
\end{aligned}
$$

in the r coordinate frame. We derive the relation between the spin connection and these Christoffel symbols. For this, one determines the covariant derivative of a vector field in both the original formalism and the vielbein formalism. First, one has

$$
\begin{aligned}
\nabla X &= \left(\nabla_\mu X^\nu\right) \mathrm{d}x^\mu \otimes \partial_\nu \\
&= \left(\partial_\mu X^\nu + \Gamma_{\mu\alpha}^\nu X^\alpha\right) \mathrm{d}x^\mu \otimes \partial_\nu
\end{aligned}
$$

while on the other hand

$$
\begin{aligned}
\nabla X &= \left(\nabla_\mu X^{\underline{a}}\right) \mathrm{d}x^\mu \otimes \hat{e}_a \\
&= \left(\partial_\mu X^{\underline{a}} + \omega_{\mu\underline{b}}^{\underline{a}} X^{\underline{b}}\right) \mathrm{d}x^\mu \otimes e_{\underline{a}}^\nu \partial_\nu \\
&= e_{\underline{a}}^\nu \left(\partial_\mu \left(e_{\alpha}^{\underline{a}} X^\alpha\right) + \omega_{\mu\underline{b}}^{\underline{a}} e_{\alpha}^{\underline{b}} X^\alpha\right) \mathrm{d}x^\mu \otimes \partial_\nu \\
&= \left(\delta_\alpha^\nu \partial_\mu X^\alpha + e_{\underline{a}}^\nu \partial_\mu \left(e_{\alpha}^{\underline{a}}\right) X^\alpha + e_{\underline{a}}^\nu \omega_{\mu\underline{b}}^{\underline{a}} e_{\alpha}^{\underline{b}} X^\alpha\right) \mathrm{d}x^\mu \otimes \partial_\nu \\
&= \left(\partial_\mu X^\nu + e_{\underline{a}}^\nu \partial_\mu \left(e_{\alpha}^{\underline{a}}\right) X^\alpha + e_{\underline{a}}^\nu \omega_{\mu\underline{b}}^{\underline{a}} e_{\alpha}^{\underline{b}} X^\alpha\right) \mathrm{d}x^\mu \otimes \partial_\nu.
\end{aligned}
$$

Comparing these expressions, one finds

$$\omega_{\mu\underline{ab}} = e_{\nu\underline{a}} \partial_\mu e_{\underline{b}}^\nu + e_{\nu\underline{a}} e_{\underline{b}}^\sigma \Gamma_{\sigma\mu}^\nu.$$

An important property of the spin connection is that it is anti-symmetric in its two flat indices, as is easily seen by expressing it purely in vielbeins

$$\omega_{\mu\underline{ab}} = \frac{1}{2}e_{\underline{a}}^\nu\left(\partial_\mu e_{\nu\underline{b}} - \partial_\nu e_{\mu\underline{b}}\right) - \frac{1}{2}e_{\underline{b}}^\nu\left(\partial_\mu e_{\nu\underline{a}} - \partial_\nu e_{\mu\underline{a}}\right) - \frac{1}{2}e_{\underline{a}}^\rho e_{\underline{b}}^\sigma e_\mu^{\underline{c}}\left(\partial_\rho e_{\sigma\underline{c}} - \partial_\sigma e_{\rho\underline{c}}\right).$$

Then, from the discussion in the text, the covariant derivative becomes

$$\nabla_\mu = \partial_\mu + \frac{1}{8}\omega_{\mu\underline{ab}}\left[\Gamma^{\underline{a}}, \Gamma^{\underline{b}}\right]$$

when acting on a spinor Ψ. We now calculate the various components.

First, we have $\omega_{r\underline{ab}} = 0$ for all $\underline{a},\underline{b}$, by considering all possible options. Thus,

$$\nabla_r = \partial_r.$$

Secondly, setting $\mu = i$, we find

$$
\begin{aligned}
\omega_{i\underline{ri}} &= e_{r\underline{r}} e^i_{\underline{i}} \Gamma^r_{ii} \\
&= -\frac{r}{\ell^2 \sqrt{g}}
\end{aligned}
$$

as the only non-zero independent component. Hence,

$$
\begin{aligned}
\nabla_i &= \partial_i + \frac{1}{8}\omega_{i\underline{ir}}\left[\Gamma^{\underline{i}}.\Gamma^{\underline{r}}\right] + \frac{1}{8}\omega_{i\underline{ri}}\left[\Gamma^{\underline{r}},\Gamma^{\underline{i}}\right] \\
&= \partial_i + \frac{1}{2}\frac{r}{\ell^2 \sqrt{g}}\Gamma^{\underline{i}}\Gamma^{\underline{r}},
\end{aligned}
$$

using the anti-commutation relations for the Γ matrices.

Finally, when $\mu = t$ we find

$$
\begin{aligned}
\omega_{t\underline{rt}} &= e_{r\underline{r}} e^t_{\underline{t}} \Gamma^r_{tt} \\
&= \frac{r^2}{\ell^2}\sqrt{\frac{f}{g}}\left(\frac{f'}{2f} + \frac{1}{r}\right)
\end{aligned}
$$

as the only non-zero independent component. Thus,

$$
\begin{aligned}
\nabla_t &= \partial_t + \frac{1}{8}\omega_{t\underline{rt}}\left[\Gamma^{\underline{r}},\Gamma^{\underline{t}}\right] + \frac{1}{8}\omega_{t\underline{tr}}\left[\Gamma^{\underline{t}},\Gamma^{\underline{r}}\right] \\
&= \partial_t - \frac{1}{2}\frac{r}{\ell\sqrt{g}}\partial_r\left(\frac{r}{\ell}\sqrt{f}\right)\Gamma^{\underline{t}}\Gamma^{\underline{r}}.
\end{aligned}
$$

Thus, we have shown the correctness of equation (4.6):

$$
\begin{aligned}
\nabla_r &= \partial_r \\
\nabla_i &= \partial_i + \frac{1}{2}\frac{r}{\ell^2 \sqrt{g}}\Gamma^{\underline{i}}\Gamma^{\underline{r}} \\
\nabla_t &= \partial_t - \frac{1}{2}\frac{r}{\ell\sqrt{g}}\partial_r\left(\frac{r}{\ell}\sqrt{f}\right)\Gamma^{\underline{t}}\Gamma^{\underline{r}}.
\end{aligned}
$$

Finally, an important fact used in the text is that the spin connection yields a vanishing contribution to the variation of the Dirac action on a constant radius hypersurface. Thus, all covariant derivatives can be replaced by partial derivatives. To prove this, consider the term in the Dirac action on the surface $r = r_0$. Since $\Gamma^{\underline{a}} = \gamma^{\underline{a}}$ when d is even - see (4.1), we obtain

$$
\begin{aligned}
\bar{\Psi}\left(\Gamma^\mu \nabla_\mu - m\right)\Psi &= \Psi^\dagger \Gamma^{\underline{t}}\left(\Gamma^t \nabla_t + \Gamma^i \nabla_i - m\right)\Psi \\
&= \Psi^\dagger \Gamma^{\underline{t}}\left(e^t_{\underline{t}}\Gamma^{\underline{t}}\partial_t + e^i_{\underline{i}}\Gamma^{\underline{i}}\partial_i - m\right)\Psi \\
&\quad + \Psi^\dagger \Gamma^{\underline{t}}\left(-e^t_{\underline{t}}\frac{r}{2\ell\sqrt{g}}\partial_r\left(\frac{r}{\ell}\sqrt{f}\right)\left(\Gamma^{\underline{t}}\right)^2\Gamma^{\underline{r}} + \Gamma^{\underline{i}}\frac{r}{\ell^2 \sqrt{g}}\left(\Gamma^{\underline{i}}\right)^2\Gamma^{\underline{r}}\right)
\end{aligned}
$$

on the surface $r = r_0$. Thus the contributions are proportional to

$$\left(\Gamma^{\underline{t}}\right)^2\Gamma^{\underline{t}}\Gamma^{\underline{r}}, \quad \Gamma^{\underline{t}}\left(\Gamma^{\underline{i}}\right)^2\Gamma^{\underline{r}},$$

which vanish in the representation (4.1) of the Γ matrices.

Appendix C

The Lifshitz electron star

We provide some results regarding the Lifshitz electron star, for future work. To this end, we study the action for the Lifshitz spacetime, to which we add fermions treated in the fluid limit. We begin from an action which combines the Lifshitz black brane action (2.19) and the Electron star action (3.8):

$$S = \int d^{d+1}x \sqrt{-g} \left[\frac{1}{2\kappa^2} \left(R + \frac{6}{\ell^2} - \partial_\mu \phi \partial^\mu \phi \right) - \frac{1}{4} \sum_i \frac{1}{e_i^2} e^{\lambda_i \phi} F_{i\mu\nu}^2 - p(\mu_l) \right],$$

where ϕ is the dilaton field, and where $i = 1, 2$ indexes the two gauge fields A_i, the constants λ_i and the charges e_i. Again, we write down a metric ansatz

$$ds^2 = \ell^2 \left(-f(u) dt^2 + g(u) du^2 + u^{-2} dx_i^2 \right)$$

where we require the asymptotic behavior $f \to u^{-2\alpha}, g \to u^{-2}$ for an asymptotically Lifshitz spacetime. This time, the equations of motion read

$$\nabla_\mu \left(T_A^{\mu\nu} + T_\phi^{\mu\nu} + T_f^{\mu\nu} \right) = 0$$

$$R_{\mu\nu} + \left(\Lambda - \frac{1}{2} R \right) g_{\mu\nu} = T_{\mu\nu}^\phi + \kappa^2 \left(\sum_i \frac{1}{e_i^2} e^{\lambda_i \phi} \left(F_{i\mu\sigma} F_{i\nu}^\sigma - \frac{1}{4} g_{\mu\nu} F_i^2 \right) + T_{\mu\nu}^f \right)$$

$$\nabla_\mu \left(e^{\lambda_1 \phi} F_1^{\nu\mu} \right) = 0$$

$$\nabla_\mu \left(e^{\lambda_2 \phi} F_2^{\nu\mu} \right) = e_2^2 \sigma u^\nu$$

$$\Box \phi - \frac{1}{4} \sum_i \lambda_i e^{\lambda_i \phi} F_i^2 = 0.$$

with $T_{\mu\nu}^A = \sum_i \frac{1}{e_i^2} e^{\lambda_i \phi} \left(F_{i\mu\sigma} F_{i\nu}^\sigma - \frac{1}{4} g_{\mu\nu} F_i^2 \right)$, $T_{\mu\nu}^\phi = \partial_\mu \phi \partial_\nu \phi - \frac{1}{2} (\partial \phi)^2 g_{\mu\nu}$ and $T_{\mu\nu}^f = (\rho + p) u_\mu u_\nu + p g_{\mu\nu}$. Also, we will take

$$A_{i,t} = \frac{e_i \ell}{\kappa} h_i$$

generalizing our earlier discussion. Then, repeating the same steps as we have taken in Appendix A, we find the equations of motion

$$\hat{p}' + (\hat{\rho} + \hat{p})\,\frac{f'}{2f} + \frac{\phi'^2}{g}\left[\frac{\phi''}{\phi'} - \frac{g'}{2g} + \frac{1-d}{u} + \frac{f'}{2f}\right] \tag{C.1}$$

$$+ \frac{\phi'}{2gf}\left[h_1'^2\lambda_1 e^{\lambda_1\phi} + h_2'^2\lambda_2 e^{\lambda_2\phi}\right] - \hat{\sigma}\frac{h_2'}{\sqrt{f}} = 0 \tag{C.2}$$

$$\frac{d-1}{2u}\left(\frac{4}{u} + \frac{g'}{g} + \frac{f'}{f}\right) + g\,(\hat{\rho} + \hat{p}) + \phi'^2 = 0 \tag{C.3}$$

$$\frac{f'}{fu} - \frac{d-2}{u^2} + g\left(\frac{d\,(d-1) + 2\hat{p}}{d-1}\right) - \frac{h_1'^2 e^{\lambda_1\phi}}{(d-1)\,f} - \frac{h_2'^2 e^{\lambda_2\phi}}{(d-1)\,f} + \frac{\phi'^2}{d-1} = 0 \tag{C.4}$$

$$h_2'' - h_2'\left(\frac{d-1}{u} + \frac{g'}{2g} + \frac{f'}{2f}\right) - g\sqrt{f}\hat{\sigma} = 0 \tag{C.5}$$

$$h_1'' - h_1'\left(\frac{d-1}{u} + \frac{g'}{2g} + \frac{f'}{2f} - \lambda_2\phi'\right) = 0 \tag{C.6}$$

$$\phi'' - \phi'\left(\frac{g'}{2g} - \frac{f'}{2f} + \frac{d}{u}\right) + \frac{\lambda_1 h_1'^2 e^{\lambda_1\phi}}{2f} + \frac{\lambda_2 h_2'^2 e^{\lambda_2\phi}}{2f} = 0. \tag{C.7}$$

The last equation was obtained using

$$\begin{aligned}
\Box\phi &= g^{\mu\nu}\left(\partial_\mu\partial_\nu\phi - \Gamma_{\mu\nu}^\alpha\partial_\alpha\phi\right) \\
&= g^{rr}\phi'' - \phi'\left(g^{rr}\Gamma_{rr}^r + (d-1)\,g^{ii}\Gamma_{ii}^r + g^{tt}\Gamma_{tt}^r\right) \\
&= \frac{\phi''}{g\ell^2} - \frac{\phi'}{g\ell^2}\left(\frac{g'}{2g} - \frac{f'}{2f} + \frac{d-1}{r}\right).
\end{aligned}$$

One verifies that letting $\phi \to 0$, $h_2 \to 0$ and $\lambda_{1,2} \to 0$, that the electron-star equations of motion are retrieved. Next, one substitutes equation (C.7) into the first equation of motion and finds that the dilaton does not contribute in this equation, leaving simply

$$\hat{p}' + (\hat{\rho} + \hat{p})\,\frac{f'}{2f} - \hat{\sigma}\frac{h_2'}{\sqrt{f}} = 0.$$

This is precisely the first equation of motion that we derived in Chapter 3. It is solved trivially by the zero-temperature equation of state, $-p = \rho - \mu\sigma$, in terms of the fluid parameters

$$\hat{\rho} = \hat{\beta}_d \int_{\hat{m}}^{\frac{h_2}{\sqrt{f}}} \epsilon^2\left(\epsilon^2 - \hat{m}^2\right)^{(d-3)/2}d\epsilon, \quad \hat{\sigma} = \hat{\beta}_d \int_{\hat{m}}^{\frac{h_2}{\sqrt{f}}} \epsilon\left(\epsilon^2 - \hat{m}^2\right)^{(d-3)/2}d\epsilon.$$

Because these expressions are identical to the expressions of the electron star, we also expect the same generalization to a non-zero temperature fluid. That is, we expect the first equation of motion to also be solved by invoking a non-zero temperature equation of state with a local temperature.

Having solved the first equation of motion, one now substitutes (C.3) into the Maxwell equations,

as before, to find

$$\frac{d-1}{2u}\left(\frac{4}{u}+\frac{g'}{g}+\frac{f'}{f}\right)+g\frac{h_2}{\sqrt{f}}\hat{\sigma}+\phi'^2 = 0$$

$$\frac{f'}{fu}-\frac{d-2}{u^2}+g\left(\frac{d\,(d-1)+2\hat{p}}{d-1}\right)-\frac{h_1'^2 e^{\lambda_1\phi}}{(d-1)\,f}-\frac{h_2'^2 e^{\lambda_2\phi}}{(d-1)\,f}+\frac{\phi'^2}{d-1} = 0$$

$$h_2''-\frac{h_2'\,(d-3)}{u}+\frac{g\hat{\sigma}}{\sqrt{f}}\left(\frac{uh_2 h_2'}{d-1}-f\right)+h_2'\left(\frac{u\phi'^2}{d-1}+\lambda_2\phi'\right) = 0$$

$$h_1''-\frac{h_1'\,(d-3)}{u}+\frac{g\hat{\sigma}}{\sqrt{f}}\frac{uh_1 h_1'}{d-1}+h_1'\left(\frac{u\phi'^2}{d-1}+\lambda_1\phi'\right) = 0$$

$$\phi''-\phi'\left(\frac{g'}{2g}-\frac{f'}{2f}+\frac{d}{u}\right)+\frac{\lambda_1 h_1'^2 e^{\lambda_1\phi}}{2f}+\frac{\lambda_2 h_2'^2 e^{\lambda_2\phi}}{2f} = 0.$$

This is the set of equations of motion for the Lifshitz electron star, analogous to the equations of motion (3.16)-(3.18). The presence of the extra equations of motion is due to the fact that additional matter fields are required for the support of the Lifshitz geometry. These equations have to solved throughout the spacetime, providing a background geometry on which, for instance, fermion correlator can be computed as we have done.

Acknowledgments

There are several people I would like to thank for their help and support in writing this thesis.

First and foremost, I would like to thank my two supervisors, Henk and Vivian. You were a tremendous help in writing this thesis from the outset and throughout. Our weekly meetings were always incredibly helpful, and I feel grateful to have had the opportunity to drop by at any time for questions and discussions. Henk, thank you for helping me prepare for my talks, your continuous support throughout the year and for recommending me for the PhD position in Germany. Vivian, thank you proofreading many documents and devoting so much of your time helping me solve numerical issues and figure out conceptual details. I think you are both tremendous supervisors and I look forward to hearing about the results in the follow-up of this project. Thank you!

Further, I would like to thank my fellow students in the master room for creating a great atmosphere to work in. Special thanks go to Tom, Stella, Jeemijn, Pieter, Tycho, and Peter. I enjoyed our many - sometimes much needed - lunch and coffee breaks, especially those outdoors. I wish you all good luck in the future. Finally, I would like to thank Suzanne for keeping me motivated throughout the year and helping me prepare for several talks and interviews.